REMARKS

I. Status of the Claims

Claims 1-35 were originally filed. As the result of a restriction requirement, claims 10-17 and 20-35 have been withdrawn from consideration.

Upon entry of the present amendment, claims 8, 9, and all withdrawn claims are canceled. Claim 1 is amended to recite the full name for the abbreviation of CNG3B, as requested by the Examiner. Support for the full name can be found throughout the specification, *e.g.*, on page 11, lines 19-20. The word "additional" is deleted in claim 1. Claims 1, 2, and 7 are amended to recite a sequence identity of at least 85%, 90%, and 95% to SEQ ID NO:1, which finds support in the specification, *e.g.*, on page 11, lines 22-27. No new matter is introduced. Claims 1-7, 18, and 19 remain pending.

II. Specification

The specification is amended to delete all reference to browser-executable codes embedded in the specification, as requested by the Examiner. No new matter is introduced.

III. Claim Rejections

A. 35 U.S.C. §101

Claims 1-9, 18, and 19 were rejected under 35 U.S.C. §101 for alleged lack of either a specific, substantial, and credible asserted utility or a well established utility. Applicants respectfully traverse the rejection.

1. Standard to Assess Utility

According to MPEP §2107, the Examiner should review the claims and the supporting written description to determine whether the utility requirement under 35 U.S.C. §101 is met. No rejection based on lack of utility should be made if an invention has a well-established utility, *i.e.*, a utility that will be immediately appreciated by one of ordinary skill in the art based on the characteristics of the invention, regardless of whether any such utility has been asserted. Neither should any rejection be made for lack of utility if an applicant has

asserted a specific and substantial utility that would be considered credible by one of ordinary skill in the art.

In most cases, an applicant's assertion of utility creates a presumption of utility that will be sufficient to satisfy the utility requirement of 35 U.S.C. §101. MPEP §2107.02 III A. The Court of Customs and Patent Appeals stated in *In re Langer*:

> As a matter of Patent Office practice, a specification which contains a disclosure of utility which corresponds in scope to the subject matter sought to be patented must be taken as sufficient to satisfy the utility requirement of §101 for the entire claimed subject matter unless there is a reason for one skilled in the art to question the objective truth of the statement of utility or its scope.

In re Langer, 183 USPQ 288, 297 (CCPA, 1974, emphasis in original). To overcome the presumption of sufficient utility as asserted by an applicant, the Examiner must carry the initial burden to make a *prima facie* showing of lack of utility and provide a sufficient evidentiary basis for the conclusion. In other words, the Examiner "must do more than merely question operability--[he] must set forth factual reasons which would lead one skilled in the art to question objective truth of the statement of operability." *In re Gaubert*, 187 USPQ 664, 666 (CCPA 1975).

MPEP §2107.02 IV further states, a detailed explanation should be given for a utility rejection as to why the claimed invention has no specific and substantial asserted utility. Documentary evidence should be provided when possible. Otherwise the Examiner should specifically explain the scientific basis for his factual conclusions.

2. The Asserted Utility and the Examiner's Rejection

In the Office Action mailed November 2, 2004, the Examiner alleged that the instant specification fails to establish a well-established utility or a specific and substantial asserted utility of the claimed invention. As the basis of this conclusion, the Examiner stated that since the instant specification does not provide any experimental data demonstrating that the claimed CNG3B protein functions as a cyclic nucleotide-gated channel, the determination or

confirmation of such claimed biological activity would require undue experimentation. *See, e.g.*, paragraph 10 bridging pages 4 and 5 of the Action.

The instant application asserts a specific and substantial utility of the claimed invention. For example, it is asserted on page 7, line 26, to page 8, line 6, that CNG3B is a beta subunit capable of complexing with alpha subunits of the family of cyclic nucleotide-gated cation channels and that the identification of CNG3B subunits allows screening for modulators of cyclic nucleotide-gated cation channels comprising a CNG3B subunit. Because of the involvement of known CNG channels in regulating intracellular Ca^{2+} level and therefore in regulating various biological processes such as light sensory and chemotaxis of sperm, and also because of the expression pattern of CNG3B in the retina and testis, it is asserted that these modulators are useful for treating visual disorders and for modulating male fertility.

3. The Claimed CNG3B Polypeptides Are Useful for Screening of New Therapeutics for Treating Neurological Disorders Related to Cell Excitability

The CNG3B polypeptides are beta subunits of cyclic nucleotide-gated cation channels most highly expressed in the retina and testes. It is well known in the art that this type of cyclic nucleotide-gated cation channel plays an important role in regulating intracellular cation concentration, *e.g.*, Ca^{2+} concentration, which can act as a second messenger to regulate a number of cellular events and therefore affect the biological functions of the tissue in which the cation channels are expressed. See, *e.g.*, page 2, line 8, to page 3, line 2, of the specification and references cited therein.

Because the CNG3B channels are capable of modulating cytoplasmic Ca^{2+} concentration, which in turn participates in the regulation of biological functions of tissues expressing the channels, these cation channels are therapeutic targets for treating diseases and conditions related to abnormal cation influx in the relevant tissues, such as retina and testis. For example, modulators of the CNG3B channels can be expected to be useful for treating diseases or conditions in the retina and testis, such as vision problems and male infertility (*see, e.g.*, page 7, line 30, to page 8, line 2, of the specification).

The assertion that the CNG3B polypeptide identified by the present inventors is a subunit of a cyclic nucleotide-gated ion channel implicated in visual disorders has been confirmed by studies published after the effective filing date of this application. For example, the work by Kohl *et al.* (*Human Mol. Genet.*, 2000, **9**:2107-2116, attached as Exhibit A) demonstrates that human CNG3B (termed CNGB3 in the reference), a homolog of CNGA3, is specifically expressed in the retina and its mutants are found in families with hereditary visual abnormalities such as achromatopsia. Moreover, two papers by Peng *et al.* (Peng *et al.*, *J. Biol. Chem.*, 2003, **278**:24617-24623, attached as Exhibit B; and Peng *et al.*, *J. Biol. Chem.*, 2003, **278**:34533-34540, attached as Exhibit C) further provide convincing evidence that CNG3B (termed CNGB3 in the papers) is indeed a subunit that can participate in forming a cyclic nucleotide-gated cation channel, which is important for proper visual functions.

The present application provides the amino acid sequence of CNG3B channel beta subunit, methods of activating the CNG3B channels, and methods of assaying for modulators of the CNG3B channels. A skilled artisan, after reading the present application, would therefore be able to (1) routinely identify potential modulators of the CNG3B channels and (2) determine if such a modulator increases or decreases cytoplasmic cation concentration. Treating diseases related to abnormal ion influx by targeting ion channels is a well known strategy in the art. Modulators of CNG3B channels, therefore, have utility for (1) altering cation influx and intracellular cation levels, (2) modulating the biological functions of relevant tissues, and (3) treating diseases and conditions found in these tissues, such as vision problems and male infertility.

Once an ion channel is identified, its modulators can be routinely identified using an assay system that assesses the function characteristics of the ion channel. The present application provides CNG3B polypeptides, as well as methods for activating a CNG3B channel, *e.g.*, by increasing the concentration of a cyclic nucleotide. Activators and inhibitors of a CNG3B channel can be routinely identified by applying a candidate compound to cells expressing the CNG3B channel while applying a cyclic nucleotide, *e.g.*, cAMP, to the cells and measuring the effect on the level of cation flow through the CNG3B channel. After reading the

present application, one of ordinary skill in the art would therefore know how to identify CNG3B channel modulators that are useful for modulating intracellular cation concentrations in the relevant tissues.

Applicants thus contend that the asserted utility for the present invention is one supported by the general knowledge in the relevant field and a person of ordinary skill in the art would find such utility credible.

4. The Asserted Utility is Specific, Substantial, and Credible

Applicants contend that the disclosure of CNG3B polypeptides as subunits of functional cyclic nucleotide-gated cation channels, combined with the methods disclosed in the specification and the level of skill in the art, is sufficient to establish a credible specific and substantial utility under the definitions provided by the MPEP.

Specific Utility

Applicants assert that the present invention has a specific utility. Specific utility is defined by the MPEP as a utility that is specific to the subject matter claimed. The MPEP explains that applications show sufficient specific utility when applicants disclose a "specific biological activity" and reasonably correlate that activity to a "disease condition." MPEP §§2107.01 and 2107.02. In the present application, Appellant discloses a "disease condition," *i.e.*, altered cytoplasmic cation concentration, that correlates with a "biological activity," *i.e.*, the opening and closing of the CNG3B channels. This application teaches that the CNG3B channels modulate intracellular cation concentration. The application further provides methods for identifying modulators of the CNG3B channels capable of modulating cation influx, *e.g.*, for the treatment of altered biological functions in tissues expressing the CNG3B channels, such as abnormalities found in the retina (*e.g.*, vision disorders) or testes (*e.g.*, male infertility). Applicants thus submit that the present invention has a specific utility, namely that CNG3B channels can regulate cation concentrations in the cells of certain tissues, which is clearly specific for the claimed CNG3B channels and not just any ion channels.

Substantial Utility

Applicants also assert that the present invention has a substantial or "real-world" use. This invention provides CNG3B polypeptides. The application also teaches that CNG3B channels modulate intracellular cation concentration in certain tissues and teaches how to assay the function of a CNG3B channel and how to identify modulators of the CNG3B channels. For example, on pages 42-45 of the specification, assays are provided that can be used to screen for inhibitors and activators of the CNG3B channels, *e.g.*, assays that involve measuring current, measuring membrane potential, measuring ion flux, or measuring patch-clamp electrophysiology. The present invention therefore has a real-world use in the modulation of intracellular cation concentration, as well as in the identification of compounds that modulate the CNG3B channels and thus can be useful as therapeutic agents for treating diseases related to altered functions in tissues expressing CNG3B, such as vision disorder or male infertility.

Credible Utility

Finally, Applicants contend that the asserted utility of the present invention is credible, *i.e.*, would be believable to one of skill in the art. Applicants submit that an ordinarily skilled artisan, after reading this application, would know (a) how to identify the CNG3B channels; (b) how to identify modulators of the CNG3B channels; and (c) how to use these modulators so identified to modulate cellular cation concentration and therefore cellular function. Because many currently marketed drugs treat a wide variety of diseases or conditions by targeting ion channels, one skilled in the art would believe that the identification of a new cation channel is useful for developing new therapeutics.

5. The Examiner's Rejection Is Not Supported by Objective Reasons

Despite the assertion of a specific and substantial utility of the claimed invention in the specification, the Examiner apparently did not believe this asserted utility. For example, the Examiner stated in the Office Action that "[t]he instant specification fails to provide any experimental data or information on whether the CNG3B protein encoded by the claimed nucleic acids set forth as SEQ ID NO:2 or SEQ ID NO:3, functions like a cyclic nucleotide-gated ion channel " (page 5, lines 6-9, of the Office Action). The Examiner cited three references by Finn

et al., Skolnick *et al.*, and Bork to question the assertion that the CNG3B polypeptide is a subunit of a cyclic nucleotide-gated cation channel.

According to the MPEP, raising a rejection for lack of utility requires the Examiner to carry the initial burden, not Applicants, to provide evidence to support a factual conclusion of the credibility of an asserted utility. In fact, MPEP §2107.02 III.B. specifically cautions Office personnel that, once an assertion of a particular utility is made, "that assertion cannot simply be dismissed ..... as 'wrong,' even when there may be reason to believe the assertion is not entirely accurate." Instead, the Examiner must provide an explanation setting forth the reasoning used in concluding that the asserted specific and substantial utility is not credible; support for factual findings relied upon in reaching the conclusion; and an evaluation of all relevant evidence of record, including utilities taught in the closest prior art. MPEP §2107.02 IV.

In the present application, it is asserted that human CNG3B is a subunit of a cyclic nucleotide-gated ion channel, since it has a significant level of overall amino acid sequence homology to human CNG1A and CNG3A as well as a particularly high level of homology in the region of 210-661 of CNG3B, a region known in the art for defining members of the CNG family (see Figure 1 and Example 1 on pages 62-63). Also, the 210-661 region of CNG3B has a greater than 81% sequence identity to the corresponding regions of mouse CNG6 (see the bridging paragraph between pages 62 and 63).

In contrast, the Examiner relied on the three references by Finn *et al.*, Skolnick *et al.*, and Bork to conclude a lack of credible asserted utility. Applicants contend that this reliance is misplaced, because these references are not immediately relevant to the credibility of CNG3B's asserted role as a subunit of a cyclic nucleotide-gated cation channel and therefore do not provide reasonable support for the Examiner's doubts about the credibility of the asserted utility of the claimed invention. For example, the Bork *et al.* and Skolnick *et al.* references provide some general discussions about the pitfalls in predicting protein function on the basis of amino acid sequence homology. Applicants do not dispute that such sequence-based functional prediction for newly identified open reading frames has only limited accuracy and reliability. It

is noted, however, that there exists an increasingly high probability of correct functional predication as the level of sequence homology increases both overall and in regions that are known to be characteristic of a particular type of proteins, *e.g.*, the common motif of the six transmembrane domains found among subunits of cyclic nucleotide-gated ion channels.

The Examiner pointed to Box 2 of the Skolnick reference to argue that similar protein structure does not support the conclusion of similar protein function. Applicants do not agree with the Examiner's overly broad interpretation of the teaching by Skolnick *et al.*, particularly the interpretation of Box 2. What Box 2 teaches is that generally similar protein structures (such as how the proteins fold) that are used for defining protein super families do not indicate similar functions of these proteins. This is without question a correct statement when protein structural similarities are viewed at such a large scale, *e.g.*, at the level of general organization of major domains. Anyone of skill in the art would know that, as an example, the immunoglobulin-like superfamily encompasses a huge variety of proteins of drastically diverse functions, *e.g.*, antibodies, cell surface receptors, *etc.* Yet, Applicants contend that such lack of similarity in protein functions resides in the fact that the structural similarity at this level does not necessarily require any significant homology in the primary amino acid sequence. When protein structure similarity refers to similarity at a much smaller scale, *e.g.*, at the level of amino acid sequence identity, the amino acid sequence similarity and the structural similarity resulted therefrom are far more likely to support a functional similarity.

Moreover, as far as ion channels are concerned, there exists an abundance of knowledge of well-defined ion channel families and the common structural features for each family, for instance, the conserved region of a cyclic nucleotide-gated cation channel containing the signature six transmembrane domains, or the pore region, or the cytoplasmic cyclic nucleotide binding domain (see, *e.g.*, Finn *et al.*). This is precisely why there is a much higher likelihood that a new member of a ion channel family can be correctly recognized based on sequence homology and structural similarity. The Bork and Skolnick references simply do not address this particular consideration. Applicants contend that, given the state of the art in the field of ion channel research, a sequence homology set forth in the present application (*e.g.*,

Figure 1) is sufficient to support a conclusion that CNG3B belongs to the cyclic nucleotide-gated ion channel family.

The Finn *et al.* reference discusses the diverse features among cyclic nucleotide-gated ion channels. These discussions focus on the different signaling pathways these ion channels are involved in (*e.g.*, in the visual and olfactory sensory pathways) and the different mechanisms by which they are regulated (*e.g.*, cyclic nucleotide-activated or cyclic nucleotide-modulated). This review article provides general discussions about various ion channels expressed in different tissues and having different functional characteristics. Yet the discussions do not address what level of sequence homology would reasonably support a conclusion that a newly described protein is a member of a known class of ion channels. Thus, the Finn *et al.* reference is not directly relevant to the question whether a protein such as CNG3B described by the present inventors can be reasonably accepted as a cyclic nucleotide-gated cation channel, when the protein has a significant level of sequence homology to known cyclic nucleotide-gated ion channels, particularly in a region recognized in the art as a characteristic for this class of ion channels. At the very least, this reference does not provide sufficient basis, as described by MPEP §2107.02.III.B., for the Examiner to doubt the role of CNG3B as a cyclic nucleotide-gated cation channel.

As such, Applicants submit that the Examiner has not provided any reasonable objective reasons why CNG3B's asserted functional role as a cyclic nucleotide-gated cation channel is not credible or why the asserted utility of the claimed invention based on this asserted function is not credible, particularly when post-filing information has already confirmed the role of CNG3B as a subunit of a cyclic nucleotide-gated ion channel as asserted in the specification.

6. Claims Drawn to Fully Characterized Proteins Meet the Utility Requirement under 35 U.S.C. §101

The claimed CNG3B channels are fully characterized both structurally and functionally. The CNG3B polypeptides are claimed by shared structural features, *e.g.*, having at least 85% identity to the amino acid sequence of SEQ ID NO:1, and shared functional features,

e.g., capable of forming a cyclic nucleotide-gated cation channel with at least one additional CNG alpha subunit.

According to the Revised Interim Utility Guidelines Training Materials (the "Guidelines") promulgated by the PTO (http://www.uspto.gov/web/menu/utility.pdf), a characterized protein has sufficient utility for patentability. This standard is made evident from Example 8 on page 45 of the Guidelines, wherein a compound A is disclosed to inhibit enzyme XYZ, a well known enzyme, *in vitro*. The hypothetical specification states that the compound A can be used to treat diseases caused or exacerbated by enzyme XYZ. No such diseases are named. Claim 1 is directed to compound A. Claim 2 is directed to a method of treating a disease caused or exacerbated by enzyme XYZ consisting of administering an effective amount of compound A to a patient. In the subsequent analysis, claim 2 is deemed to be insufficiently supported by a real world context of use. This is because neither the specification nor the art of record discloses any disease or conditions caused or exacerbated by enzyme XYZ and therefore, the asserted utility is seen as a method of treating an unspecified and undisclosed disease or condition, which does not define a "real world" context of use. Claim 1, however, is regarded as having utility because claim 1 is directed to a compound that inhibits an enzyme and enzymes have well established utility in the art, i.e., catalyzing certain reactions.

This hypothetical example can be compared to the present application. The present application claims CNG3B cation channels, which are analogous to compound A in the Guidelines that inhibits enzyme XYZ. The present specification states that the CNG3B channels are likely involved in modulating cytoplasmic cation concentration and cellular functions in the relevant tissues. Thus, the ion channels can be used as targets for treating disorders related to abnormal cellular functions in these tissues. In Example 8 of the Guidelines, claim 1 directed to compound A is found to have utility even though there is no disclosure of specified disease to be treated. Accordingly, even if the Examiner is not convinced that the claimed CNG3B channels are involved in regulation of intracellular cation levels and cellular function in tissues expressing the channels, a claim directed to compound A, *i.e.*, the CNG3B cation channels in the present case, have sufficient utility for patentability. The utility resides in the fact that the claimed

polypeptides are cation channels subunits, which, like enzymes, have a well-established utility in the art: modulating the passage of caions according to varying conditions.

Analysis of the pending claims according to the Guidelines therefore further supports Applicants' position that the rejection for lack of utility is improper.

7. Finding Sufficient Utility in the Present Application is Consistent with the Policy of Encouraging Early Disclosure

Our patent law places much emphasis on encouraging early disclosure of inventions. This is a particularly relevant policy consideration in case law involving the utility standard under 35 U.S.C. §101. In *Brenner v. Manson*, 148 USPQ 689 (US Sup. Ct. 1966), for instance, the Supreme Court ruled that a process to produce a compound may be patented only if the compound has "substantial utility," "specific benefit ... in currently available form." Whether granting patent protection to the discovery of a new process or compound with a yet unknown practical utility would encourage prompt disclosure of inventions was one factor the Court carefully considered and to a significant extent relied upon in reaching the landmark decision. 148 USPQ at 695.

In *Nelson v. Bowler*, 206 USPQ 881 (CCPA 1980), the CCPA was confronted with a situation where the claimed compound, 16-phenoxy-substituted prostaglandin, was shown to have some pharmacological activity, *i.e.*, causing changes in blood pressure in the rat blood pressure test and stimulation of smooth muscles in the gerbil colon smooth muscle stimulation test, yet no specific therapeutic use for the compound was established. In deciding the question of utility, the CCPA stated:

> Knowledge of the pharmacological activity of any compound is obviously beneficial to the public. It is inherently faster and easier to combat illness and alleviate symptoms when the medical profession is armed with an arsenal of chemicals having known pharmacological activities. Since it is crucial to provide researchers with an incentive to disclose pharmacological activities in as many as compounds as possible, we conclude that adequate proof of any such activity constitute a showing of practical utility.

Nelson, 206 USPQ at 883. The present case is analogous to *Nelson*. Because abnormal ion influx and altered cellular functions are known to cause or are related to various diseases and disorders, compounds capable of modulating ion channels, such as cyclic nucleotide-gated cation channels, are useful as therapeutic agents for treating these conditions. Assays for screening of these ion channel modulators is thus beneficial to the public and the disclosure of how to perform these assays should be encouraged. The present application provides just this kind of disclosure. To hold that the present invention lacks sufficient utility under 35 U.S.C. §101 to warrant patent protection would be inconsistent with the underlying policy of case law and create a strong disincentive for researchers to disclose their inventions of this type.

8. Summary

In light of the foregoing discussion, Applicants believe that the utility rejection under 35 U.S.C. §101 is improper and should be withdrawn.

B. 35 U.S.C. §112, First Paragraph: Enablement

Utility-Based Enablement Rejection

Claims 1-9, 18, and 19 were also rejected under 35 U.S.C. §112, first paragraph, for alleged lack of enablement. The Examiner asserted that since the claimed invention does not have a patentable utility, one of skill in the art would not know how to use the invention. In light of the above discussion, Applicants trust that sufficient utility under 35 U.S.C. §101 has been established. Thus, the withdrawal of the enablement rejection based on the alleged lack of utility is respectfully requested.

Scope-Based Enablement Rejection

Claims 1, 2, 5, and 7-9 were further rejected under 35 U.S.C. §112, first paragraph, for alleged lack of enablement, as the Examiner argued that the specification does not properly enable the full scope of the claimed invention. Applicants respectfully traverse the rejection in light of the present amendment.

A claimed invention is enabled when the disclosure allows one of ordinary skill in the art to make and use the invention without undue experimentation. MPEP §2164.01. The test

for enablement as set forth in *In re Wands*, 8 USPQ2d 1400 (Fed. Cir. 1988), requires the consideration of multiple factors: the breadth of the claims; the nature of the invention; the state of the prior art; the level of predictability in the art; the amount of direction provided by the inventor; the existence of working examples; and the quantity of experimentation needed to make or use the invention based on the content of the disclosure.

In the present case, the claims are directed to a nucleic acid encoding a CNG3B subunit of a cyclic nucleotide-gated cation channel, which has well-defined structures and readily testable functional features. The specification contains ample directions to practice the invention. For example, the application provides cloning methods for isolating the polynucleotide sequences encoding CNG3B (*e.g.*, page 26, line 28, to page 29, line 18; Example I on pages 61-63); the application also teaches the methods for expressing CNG3B in prokaryotic and eukaryotic cells (*e.g.*, page 29, line 21, to page 31, line 32) and purifying recombinant CNG3B polypeptide (*e.g.*, page 32, line 6, to page 35, line 3); the application further describes the methods for immunological detection of CNG3B polypeptide (*e.g.*, page 35, line 6, to page 42, line 19); the application in addition offers assays for analyzing the electrophysiological characteristics of CNG3B and assays for screening compounds that modulate ion flow through a CNG3B (*e.g.*, page 42, line 23, to page 46, line 2). As such, a large amount of detailed direction is given in the present disclosure for practicing the claimed invention.

The level of technical sophistication is high in the art, and variants of the cyclic nucleotide-gated cation channel subunit can be readily tested according to the methods commonly used by those skilled in the art or the methods taught by the specification (such as nucleic acid or amino acid sequence comparison, nucleic acid hybridization assays, and assays for ion channels with the characteristics of cyclic nucleotide-gating) to eliminate inoperable embodiments. MPEP §2164.01 states, complex experimentation is not necessarily undue, if the art typically engages in such experimentation. In the present case, although some experimentation may be involved to practice the claimed invention using embodiments other than those specifically described in the application, such experimentation utilizes well-

established techniques and is the type routinely conducted in the art. Thus, the experimentation does not constitute undue experimentation.

Taken together, analysis of the *Wands* factors indicates proper enablement of the claimed invention. Applicants thus respectfully request the withdrawal of the enablement rejection.

C. 35 U.S.C. §112, First Paragraph: Written Description

Claims 1-9, 18, and 19 were further rejected under 35 U.S.C. §112, first paragraph, for alleged lack of sufficient written description. Applicants respectfully traverse the rejection, particularly in light of the present amendment.

Possession of claimed invention may be shown by a variety of descriptive means, including words, structure, figures, diagrams, and formulas. MPEP §2163 I. Case law provides more specific guidance in setting the standard for written description.

As discussed above, the amended claims are now directed to an isolated nucleic acid that encodes for a polypeptide, which can form a cyclic nucleotide-gated cation channel with at least one alpha subunit and comprises a subsequence having at least 85% amino acid sequence identity to SEQ ID NO:1. The amended claims fully comply with the requirements for written description of a chemical genus as set forth in *University of California v. Eli Lilly & Co.*, 43 USPQ2d 1398 (Fed. Cir. 1997). As described by the Federal Circuit in *Lilly*, "[a] description of a genus of cDNAs may be achieved by means of . . . a recitation of structural features common to the members of the genus . . . ." *Lilly*, 43 USPQ2d at 1406. Furthermore, the court in *Fiers v. Revel* stated that an adequate written description "requires a precise definition, such as by structure, formula, chemical name, or physical properties." *Fiers*, 25 USPQ2d 1601, 1606 (Fed. Cir. 1993).

On the other hand, proper description of functional features of a claimed invention can play an important role in satisfying the written description requirement. The Federal Circuit recently stated that "*Lilly* did not hold that all functional descriptions of genetic material necessarily fail as a matter of law to meet the written description requirement; rather,

the requirement may be satisfied if in the knowledge of the art the disclosed function is sufficiently correlated to a particular, known structure." *Amgen Inc. v. Hoechst Marion Roussel Inc.*, 65 USPQ2d 1385, 1398 (Fed. Cir. 2003).

With regard to the claimed nucleic acids, pending claims set forth both functional features, *e.g.*, encoding a CNG3B polypeptide capable of forming a cyclic nucleotide-gated cation channel with at least one alpha subunit, and structural features, *e.g.*, comprising a subsequence having at least 85% amino acid sequence identity to SEQ ID NO:1. The percentage sequence identity between a polypeptide and a reference amino acid sequence is a physical/structural property of the polypeptide, because such percentage identity relies upon the amino acid sequence of the polypeptide. In turn, this is a physical/structural property of the nucleic acid encoding for the polypeptide, because the amino acid sequence of the polypeptide depends on the polynucleotide sequence of the nucleic acid. The pending claims therefore set forth commonly shared structural features of the claimed nucleic acids.

Thus, both structural and functional features commonly shared by the claimed genus have been described in detail, which "clearly allow persons of ordinary skill in the art to recognize that [the applicant] invented what is claimed." *Vas-Cath Inc. v. Mahurkar*, 19 USPQ2d 1111, 1116 (Fed. Cir. 1991). Such description is consistent with the standards set forth in both *Lilly* and *Amgen*. Applicants thus respectfully request the withdrawal of the written description rejection.

D. 35 U.S.C. §112, Second Paragraph

Claims 1-9, 18, and 19 were also rejected under 35 U.S.C. §112, second paragraph, for alleged indefiniteness. Specifically, the Examiner objected to the use of the abbreviation of CNG3B in claims 1 and 8. In response, claim 1 has been amended to spell out the full name of CNG3B. Claim 8 is canceled. The Examiner also held that the term "at least one additional alpha subunit" in claim 1 indefinite, since there is no previous reference to any alpha subunit. Upon entry of the present amendment, the word "additional" has been deleted from claim 1. In addition, claim 7 was rejected for alleged indefiniteness for reciting the term "moderately stringent conditions." As amended, claim 7 no longer recites this term.

In light of the present claim amendment, Applicants submit that all indefiniteness rejections have been properly addressed. Their withdrawal is respectfully requested.

CONCLUSION

In view of the foregoing, Applicants believe all claims now pending in this Application are in condition for allowance. The issuance of a formal Notice of Allowance at an early date is respectfully requested.

If the Examiner believes a telephone conference would expedite prosecution of this application, please telephone the undersigned at 925-472-5000.

Respectfully submitted,

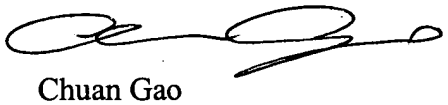

Chuan Gao
Reg. No. 54,111

TOWNSEND and TOWNSEND and CREW LLP
Two Embarcadero Center, Eighth Floor
San Francisco, California 94111-3834
Tel: 415-576-0200
Fax: 415-576-0300

Attachment (Exhibit A: Kohl *et al.*, *Human Mol. Genet.*, 2000, **9**:2107-2116; Exhibit B: Peng *et al.*, *J. Biol. Chem.*, 2003, **278**:24617-24623; Exhibit C: Peng *et al.*, *J. Biol. Chem.*, 2003, **278**:34533-34540)

CG:cg
60403182 v1

Human Molecular Genetics, 2000, Vol. 9, No. 14 2107–2116

ARTICLE

Mutations in the *CNGB3* gene encoding the β-subunit of the cone photoreceptor cGMP-gated channel are responsible for achromatopsia (*ACHM3*) linked to chromosome 8q21

Susanne Kohl[1], Britta Baumann[1], Martina Broghammer[1], Herbert Jägle[2], Paul Sieving[3], Ulrich Kellner[4], Robert Spegal[5], Mario Anastasi[6], Eberhart Zrenner[1], Lindsay T. Sharpe[2] and Bernd Wissinger[1+]

[1]Molekulargenetisches Labor and [2]Psychophysisches Labor, Universitäts-Augenklinik, Auf der Morgenstelle 15, D-72076 Tübingen, Germany, [3]Kellogg Eye Center, University of Michigan, Ann Arbor, MI, USA, [4]Augen-Poliklinik, Universitätsklinikum Benjamin Franklin, Berlin-Steglitz, Germany, [5]Micronesia Human Resource Development Center, Kolonia, Pohnpei State, Federated States of Micronesia and [6]Clinica Oculistica, Palermo, Italy

Received 26 May 2000; Revised and Accepted 28 June 2000

DDBJ/EMBL/GenBank accession no. AF272900

Achromatopsia is an autosomal recessive disorder featuring total colour blindness, photophobia, reduced visual acuity and nystagmus. While mutations in the *CNGA3* gene on chromosome 2q11 are responsible for achromatopsia in a subset of patients, previous linkage studies have localized another achromatopsia locus, *ACHM3*, on chromosome 8q21. Using achromatopsia families in which *CNGA3* mutations have been excluded, we refined the *ACHM3* locus to a 3.7 cM region enclosed by markers *D8S1838* and *D8S273*. Two yeast artificial chromosome (YAC) contigs covering nearly the entire *ACHM3* interval were constructed. Database searches with YAC content sequences identified two overlapping high throughput genomic sequencing phase (HTGS) entries which contained sequences homologous to the murine *cng6* gene encoding the putative β-subunit of the cone photoreceptor cGMP-gated channel. Using RT–PCR and RACE, we identified and cloned the human cDNA homologue, designated *CNGB3*, which encodes an 809 amino acid polypeptide. Northern blot analysis revealed a major transcript of ~4.4 kb specifically expressed in the retina. The human *CNGB3* gene consists of 18 exons distributed over ~200 kb of genomic sequence. Analysis of the *CNGB3* gene in achromats revealed six different mutations including a missense mutation (S435F), two stop codon mutations (R203X and E336X), a 1 bp and an 8 bp deletion (1148delC and 819–826del) and a putative splice site mutation of intron 13. The 1148delC mutation was identified recurrently in several families, and in total was present on 11 of 22 disease chromosomes segregating in our families.

INTRODUCTION

Achromatopsia (rod monochromacy, total colour blindness) is a rare, autosomal recessively inherited ocular disorder characterized by low visual acuity, central scotoma, nystagmus, photophobia and the complete disability to discriminate between colours (1). Electroretinographic recordings (ERGs) in patients show that rod photoreceptor function is normal, whereas cone photoreceptor function cannot be established.

Recently, we showed that mutations in the *CNGA3* gene cause achromatopsia linked to the *ACHM2* locus on chromosome 2q11 (2). *CNGA3* encodes the α-subunit of the cGMP-gated channel in cone photoreceptors, a key player of the phototransduction cascade responsible for the membrane hyperpolarization on light stimulation of photoreceptors. Analysis of the homologous knock-out mouse model showed complete absence of physiologically measurable cone function, decrease in the number of cones in the retina and morphological abnormalities of the remaining cones (3).

However, achromatopsia in man is not a genetically homogenous condition. Linkage analysis in pedigrees from the Pingelap islander population and a large Irish pedigree excluded the *ACHM2/CNGA3* locus but detected linkage with markers on chromosome 8q21 and defined a new achromatopsia locus *ACHM3* (4,5). Homozygosity intervals identified in the Pingelap pedigrees localized the *ACHM3* locus to an interval of ~5 cM between markers *D8S1757* and *D8S273*. Yet no cone

+To whom correspondence should be addressed. Tel: +49 7071 2985032; Fax: +49 7071 295725; Email: wissinger@uni-tuebingen.de

photoreceptor-specific candidate gene has been mapped to this region, making it necessary to employ positional cloning strategies to identify the gene responsible for *ACHM3*.

Here we report the genetic and physical mapping of the *ACHM3* region, the identification and cloning of the *CNGB3* gene within the critical region and the detection of mutations responsible for achromatopsia linked to chromosome 8q21.

RESULTS

Genetic mapping

We defined a subset of 11 achromatopsia families based on the exclusion of *CNGA3* mutations and discordant marker segregation for the corresponding *ACHM2* locus on chromosome 2q11 (Fig. 1A). Linkage analysis in the combined set of families with polymorphic markers spanning an interval of ~20 cM on chromosome 8q21 resulted in a two-point LOD score of >3.0 for markers *D8S1697*, *D8S1838*, *D8S167* and *D8S273*. The highest combined LOD score of 5.1 was obtained for *D8S1838* at $\theta = 0.0$ (data not shown). The order of markers used for genetic fine mapping was based primarily on published genetic data (6,7; http://www.genethon.fr , http://www.marshmed.org/genetics/) and physical mapping data (8; http://www.genome.wi.mit.edu/cgi-bin/contig/phys-map). The order cen–*D8S543*–*D8S279*–*D8S2324*–*D8S541*–*D8S1705*–*D8S1757*–*D8S275*–*D8S525*–*D8S169*–*D8S1838*–*D8S167*–*D8S1707*–*D8S273*–*D8S88*–*D8S270*–*D8S1699*–*D8S1822*–tel was most consistent with already published data and results herein derived from meiotic breakpoint mapping, homozygosity intervals and sequence-tagged site (STS) content mapping data (see below). On haplotype reconstruction, closest meiotic recombinations were observed for *D8S1757* at the centromeric border in an affected subject (II:1) in family CHRO8 and for *D8S88* at the telomeric border in an unaffected sibling (II:3) in family CHRO17 (Fig. 1B). However, due to the small size of the respective families, those data had to be considered preliminary. Additional mapping evidence was obtained with the observation of significant marker homozygosity intervals in patients from four families (CHRO4, CHRO19, CHRO92 and CHRO183). Among these, a patient of the Pingelap islander population (subject II:1 in family CHRO183) showed homozygosity for eight consecutive markers telomeric to *D8S1838* (Fig. 1B). Taking into account the data reported by Winick *et al.* (4), our results suggest the *ACHM3* locus to be localized within a 3.7 cM region between *D8S1838* and *D8S273*.

Physical mapping

Based on the Whitehead framework map and additional screening efforts, we collected yeast artificial chromosome (YAC) clones mapping to 8q21 in order to build a physical map of the *ACHM3* region. Individual YAC colonies were typed for known short tandem repeat (STR) and STS markers retrieved from public databases (8,9; http://www.genome.wi.mit.edu/cgi-bin/contig/phys-map/ and http://www.ncbi.nlm.nih.gov/genemap/) as well as for additional STSs generated from YAC end and Alu-vectorette PCR products. We thus obtained a YAC contig of ~6.5 Mb size between markers *D8S1757* and *D8S167*, and another contig including marker *D8S273* and further distal markers (Fig. 2). Efforts to cover the gap between both contigs with additional YAC clones from either the CEPH or the ICRF YAC library failed. Right end sequences of both CEPH 790_a_07 and CEPH 952_g_02 clones matched to unordered sequences of the chromosome 8 bacterial artificial chromosome (BAC) clone RP11-386D6 (GenBank accession no. AC021132). BLAST analysis showed that AC021132 also contains *D8S1707*, thus extending the YAC contig to this marker. Similarly, the left end sequence of CEPH 765_g_08 gave a hit to high throughput sequencing phase (HTGS) BAC clone RP11-480D11 (GenBank accession no. AC021991) which also contains STS WI-2030 and overlaps with the finished *D8S273*-containing BAC clone CTB-118P5 (GenBank accession no. AC005066). Sequence sampling of YAC content sequences and their use in database searches proved particularly useful to link unmapped HTGS sequences to the *ACHM3* region. For example, sequences encoding the *IMPA* and the *CA1* genes were identified and placed on the physical map (STS IMPA-PM and SHGC-31642 in Fig. 2).

Identification of the human *CNGB3* gene

The HTGS sequence AC021132 identified with YAC end sequences (see above) virtually overlaps with another HTGS sequence (AC013751) derived from BAC RP11-298P6. Analysis of these sequences with the NIX software package provided significant sequence matches with the mouse *cng6* cDNA encoding the putative β-subunit of the cGMP-gated channel in cone photoreceptors (10).

Amplification of a human genomic segment encompassing sequences homologous to the mouse cDNA with samples of the NIGMS monochromosomal hybrid panel resulted in a product only with DNA from the human chromosome 8 cell line NA10156B, and thus provided additional experimental evidence for the location of *cng6*-homologous sequences on human chromosome 8 (data not shown).

Using primers derived from the *cng6*-homologous human genomic sequence, we performed RT–PCR and RACE experiments with human retinal RNA to amplify and clone the orthologous human cDNA, designated *CNGB3*, according to the HUGO nomenclature committee. Two cDNA species differing in length by 250 bp were identified by 3′ rapid amplification of cDNA ends (RACE). Comparison with the genomic sequence indicated that these different cDNAs represent transcripts with alternative polyadenylation sites. The overlapping cDNA sequences revealed a combined cDNA length of 4119 and 4369 bp, respectively, with an open reading frame of 809 codons from the first in-frame ATG, 46 bp of 5′-untranslated region (UTR) and 1896 bp of 3′-UTR sequence for the longer transcript. Three heterozygous polymorphisms were detected at the cDNA level in directly sequenced RT–PCR products: an A→C single nucleotide polymorphism (SNP) at nucleotide position 892 (nucleotide 1 refers to the first nucleotide of the ATG start codon) resulted in a threonine to proline substitution at amino acid position 298 (T298P) in comparison with the genomic BAC sequence, a silent A→G SNP at nucleotide 2214 and an A→G SNP at nucleotide 2264 exchanging glycine for glutamic acid at amino acid position 755 (E755G). Analysis of the expressed sequence tag database (dbEST) identified only few matching human cDNA sequences, mainly from

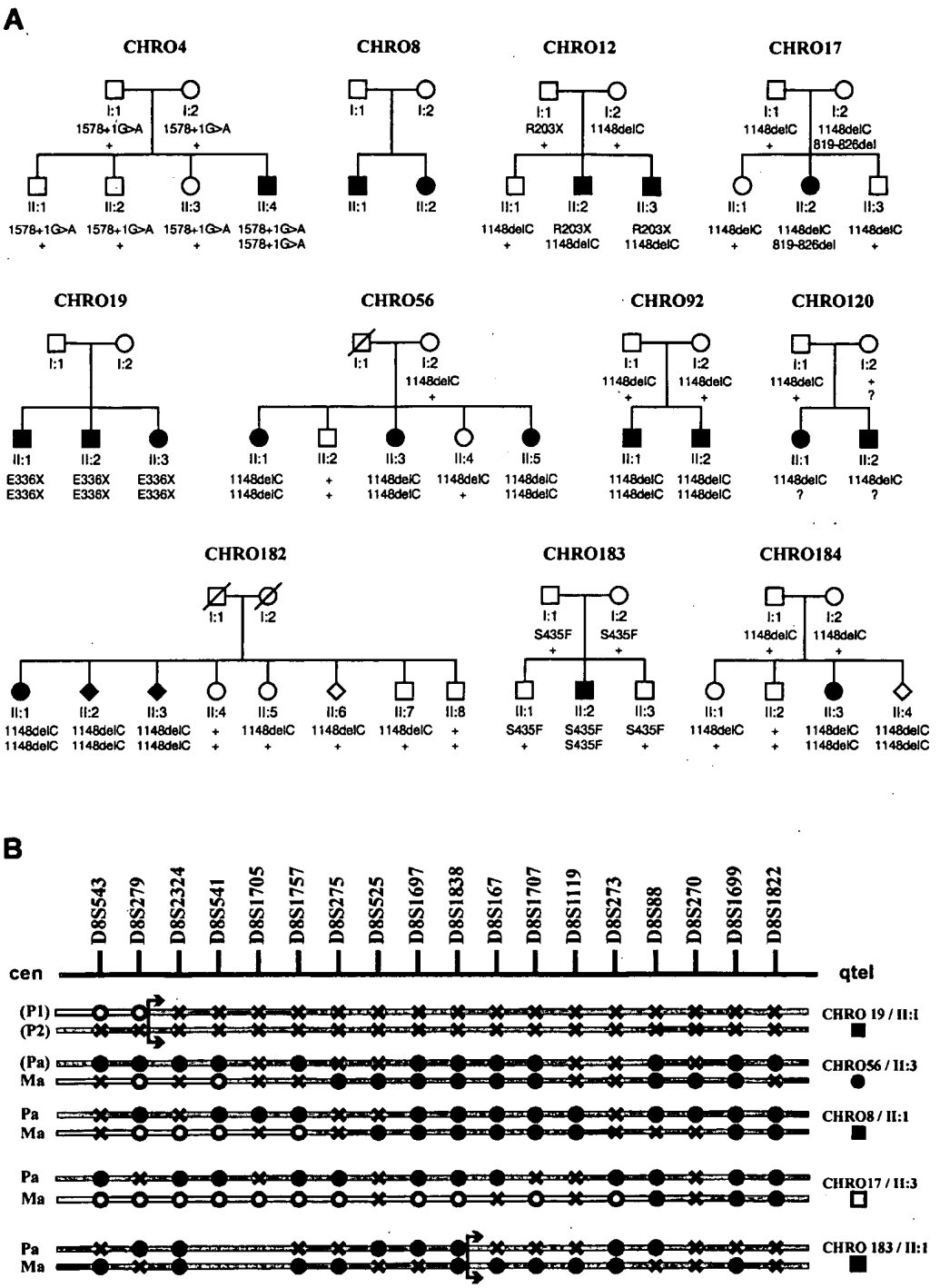

Figure 1. Pedigrees of achromatopsia patients analysed in this study and refined genetic mapping of the *ACHM3* locus. (**A**) Pedigrees of the 11 *ACHM3*-linked achromatopsia families investigated. Segregation of *CNGB3* mutations for available family members is indicated: +, wild-type allele; ?, an as yet unidentified mutation (see text). (**B**) Schematic summary of refined genetic mapping results. Shaded bars represent disease-associated sections, and clear bars recombinant normal sections of chromosome 8q for four affected patients and one unaffected sibling (pedigree identifier and status symbol given on the right) as reconstructed from genotyping of ordered markers from centromere to telomere (top line). The maternal (Ma) and paternal (Pa) origin of the inherited chromosomes is indicated on the left. P1 and P2 indicate unresolved parental origin (both parents not available), and parentheses indicate parental haplotypes reconstructed from the offspring. On the haplotype bars, solid circles represent disease-associated marker alleles, open circles non-disease-associated alleles, and crosses non-informative marker alleles. Sections distal to the arrowheaded brackets represent regions of marker homozygosity in pedigrees CHRO19 and CHRO183.

pineal gland, which cluster in three separate Unigene entries (Hs.114100, Hs.154433 and Hs.180136).

The deduced human CNGB3 polypeptide is 115 amino acids longer than the murine counterpart due to a C-terminal extension. Its molecular mass was calculated as 92.2 kDa and it contains a high proportion of hydrophobic amino acids typical for membrane proteins. Functional domains including transmembrane helices and the cGMP-binding domain are highly

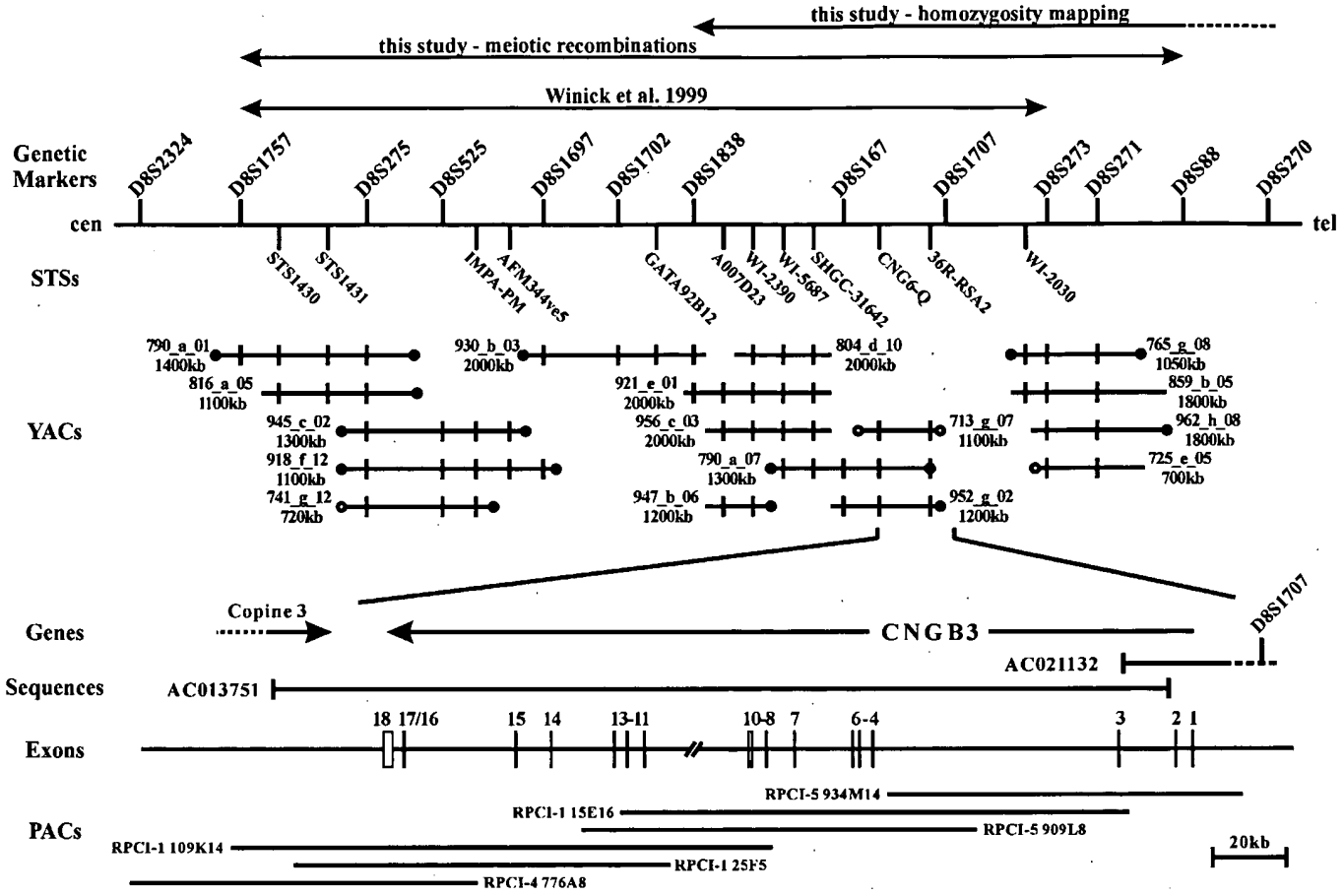

Figure 2. Physical mapping of the *ACHM3* region and location and structure of the *CNGB3* gene. From top to bottom: genetic mapping intervals reported by Winick *et al.* (4) and those found in this study. Below is given the order of genetic markers and STSs used to generate the physical map of the *ACHM3* region. Two non-overlapping YAC contigs were constructed based on STS content mapping. Vertical lines on the individual YAC bars indicate the presence of the respective marker or STS given above. YAC sizes as determined by PFGE are given below the individual YAC address. Filled circles represent YAC end sequences matching various chromosome 8 database sequences by BLAST analysis, and open circles represent end sequences with matches to sequences located on other chromosomes. Below is given an enlarged view of the *CNGB3* region. The *CNGB3* gene is orientated in telomere to centromere direction, and terminal parts of the *Copine 3* gene were found in opposite orientation distal to *CNGB3*. Two HTGS phase sequences AC013751 and AC021132 cover the *CNGB3* region including all exons (1–18) of the *CNGB3* gene. Contigs within the HTGS phase sequences were ordered and experimentally verified by additional PAC clones (bottom).

conserved and display 82% identity at the amino acid sequence level between human and mouse (Fig. 3). Neither the murine *cng6* nor the orthologous human *CNGB3* gene encode sequences similar to the glutamic acid-rich segment (GARP) of the rod cGMP-gated channel β-subunit which is involved in the structural organization of the phototransduction components in rod photoreceptors (11) (Fig. 3).

Northern blot analysis showed a major transcript of ~4.4 kb in human retina (Fig. 4). In addition, much less abundant transcripts of ~3.6 and 3.0 kb were detected after longer exposures. Northern blot and multiple tissue dot-blot hybridizations (data not shown) demonstrated that *CNGB3* transcripts are expressed specifically in the retina. Only after long exposure were some faint signals observed in RNA from testis and the WERI-Rb1 retinoblastoma cell line (data not shown).

Comparison of the cDNA with the genomic sequence (HTGS BAC sequences AC013751 and AC021132) showed that the human *CNGB3* gene is encoded by 18 exons covering ~200 kb of genomic sequence (Fig. 2 and Table 1). Exons 1 and 2 are present on AC021132, whereas the remaining 16 exons are located in AC013751. AC021132 and AC013751 overlap by ~15 kb of non-coding sequence between exons 2 and 3. Links between the unordered sequence pieces in the HTGS entries and the sizes of all but one non-contiguously covered intron sequence were obtained by PCR mapping of individual exons and linking PCR amplification with DNA from additional phage P1-derived artificial chromosomes (PACs) isolated for the *CNGB3* gene (Fig. 2, bottom). The exon sizes of the *CNGB3* gene range between 51 and 2197 bp for the 3′-terminal exon. Exon–intron boundaries show typical sequence features and follow the GT–AG rule, except the splice donor downstream of exon 13 which presents a GC instead of GT (Table 1). In a few instances, the presence of a GC dinucleotide at the 5′ end of an intron has been described (12).

The *CNGB3* gene is orientated in telomere to centromere direction. Downstream of the *CNGB3* gene we could identify eight terminal exons of the *Copine 3* gene also present on AC013751. *CNGB3* and *Copine 3* are arranged in tail-to-tail

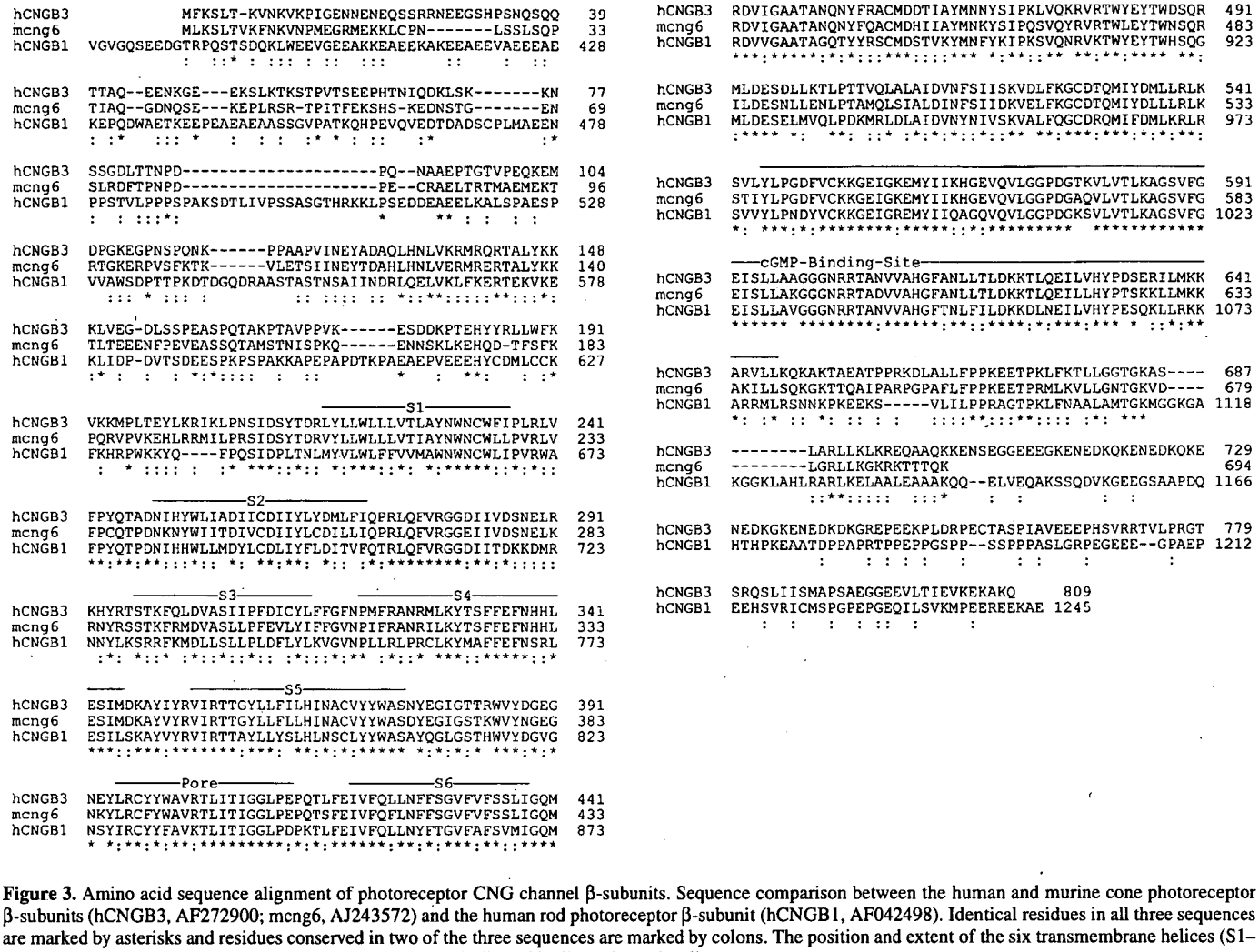

Figure 3. Amino acid sequence alignment of photoreceptor CNG channel β-subunits. Sequence comparison between the human and murine cone photoreceptor β-subunits (hCNGB3, AF272900; mcng6, AJ243572) and the human rod photoreceptor β-subunit (hCNGB1, AF042498). Identical residues in all three sequences are marked by asterisks and residues conserved in two of the three sequences are marked by colons. The position and extent of the six transmembrane helices (S1–S6), the pore and the cyclic nucleotide-binding domain are indicated by lines above the alignment.

configuration and their 3′ ends are separated by ~12.5 kb of genomic sequence (Fig. 2).

Mutations in the *CNGB3* gene in patients with achromatopsia

We then screened the *CNGB3* gene in patients from our 11 *ACHM3*-linked families by direct sequencing of PCR products obtained from amplification of exon segments with primers located in flanking intron or UTR sequences. We identified six different mutations including a missense mutation (1304C→T, S435F), two stop codon mutations (607C→T, R203X and 1006G→T, E336X), two frameshift deletions of 1 and 8 bp (1148delC and 819–826del), respectively, and a putative splice site mutation between exons 13 and 14 (1578+1G→A) (Table 2). Sequence examples of these mutations are outlined in Figure 5. Mutations were found in all *ACHM3*-linked families except CHRO8, and only a single heterozygous mutation was identified in patient II:1 of family CHRO120. Homozygous mutations were present in seven cases, including those in which marker homozygosity intervals were defined initially (Fig. 1). Interestingly, we found the 1 bp deletion mutation (1148delC) recurrently in several patients of different geographic origin. Patients in families CHRO56, CHRO92, CHRO182 and CHRO184 were homozygous for this mutation, and patients in families CHRO12, CHRO17 and CHRO120 harbour this mutation on one of the two disease chromosomes. Patient II:4 in family CHRO4 carried a homozygous G→A substitution at the first nucleotide of intron 13. Thus, the splice donor sequence of this intron is changed from GC to AC. This substitution probably abolishes effective splicing between exons 13 and 14 and thus leads to premature translation termination. Numerous examples of aberrant splicing in cases of G→A substitutions at the first nucleotide position of an intron have been described in the literature (13).

Co-segregation analysis by PCR/restriction fragment length polymorphism (RFLP) or single strand conformation polymorphism (SSCP) was performed in all families and was found to be consistent with the autosomal recessive mode of inheritance in all cases. Moreover, it proved the independent segregation of the mutant alleles (Fig. 6). None of the mutations were found in 100 healthy controls.

The S435F mutation was found to be homozygous in patient II:2 in family CHRO183, originating from the South Pacific

Table 1. Exons and exon–intron boundary sequences of the *CNGB3* gene

Exon	Size (bp)	cDNA sequence[a]	Genomic sequence[b]	Splice acceptor[c]	Splice donor[c,d]
1	175	1–175	132 723–132 549		GCACAGgtatgt
2	82	176–257	128 786–128 705	tgtttttctcaaagGAAGAA	TACAAGgtcaga
3	127	258–384	131 176–131 302	attttttttcatagACAAAC	AAACAGgtgagc
4	155	385–539	186 738–186 892	ttttttctcatttagCCCACA	AAACTGgtaagc
5	150	540–689	189 668–189 817	tttttccctatgaagCAAAGC	ACACAGgtatta
6	209	690–898	190 703–190 911	ttgctgtttttccagATCGAC	ATAATAgtaagt
7	51	899–949	203 774–203 824	acaaatatctttcagGTGGAT	TTTCAGgtaggt
8	87	950–1036	12 801–12 715	gtgttctttcaacagTTGGAT	TTAAAGgtaaga
9	65	1037–1101	9600–9536	tgcttttctatatagTACACT	CTACAGgtaaag
10	123	1102–1224	8787–8665	tattctctctgacagAGTTAT	AAACGAgtaagt
11	142	1225–1366	35 475–35 616	cttctgttttcacagGTATCT	GGTCAGgtaagc
12	160	1367–1526	39 290–39 449	tatttgtggttttagATGAGA	TGCTAGgtaagc
13	98	1527–1624	42 289–42 386	tttatctttataaagATGAGT	TTCAAGgcaagt
14	84	1625–1708	56 699–56 782	tttctttttatatagGGTTGT	AAAAAGgtgagt
15	119	1709–1827	64 435–64 553	atatttaaaatgtagGGAGAA	AATCAGgtatct
16	147	1828–1974	89 394–89 540	ttttctctcttacagCCTTCT	AGCCAGgtacaa
17	175	1975–2149	89 783–89 957	ctctcttacccacagAGTGCT	GCTCAGgtaata
18	2197	2150–4346	92 517–94 712	aattgctccttccagAAGAAA	

[a]Sequence positions according to GenBank entry AF272900.
[b]Sequence positions within GenBank entries AC021132 (exons 1 and 2) and AC013751 (remaining exons).
[c]Exon sequences in upper case and intron sequences in lower case letters.
[d]The nucleotide mutated in family CHRO4 is underlined.

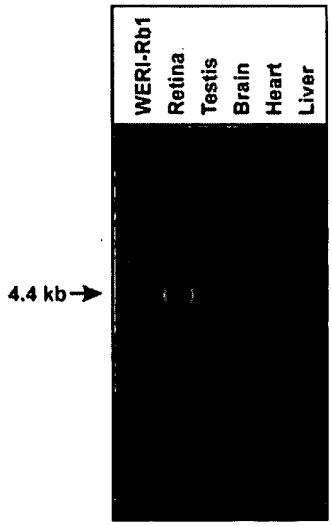

Figure 4. Expression of the human *CNGB3* gene. Northern blot hybridization with a *CNGB3* cDNA probe detected a major transcript of 4.4 kb in retinal RNA. Minor retinal transcripts of ~3.6 and 3.0 kb were detectable after prolonged exposures, as well as low levels of *CNGB3* transcripts in WERI-Rb1 and testis RNA samples (data not shown).

Table 2. *CNGB3* mutations in patients with achromatopsia

Location	Alteration in nucleotide sequence[a]	Alteration in polypeptide/mRNA[b]
Exon 5	607C→T	R203X
Exon 6	819–826del	P273fs
Exon 9	1006G→T	E366X
Exon 10	1148delC	T383fs
Exon 11	1304C→T	S435F
Intron 13	1578+1G→A	Splice defect

[a]Sequence position within the *CNGB3* cDNA (GenBank accession no. AF272900) with nucleotide 1 denoting the first nucleotide of the ATG start codon.
[b]fs, frameshift.

islander population known to exhibit a dramatically increased gene frequency for achromatopsia (14,15). The S435F mutation is located in transmembrane domain S6 and affects an amino acid position conserved between human and mouse and also conserved in the homologous sequence of the rod β-subunit. All other mutations result in a severely truncated polypetide lacking important functional elements, i.e. the pore or the cyclic nucleotide-binding domain, and thus most probably represent null alleles.

DISCUSSION

We have shown recently that mutations in the *CNGA3* gene, which encodes the α-subunit of the cone cGMP-gated channel, are responsible for achromatopsia linked to the *ACHM2* locus on

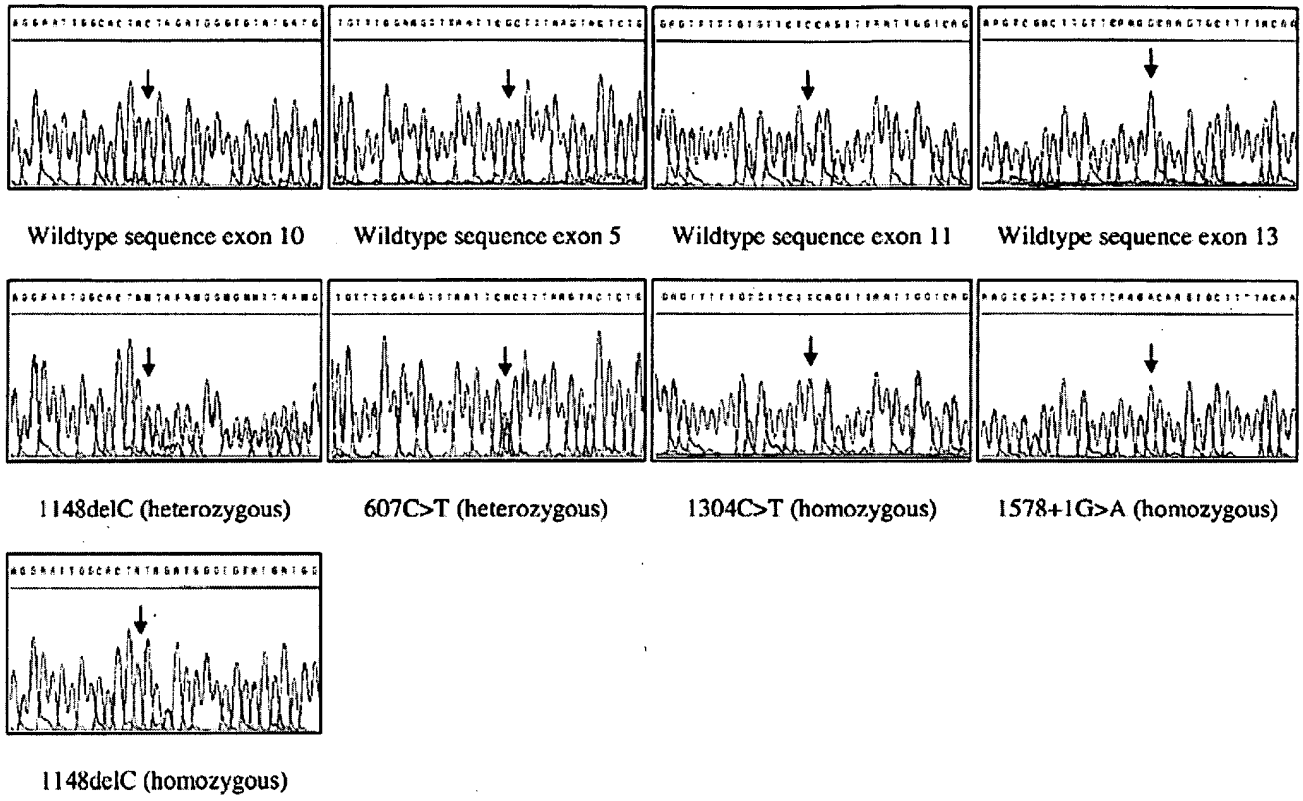

Figure 5. Identification of *CNGB3* mutations in achromatopsia patients. Electropherogram sections of selected heterozygous or homozygous mutant sequences (middle and bottom rows) in comparison with the respective wild-type sequence (top row). The nucleotides altered by the mutations are indicated by arrows.

chromosome 2q11 (2). In this study, we used a positional genomics approach to identify the second gene involved in achromatopsia, *CNGB3*, the gene defective in families linked to the *ACHM3* locus on chromosome 8q21.

Interestingly, *CNGB3* encodes the putative modulatory β-subunit of the cGMP-gated channel of cone photoreceptors. Gerstner *et al.* (10) recently have demonstrated for the mouse orthologue *cng6* that in co-expression experiments the *cng6* gene product modulates the biophysical and electrophysiological behaviour of the functional channel-forming α-subunit. It induces flickering channel gating, a decrease in outward rectification and sensitivity to the blocking agent L-*cis*-diltiazem, similar to native cone cyclic nucleotide-gated (CNG) channels (10).

It has been suggested that native CNG channels represent heterotetramers of two α- and β-subunits (16). In heterologous expression systems, the α-subunit *per se* is able to form functional cation channels (17). In contrast, the β-subunit alone cannot conduct measurable ion currents, although the secondary structure of the polypeptide is conserved between α- and β-subunits, and relevant functional domains (transmembrane helices, pore and cyclic nucleotide-binding domain) are also present in the β-subunit (18). Since mutations in either of the two genes give rise to a clinically indistinguishable phenotype of complete achromatopsia, it has to be assumed that the β-subunit confers some essential function to the native channel complex within the context of phototransduction.

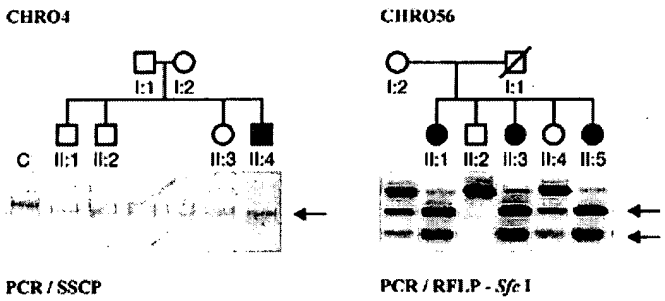

Figure 6. Segregation of *CNGB3* mutations within selected achromatopsia families. Gel lanes are mounted according to the respective subjects in the pedigrees above. The arrows indicate mutant-specific gel bands. (Left) SSCP separation of the 1578+1G→A splice site mutation in family CHRO4. Patient II:4 carries this mutation on both alleles, whereas all siblings and the parents are heterozygous carriers. Lane C, normal control. (Right) Segregation of the 1148delC mutation in family CHRO56 performed by PCR–RFLP analysis with *Sfc*I. All three affecteds are homozygous for this mutation, whereas the mother and sibling II:4 are heterozygous carriers and sibling II:2 does not carry the mutation.

Whereas mutations in the *CNGA3* and *CNGB3* genes cause achromatopsia, a congenital, stationary disorder of the cone photoreceptor system, mutations in the gene for the α-subunit homologue in rod photoreceptors have been shown to cause autosomal recessive retinitis pigmentosa, a progressive form of retinal dystrophy (19). No retinal disorder has yet been

associated with the gene encoding the β-subunit of the rod cGMP-gated channel.

We have identified mutations in the *CNGB3* gene in all but one of our *ACHM3*-linked achromatopsia families. No mutations could be identified in family CHRO8 and only a single heterozygous mutation was detected in family CHRO120. The simplest explanation for this is that these missing mutations are located in an as yet unidentified regulatory region of the *CNGB3* gene, i.e. the promoter region, or that some disease alleles constitute larger deletions unable to be detected by our screening strategy. However, due to the low statistical significance of linkage to the *ACHM3* locus in the individual family, we cannot exclude that achromatopsia in family CHRO8 is not caused by mutations in the *CNGB3* gene but by another gene defect.

The 1 bp deletion mutation, 1148delC, was found recurrently in our patient sample. In total, 11 of the 22 disease chromosomes carry this common mutation. Haplotype analysis based on linked microsatellite markers provided no significant evidence for a linkage disequilibrium among chromosomes carrying the 1148delC mutation (data not shown). Additional studies with a larger number of disease chromosomes and inclusion of closely spaced, robust markers (i.e. SNPs) will be necessary to address the question on the origin of this particular mutation. Another reason for its high frequency might be that this particular nucleotide position is prone to deletion and thus represents a mutational hot spot. Several other examples of disease genes with a high frequency of particular deletion mutations either due to a founder effect or recurrent new mutation have been described, i.e. *CFTR* (20), *GJB2* (21) and *USH2A* (22).

The *ACHM3* locus was mapped originally to chromosome 8q21 in pedigrees from a South Pacific islander population, in which achromatopsia is highly frequent and affects nearly 10% of the native population. Therefore, this conditon has also been acknowledged as Pingelapese blindness (OMIM 262300). It has been assumed that this >1000-fold increased incidence in comparison with the European population (23) results from genetic drift following a devastating typhoon in the 18th century killing most of the inhabitants. These instances have come to public attention through Oliver Sacks' book *The Island of the Colorblind* (14) and a recent BBC television documentary (24). Family CHRO183 investigated in this study originates from this particular population. Since we have identified a homozygous S435F mutation as the sole alteration in the *CNGB3* gene in this family, we argue that this particular mutation is the cause of Pingelapese blindness.

MATERIALS AND METHODS

Achromatopsia patients

Caucasian patients were enrolled at several clinical centres in Germany (Tübingen, Berlin), the USA (Ann Arbor, MI) and Italy (Palermo). The clinical diagnosis of achromatopsia was based on ophthalmological examination including ERG recordings, fundus examination, visual acuity and visual field testing, and standard colour vision analysis. In addition, this study included a family from a South Pacific islander population, in which achromatopsia is highly frequent (14,15).

Blood samples from patients and family members were collected after informed consent. Total genomic DNA was extracted from the blood samples according to standard procedures (25).

Marker analysis

Seventeen polymorphic STR markers spanning a region of ~20 cM on human chromosome 8q21 (6,7) were genotyped by means of PCR amplification with fluorescence-labelled primers and electrophoretic sizing on an ABI 373 DNA sequencer (PE Biosystems, Weiterstadt, Germany) as described previously (26).

Statistical methods and haplotype reconstruction

Two-point LOD scores were calculated using the LINKAGE program package (27). A disease allele frequency of 0.005 and a penetrance of 1.0 were taken for calculations. Marker allele frequencies were assumed to be equal. Haplotypes were reconstructed manually, minimizing the number of recombinations.

Isolation and analysis of YAC clones

Individual YAC clones positive for chromosome 8q21 STSs were obtained from the German Human Genome Resource Center (RZPD, Berlin, Germany) or Research Genetics (Huntsville, AL). In addition, DNA pools of the CEPH Mark I and Mark II YAC libraries were screened by PCR to identify additional clones for known and newly developed STSs. Preparation of total yeast DNA and agarose plugs for pulsed-field gel electrophoresis (PFGE) was performed as previously described (26) or following standard procedures (28). YAC sizes were determined by probing PFGE blots with ^{32}P-labelled human cot-1 DNA to visualize artificial chromosomes.

STS content mapping was done with 5 ng of total yeast DNA and PCRs limited to 25 thermal cycles.

Isolation of YAC sequences and STSs

YAC end sequences were isolated by established vectorette PCR methods (28). In addition, internal YAC sequences were obtained by Alu vectorette PCR: briefly, 200 ng of total yeast DNA was digested separately with *Alu*I, *Rsa*I, *Pvu*II, *Bsp*143I, *Bgl*II or *Bam*HI, and ligated with compatible double-stranded vectorettes. Vectorette libraries were subjected to PCR amplification with vectorette and Alu repeat primers; products were size selected and cloned with the TA Cloning System (Invitrogen, Groningen, The Netherlands). Purified plasmid DNA was then sequenced with standard pUC/M13 forward and reverse primers. The chromosomal origin of newly developed STSs was determined by PCR amplification using selected DNA samples (NA10156B, NA14064 and NA11619) of a chromosome 8 regional mapping panel (Coriell Institute, Camden, NJ).

PAC isolation and analysis

Human PAC clones from the RPCI 1,3-5 library were identified by screening high density clone filters (provided by the RZPD) with ^{32}P-labelled probes. PAC DNA was isolated by standard alkaline lysis methods. Insert sizes were determined by PFGE separation of *Not*I-digested PAC DNA. STS content

mapping was done with 500 pg of PAC DNA and PCRs restricted to 23 thermal cycles.

Northern blot and RNA dot-blot hybridization

A human multiple tissue dot-blot (no. 7775-1) and total RNA from human brain, testis and liver were purchased from Clontech (Heidelberg, Germany). In addition, total RNA was isolated from human donor retinae and the human retinoblastoma cell line WERI-Rb-1 using Trizol reagent (Life Technologies, Eggenstein, Germany). For northern blots, 6 μg of total RNA of each sample were separated on a 1% agarose gel containing 2.2 M formaldehyde and blotted onto a Hybond-N nylon membrane (Amersham Pharmacia, Freiburg, Germany).

A cDNA fragment encompassing nucleotides 1–2323 of the *CNGB3* cDNA was labelled with [α-^{32}P]dCTP using the NEBlot kit (New England Biolabs, Schwalbach, Germany) and used for hybridization in ExpHyb solution (Clontech) for 15 h at 65°C. The filter was washed twice in 1× SSC, 0.15% SDS at 40°C and 0.1× SSC, 0.15% SDS at 65–70°C. Blots were exposed against X-ray films for 24–96 h at –80°C with intensifying screens.

RACE and RT–PCR

A 5 μg aliquot of total human retinal RNA was reverse-transcribed into single-stranded cDNA with AMV reverse transcriptase and random 9mer oligonucleotide primers. Aliquots were used to amplify overlapping cDNA fragments of the human *CNGB3* gene. Primer sequences were derived from segments of the human HTGS sequence AC013751 which showed significant homology to the murine *cnga3* cDNA (10).

For 5′ RACE, 20 ng of Marathon-Ready Human Retinal cDNA (Clontech) were subjected to nested PCR amplifications with adaptor primers and primers derived from internal *CNGB3* cDNA sequences. For 3′ RACE, 1 μg of total human retinal RNA was reverse-transcribed with AMV reverse transcriptase and an oligo(dT) adaptor primer (RNA PCR kit; Takara, Shiga, Japan). First strand cDNA was then used for hemi-nested PCR amplifications with adaptor primers, and primers derived from internal *CNGB3* cDNA sequences. RACE products were purified by gel electrophoresis and sequenced directly.

Chromosomal mapping

The chromosomal localization of the *CNGB3* gene was analysed by PCR amplification of a genomic 298 bp fragment encompassing exon 5 with DNA samples of a monochromosomal hybrid mapping panel (NIGMS mapping panel no. 2; Coriell Institute).

Mutation screening and segregation analysis

Coding exon sequences were amplified from patients' genomic DNA with primers located in flanking intron and UTR sequences. PCR products were purified with Qiaquick columns (Qiagen, Hilden, Germany), sequenced using Big Dye Terminator chemistry (PE Biosystems) and separated on an ABI 377 DNA sequencer. Sequence editing and alignments was performed using the Lasergene Software package (DNASTAR, Madison, WI).

Co-segregation analysis and screening of controls were performed by either sequencing, PCR–RFLP analysis (1148delC, gain of an *Sfc*I site; 1304C→T/S435F, loss of a *Bsr*I site) or PCR–SSCP analysis (607C→T/R203X, 819–826del, 1006G→T/E336X and the 1578+1G→A splice site mutation). For SSCP analysis, 10% polyacrylamide gels (acrylamide:bis-acrylamide 37.5:1) containing 10% glycerol were run with 1× TBE for 20 h at 4°C and visualized by silver staining.

Databases and database analysis

BLAST searches against nr, dbSTS, dbEST, GSS and HTGS segments of GenBank were done at the NCBI server (http://www.ncbi.nlm.nih.gov//). Re-analysis of deposited BAC and PAC sequences was done with the NIX package provided by the UK-HGMP service (Hinxton, UK).

Primer sequences

Primer sequences used for STS mapping, RACE, RT–PCR and amplification of *CNGB3* sequences are available from the authors on request.

NOTE ADDED IN PROOF

After acceptance of this paper, Sundin *et al.* reported the independent identification of the *CNGB3* gene and mutations therein in patients with achromatopsia [Sundin *et al.* (2000) *Nature Genet.*, **25**, 289–293]. Due to their limited cDNA sequence information mutations in the paper by Sundin *et al.* could be assigned only provisionally. The reported mutations Pro160 (8 bp del), Thr270 (1 bp del) and Ser322Phe correspond to the mutations 819–826del (Pro273fs), 1148delC (Thr383fs) and 1304C→T (Ser435Phe), respectively, described in this study (Table 2).

ACKNOWLEDGEMENTS

We thank all patients and family members for participating in this study. In addition, we kindly acknowledge contributions by Bernhard Jurklies, Samuel Jacobson, Günter Rudolph, Sten Andreasson, Thomas Rosenberg, Dorit Lev, Frans Cremers, Birgit Lorenz, Claudio Castellan, Pierre Bitoun, E.C. Sener, S. Tatlipinar and Nurten Akarsu for the collection of achromatopsia families during the course of this research project. Francis Futterman provided much valuable information on achromatopsia and helped with logistic coordinations. We also thank Eva Weber and Sabine Tippmann for excellent technical assistance, and Benjamin Kaupp and Dimitri Tränker for encouraging discussions. We kindly acknowledge the provision of filters and clones by the Resource Center of the German Human Genome Project (RZPD, Berlin) and the availability of bioinformatics services at the UK-HGMP (Hinxton, UK). This work was supported by grants IB2 and Q1 from the Bundesministerium für Bildung und Forschung (01 KS 9602) and the Interdisziplinäres Zentrum für Klinische Forschung (IZKF) Tübingen to L.T.S. and B.W. and a grant from the Deutsche Forschungsgemeinschaft (SFB430/A5) to B.W.

REFERENCES

1. Sharpe, L.T. and Nordby, K. (1990) Total colour blindness: an introduction. In Hess, R.F., Sharpe, L.T. and Nordby, K. (eds), *Night Vision: Basic, Clinical and Applied Aspects*. Cambridge University Press, Cambridge, UK.
2. Kohl, S., Marx, T., Giddings, I., Jägle, H., Jacobson, S., Apfelstedt-Sylla, E., Zrenner, E., Sharpe, L.T.S. and Wissinger, B. (1998) Total colour-blindness is caused by mutations in the gene encoding the α-subunit of the cone photoreceptor cGMP gated cation channel. *Nature Genet.*, **19**, 257–259.
3. Biel, M., Seeliger, M., Pfeifer, A., Kohler, K., Gerstner, A., Ludwig, A., Jaissle, G., Fauser, S., Zrenner, E. and Hofmann, F. (1999) Selective loss of cone function in mice lacking the cyclic nucleotide-gated channel CNG3. *Proc. Natl Acad. Sci. USA*, **96**, 7553–7557.
4. Winick, J.D., Blundell, M.L., Galke, B.L., Salam, A.A., Leal., S.M. and Karayiorgou, M. (1999) Homozygosity mapping of the achromatopsia locus in the Pingelapese. *Am. J. Hum. Genet.*, **64**, 1679–1685.
5. Milunsky, A., Huang, X.L., Milunsky, J., DeStefano, A. and Baldwin, C.T. (1999) A locus for autosomal recessive achromatopsia on human chromosome 8q. *Clin. Genet.*, **56**, 82–85.
6. Dib, C., Faure, S., Fizames, C., Samson, D., Drouot, N., Vignal, A., Millasseau, P., Marc, S., Hazan, J., Seboun, E. *et al.* (1996) Comprehensive genetic map of the human genome based on 5,264 microsatellites. *Nature*, **380**, 152–154.
7. Broman, K.W., Murray, J.C., Sheffield, V.C., White, R.L. and Weber, J.L. (1998) Comprehensive human genetic maps: individual and sex-specific variation in recombination. *Am. J. Hum. Genet.*, **63**, 861–689.
8. Hudson, T.J., Stein, L.D., Gerety, S.S., Ma, J., Castle, A.B., Silva, J., Slonim, D.K., Baptista, R., Kruglyak, L., Xu, S.H. *et al.* (1995) An STS-based map of the human genome. *Science*, **270**, 1919–1920.
9. Schuler, G.D., Boguski, M.S., Stewart, E.A., Stein, L.D., Gyapay, G., Rice, K., White, R.E., Rodriguez-Tome, P., Aggarwal, A., Bajorek, E. *et al.* (1996) A gene map of the human genome. *Science*, **274**, 540–546.
10. Gerstner, A., Zong, X., Hofmann, F. and Biel, M. (2000) Molecular cloning and functional characterization of a new modulatory cyclic nucleotide-gated channel subunit from mouse retina. *J. Neurosci.*, **20**, 1324–1332.
11. Körschen, H.G., Beyermann, M., Müller, F., Heck, M., Vantler, M., Koch, K.W., Kellner, R., Wolfrum, U., Bode, C., Hofmann, K.P. and Kaupp, U.B. (1999) Interaction of glutamic-acid-rich proteins with the cGMP signalling pathway in rod photoreceptors. *Nature*, **400**, 761–766.
12. Jackson, I.J. (1991) A reappraisal of non-consensus mRNA splice sites. *Nucleic Acids Res.*, **19**, 3795–3798.
13. Krawczak, M., Reiss, J. and Cooper, D.N. (1992) The mutational spectrum of single base-pair substitutions in mRNA splice junctions of human genes: causes and consequences. *Hum. Genet.*, **90**, 41–54.
14. Sacks, O. (1998) *The Island of the Colorblind*. Vintage Books, Random House, New York, NY.
15. Brody, J.A., Hussels, I., Brink, E. and Torres, J. (1970) Hereditary blindness among Pingelapese people of eastern Caroline Islands. *Lancet*, **1**, 1253–1257.
16. Zagotta, W. and Siegelbaum, S.A. (1996) Structure and function of cyclic nucleotide-gated channels. *Annu. Rev. Neurosci.*, **19**, 235–263.
17. Wissinger, B., Müller, F., Weyand, I., Schuffenhauer, S., Thanos, S., Kaupp, U.B. and Zrenner, E. (1997) Cloning, chromosomal localization and functional expression of the gene encoding the α-subunit of the cGMP-gated channel in human cone photoreceptors. *Eur. J. Neurosci.*, **9**, 2512–2521.
18. Chen, T.Y., Peng, Y.W., Dhallan, R.S., Ahamed, B., Reed, R.R. and Yau, K.W. (1993) A new subunit of the cyclic nucleotide-gated cation channel in retinal rods. *Nature*, **362**, 764–767.
19. Dryja, T.P., Finn, J.T., Peng, Y.W., McGee, T.L., Berson, E.L. and Yau, K.W. (1995) Mutations in the gene encoding the α-subunit of the rod cGMP-gated channel in autosomal recessive retinitis pigmentosa. *Proc. Natl Acad. Sci. USA*, **91**, 10177–10181.
20. Kerem, B.-S., Rommens, J.M., Buchanan, J.A., Markiewicz, D., Cox, T.K., Chakravarti, A., Buchwald, M. and Tsui, L.-C. (1989) Identification of the cystic fibrosis gene: genetic analysis. *Science*, **245**, 1073–1080.
21. Denoyelle, F., Weil, D., Maw, M.A., Wilcox, S.A., Lench, N.J., AllenPowell, D.R., Osborn, A.H., Dahl, H.H.M., Middleton, A., Houseman, M.J. *et al.* (1997) Prelingual deafness: high prevalence of a 30delG mutation in the connexin 26 gene. *Hum. Mol. Genet.*, **6**, 2173–2177.
22. Eudy, J.D., Weston, W.D., Yao, S., Hoover, D.M., Rehm, H.L., Ma-Edmonds, M., Yan, D. *et al.* (1998) Mutation of a gene encoding a protein with extracellular matrix motif in Usher syndrome type IIa. *Science*, **280**, 1753–1757.
23. Judd, D.B. (1943) Facts of color-blindness. *J. Opt. Soc. Am.*, **33**, 294–307.
24. Rawlence, C. and Crichton-Miller, E. (1996) The island of the colour blind. In Rawlence, C. and Crichton-Miller, E. (prods), *The Mind Traveller*. Television documentary series, Rosetta Pictures, London, UK.
25. Miller, S.A., Dykes, D.D. and Polesky, H.F. (1988). A simple salting out procedure for extracting DNA from human nucleated cells. *Nucleic Acids Res.*, **16**, 1215.
26. Wissinger, B., Jägle, H., Kohl, S., Broghammer, M., Baumann, B., Hanna, D.B., Hedels, C., Apfelstedt-Sylla, E., Randazzo, G., Jacobson, S.G. *et al.* (1998). Human rod monochromacy: linkage analysis and mapping of a cone photoreceptor expressed candidate gene on chromosome 2q11. *Genomics*, **51**, 325–331.
27. Ott, J. (1991) *Analysis of Human Genetic Linkage*. Johns Hopkins University Press, Baltimore, MD.
28. Green, E.D., Hieter, P. and Spencer, F.A. (1999) Yeast artificial chromosomes. In Birren, B., Green, E.D., Klapholz, S., Myers, R.M., Riethman, H. and Roskams, J. (eds), *Genome Analysis: A Laboratory Manual*, Vol. 3. Cold Spring Harbor Laboratory Press, Cold Spring Harbor, NY, pp. 297–565.

THE JOURNAL OF BIOLOGICAL CHEMISTRY
Vol. 278, No. 27, Issue of July 4, pp. 24617–24623, 2003
Printed in U.S.A.

Functionally Important Calmodulin-binding Sites in Both NH_2- and COOH-terminal Regions of the Cone Photoreceptor Cyclic Nucleotide-gated Channel CNGB3 Subunit*

Received for publication, February 19, 2003, and in revised form, April 23, 2003
Published, JBC Papers in Press, May 1, 2003, DOI 10.1074/jbc.M301699200

Changhong Peng‡, Elizabeth D. Rich‡, Christopher A. Thor‡, and Michael D. Varnum‡§¶

From the ‡Department of Veterinary and Comparative Anatomy, Pharmacology and Physiology, §Program in Neuroscience, Washington State University, Pullman, Washington 99164-6520

Whereas an important aspect of sensory adaptation in rod photoreceptors and olfactory receptor neurons is thought to be the regulation of cyclic nucleotide-gated (CNG) channel activity by calcium-calmodulin (Ca^{2+}-CaM), it is not clear that cone photoreceptor CNG channels are similarly modulated. Cone CNG channels are composed of at least two different subunit types, CNGA3 and CNGB3. We have investigated whether calmodulin modulates the activity of these channels by direct binding to the CNGB3 subunit. Heteromeric channels were formed by co-expression of human CNGB3 with human CNGA3 subunits in *Xenopus* oocytes; CNGB3 subunits conferred sensitivity to regulation by Ca^{2+}-CaM, whereas CaM regulation of homomeric CNGA3 channels was not detected. To explore the mechanism underlying this regulation, we localized potential CaM-binding sites in both NH_2- and COOH-terminal cytoplasmic domains of CNGB3 using gel-overlay and glutathione *S*-transferase pull-down assays. For both sites, binding of CaM depended on the presence of Ca^{2+}. Individual deletions of either CaM-binding site in CNGB3 generated channels that remained sensitive to regulation by Ca^{2+}-CaM, but deletion of both together resulted in heteromeric channels that were not modulated. Thus, both NH_2- and COOH-terminal CaM-binding sites in CNGB3 are functionally important for regulation of recombinant cone CNG channels. These studies suggest a potential role for direct binding and unbinding of Ca^{2+}-CaM to human CNGB3 during cone photoreceptor adaptation and recovery.

Cyclic nucleotide-gated (CNG)[1] channels play a fundamental role in both visual and olfactory transduction by helping to convert sensory input into electrical responses that are ultimately processed as sensory information (1). In mammals, at least six genes encode CNG channel subunits (2, 3). Native CNG channels are tetrameric proteins (4, 5) composed of at least two structurally related subunit types, α (CNGA1, CNGA2, CNGA3, and CNGA4) and β (CNGB1 and CNGB3). Each subunit contains six putative transmembrane domains, cytoplasmic NH_2 and COOH termini, a cyclic nucleotide-binding domain, and a conserved pore region (1, 6). Whereas heterologous expression of α subunits alone (except CNGA4) forms functional homomeric channels, the co-assembly of appropriate α and β subunits creates heteromeric CNG channels with properties that more closely resemble native CNG channels (7–12).

CNG channels are highly permeable to Ca^{2+}, and Ca^{2+} entry through CNG channels provides a negative feedback signal that assists in adaptation and recovery in photoreceptors and olfactory sensory neurons (13–15). Calmodulin (CaM) is thought to participate in these processes by binding Ca^{2+} and then targeting to different cellular components including CNG channels (16). Numerous studies have described Ca^{2+}-CaM regulation of the ligand sensitivity of rod and olfactory CNG channels (17–25). Olfactory CNG channels are composed of CNGA2 (26), CNGA4 (8, 9), and CNGB1b subunits (10, 11); Ca^{2+}-CaM modulates olfactory channel activity via direct binding to NH_2-terminal CaM-binding sites of CNGA2 (20) (and probably CNGB1b) subunits, whereas the presence of CNGA4 and CNGB1b subunits tunes the kinetics of the response to CaM (27, 28). Rod CNG channels contain CNGA1 (29) and CNGB1 (7) subunits. For these channels, Ca^{2+}-CaM modulation is comparatively weaker, and the CNGB1 subunit provides the CaM-binding site in the NH_2-terminal cytoplasmic domain that is critical for regulation (30–32).

For cone CNG channels, Ca^{2+}-feedback mechanisms are less well defined. Ca^{2+}-dependent regulation of apparent cGMP affinity is robust for native striped bass cone CNG channels and is thought to be of greater significance for cone photoreceptor adaptation than the corresponding changes in rods (33–35). Application of CaM to patches excised from cone outer segments inhibits these channels, but CaM only partially mimics the activity of an endogenous modulator(s) (33, 34). In contrast, CaM has no effect on CNG channels in patches excised from catfish cone outer segments (36). Recombinant homomeric CNG channels composed of chick cone CNGA3 subunits are modulated by Ca^{2+}-CaM (37). However, homomeric channels formed by the human or bovine orthologs of CNGA3 are insensitive to CaM regulation, even though these subunits possess an NH_2-terminal CaM-binding site (38–40). Thus, there appear to be species differences in sensitivity to regulation by Ca^{2+}-CaM both for native cone photoreceptor CNG channels and for heterologously expressed homomeric CNGA3 channels. With recent cloning of the cone photoreceptor β subunit (CNGB3) for mice (12) and humans (41, 42), the importance of this subunit for modulation of cone CNG channels by Ca^{2+}-CaM can now be examined.

In this study, we demonstrate that the human CNGB3 (hCNGB3) subunit forms functional heteromeric channels with human CNGA3 (hCNGA3) when co-expressed in *Xenopus* oo-

* This work was supported by National Eye Institute Grant EY12836 and the Adler Foundation (to M. D. V.). The costs of publication of this article were defrayed in part by the payment of page charges. This article must therefore be hereby marked "*advertisement*" in accordance with 18 U.S.C. Section 1734 solely to indicate this fact.

¶ To whom correspondence should be addressed. Tel.: 509-335-0701; Fax: 509-335-4650; E-mail: varnum@wsu.edu.

[1] The abbreviations used are: CNG, cyclic nucleotide-gated; CNB, cyclic nucleotide-binding; hCaM, human calmodulin; GST, glutathione *S*-transferase; N, amino; C, carboxyl; CHAPS, 3-[(3-cholamidopropyl)-dimethylammonio]-1-propanesulfonic acid.

cytes. These recombinant heteromeric channels exhibited electrophysiological properties that differed from those of homomeric hCNGA3 channels, including sensitivity to regulation by Ca^{2+}-CaM. Human CNGB3 plus CNGA3 heteromeric channels are shown to be unique compared with other CNG channel types, in that CaM regulation involves functionally important CaM-binding sites in both the NH_2- and COOH-terminal cytoplasmic domains of hCNGB3.

EXPERIMENTAL PROCEDURES

Molecular Biology—The human retinal cone CNG channel β subunit clone, hCNGB3-c22, was isolated using nested PCR from human retinal cDNA (Marathon Ready cDNA; Clontech) with adapter- and gene-specific primers. The coding region for this clone differs from the complete published sequence for human CNGB3 of Kohl *et al.* (AF272900) (42) at two positions (nucleotides 1743 G → A and nucleotides 1788 A → G); these likely sequence polymorphisms do not alter the encoded amino acid sequence. Human CNGA3 (AF065314) (38, 43) was a generous gift of Professor K.-W. Yau. Both hCNGB3 and hCNGA3 were subcloned into pGEMHE (44) for heterologous expression in *Xenopus* oocytes. A human calmodulin cDNA clone (hCaM) was also isolated from human retinal cDNA using nested PCR with gene-specific primers. hCaM was modified to include a FLAG epitope (DYKDDDDK) at the COOH terminus and subcloned in-frame with polyhistidine at the NH_2 terminus (pQE-30; Qiagen, Valencia, CA). Constructs for polypeptides representing NH_2- and COOH-terminal cytoplasmic domains of hCNGA3 (amino acids 1–164 and 400–694, respectively) and hCNGB3 (amino acids 1–214 and 441–809, respectively) were generated as in-frame gene fusions with GST (pGEX-5X-2; Amersham Biosciences) using PCR. Deletions were engineered by overlapping PCR, or by restriction digestion followed by blunt end generation using T4 DNA polymerase (New England Biolabs, Beverly, MA) and in-frame ligation. All mutations and the fidelity of PCR-amplified cassettes were confirmed by fluorescence-based automated DNA sequencing.

CaM Interaction Assays—Recombinant protein expression in bacteria and purification were carried out as previously described (25). Briefly, cells were harvested and resuspended in buffer S (50 mM Tris-HCl (pH 7.8), 150 mM NaCl, 25 mM imidazole, 1% NDSB (Calbiochem, San Diego, CA), 0.5% CHAPS, and 0.25% Tween 20) containing protease inhibitors (Roche Applied Science), then lysed using a French pressure cell (SLM Instruments, Rochester, NY) or sonication. Soluble proteins were isolated by centrifugation at 20,000 × *g* and 4 °C for 30 min. GST fusion proteins were purified using glutathione-Sepharose beads (Amersham Biosciences); His-tagged CaM was purified using Ni^{2+}-charged Sepharose (Probond resin; Invitrogen), eluted with 0.5 M imidazole (pH 6.0), and then dialyzed with buffer S. GST pull-down assays were performed using immobilized GST fusion proteins and 2 μM recombinant hCaM-FLAG, in the presence of 2 mM Ca^{2+} or 10 mM EDTA. Pull-down assays were incubated overnight in buffer S at 4 °C with rocking. Beads were centrifuged for 2 min at 700 × *g*, washed 5 times in 100 μl of buffer S (including either Ca^{2+} or EDTA), and suspended in SDS-PAGE sample buffer containing 2-mercaptoethanol. Bound proteins were separated using 12 or 4–20% SDS-PAGE and transferred to nitrocellulose. Gel overlay assays were performed using similarly blotted GST fusion proteins with 1 μg/ml hCaM-FLAG in 20 mM Tris (pH 7.5), 0.15 M NaCl, 0.1% Tween 20, 1% milk, and either 1 mM Ca^{2+} or 5 mM EDTA (maintained throughout the assay and blot processing). For both assays, interacting hCaM-FLAG was visualized using M2 monoclonal antibody (Eastman Kodak) directed against the FLAG epitope and a chemiluminescent detection system (SuperSignal West Dura Extended Duration Substrate; Pierce). Interaction assays were repeated at least 3 times with reproducible results. CaM-binding site search and analysis was performed using the Calmodulin Target database of M. Ikura and co-workers.[2]

Electrophysiology—For functional expression of hCNGA3 and hCNGB3, *Xenopus laevis* oocytes were isolated and microinjected with 5–10 ng of *in vitro* transcribed mRNA (mMessage mMachine; Ambion, Austin, TX) as previously described (45). The ratio of hCNGA3 to hCNGB3 cRNA was 1:5. Two to 7 days after microinjection of mRNA into oocytes, patch clamp experiments were performed with an Axopatch 200B patch clamp amplifier (Axon Instruments, Foster City, CA) in the inside-out configuration. Initial pipette resistances were 0.45–0.75 megohm. Currents were low-pass filtered at 2 kHz and sampled at 10 kHz. Intracellular and extracellular solutions contained 130 mM NaCl, 0.2 mM EDTA, and 3 mM HEPES (pH 7.2). Cyclic nucleotides were added to intracellular solutions as indicated. Intracellular solutions were changed using an RSC-160 rapid solution changer (Molecular Kinetics, Pullman, WA). Currents in the absence of cyclic nucleotide were subtracted. Recordings were made at 20 to 22 °C. For electrophysiological experiments involving CaM, bovine CaM (Calbiochem, San Diego, CA) was used at 250 nM. EDTA was substituted by 2 mM nitrilotriacetic acid and 704 μM $CaCl_2$ for 50 μM buffered free Ca^{2+} in the intracellular solution. Excised patches were first exposed to 5 mM EDTA for 2–10 min to remove soluble, endogenous Ca^{2+}-dependent modulators. In addition, any changes because of Ca^{2+} alone were permitted to occur before CaM was applied (10–40 min). After CaM experiments, the channels were typically tested for sensitivity to L-*cis*-diltiazem (RBI, Natick, MA) applied in the intracellular solution to verify the subunit composition of the channel, *i.e.* whether hCNGB3 and deletion constructs of hCNGB3 participated in the formation of the expressed channels. Dose-response relationships were obtained by plotting the current as a function of cyclic nucleotide concentration. Dose-response data were fitted to the Hill equation, $I/I_{max} = ([cNMP]^n/(K_{1/2}^n + [cNMP]^n))$, where I is the current amplitude, I_{max} is the maximum current, [cNMP] is the ligand concentration, $K_{1/2}$ is the apparent affinity for ligand, and n is the Hill slope. For current inhibition by L-*cis*-diltiazem, data were fit to the Hill equation in the form: $I_{diltiazem}/I = (K_{1/2}^n/(K_{1/2}^n + [diltiazem]^n))$. Data were acquired using Pulse (HEKA Elektronik, Lambrecht, Germany), and analyzed using Igor Pro (Wavemetrics, Lake Oswego, OR) and SigmaPlot (SPSS, Chicago, IL). The data were expressed as mean ± S.D. unless otherwise indicated. Statistical significance was determined using a Mann-Whitney rank sum or Student's t test (SigmaStat; SPSS), and a p value of <0.05 was considered significant.

RESULTS

The Properties of Heteromeric CNG Channels Containing hCNGB3 Subunits Differ from Homomeric hCNGA3 Channels—To examine the potential functional significance of the human CNGB3 subunit, hCNGB3 was co-expressed with hCNGA3 in *Xenopus* oocytes and macroscopic cGMP- and cAMP-activated currents were recorded from excised, inside-out membrane patches. As expected, hCNGB3 did not form functional CNG channels when expressed alone (data not shown). Co-expression of hCNGB3 and hCNGA3 generated recombinant heteromeric channels that demonstrated dramatically altered functional properties compared with homomeric hCNGA3 channels (Fig. 1, Table I). First, the fractional activation of the channels by a saturating concentration of cAMP compared with saturating cGMP (I_{cAMP}/I_{cGMP}) was significantly increased ($p < 0.001$) for heteromeric CNG channels (Fig. 1*A*). Second, a statistically significant increase in the apparent affinity for cAMP ($p < 0.05$) and decrease in the apparent affinity for cGMP ($p < 0.05$) were observed for channels containing hCNGB3 subunits compared with the homomeric channels (Fig. 1*B*). Third, sensitivity to block by L-*cis*-diltiazem applied to the cytoplasmic face of the patch was also examined. As expected, homomeric hCNGA3 channels were insensitive to block by L-*cis*-diltiazem (Fig. 1*C*, *left*, *D*; Table I). Heteromeric human cone CNG channels demonstrated much greater sensitivity to L-*cis*-diltiazem (Fig. 1*C*, *right*, *D*; Table I): the $K_{1/2}$ at +80 mV for the L-*cis*-diltiazem block of hCNGB3 + hCNGA3 channels was 7.4 ± 5.2 μM, $n = 0.92 \pm 0.13$ ($n = 16$). The voltage dependence and $K_{1/2}$ for block by diltiazem were roughly similar to that reported for native catfish cone CNG channels (46). These results show that the presence of the hCNGB3 subunit modified the ligand sensitivity of the expressed channels and dramatically enhanced susceptibility to block by L-*cis*-diltiazem. Thus, the functional properties of recombinant heteromeric channels formed by hCNGB3 and hCNGA3 subunits recapitulated some of the characteristics commonly associated with native CNG channels.

hCNGB3 Plus hCNGA3 Heteromeric Channels Are Inhibited by Ca^{2+}-CaM—We examined the sensitivity of both homomeric hCNGA3 channels and heteromeric hCNGA3 + hCNGB3 chan-

[2] calcium.uhnres.utoronto.ca/ctdb/pub_pages/classify/index.htm.

nels to regulation by Ca^{2+}-CaM. Consistent with previous studies (39), homomeric channels formed by hCNGA3 subunits alone were not inhibited by 250 nM CaM in the presence of 50 μM Ca^{2+} (Fig. 2, *A* and *C*, *left*). In contrast, heteromeric hCNGA3 + hCNGB3 channels displayed significant inhibition by Ca^{2+}-CaM under identical conditions (Fig. 2, *B* and *C*, *right*). The time course for maximum current inhibition by Ca^{2+}-CaM varied between seconds and minutes. The ratio of the current elicited by 10 μM cGMP at +80 mV with and without 250 nM CaM, *i.e.* I_{CaM}/I, was 0.96 ± 0.01 (n = 2) for homomeric hCNGA3 channels and 0.62 ± 0.09 (n = 8) for heteromeric hCNGA3 + hCNGB3 channels. Inhibition by Ca^{2+}-CaM was relieved by perfusion of the patch with calcium-free solution (Fig. 2, *B* and *C*, *right*). The apparent affinity of the heteromeric channel for cGMP was decreased slightly by Ca^{2+}-CaM (Fig. 2*D*), from a $K_{1/2}$ of 19.0 ± 2.7 μM, n = 2.0 ± 0.2 (n = 5) in the absence of CaM (see also Table I) to 25.8 ± 6.7 μM, n = 2.1 ± 0.2 (n = 5) in the presence of CaM ($p < 0.05$, paired t test). No change in the maximum current at a saturating concentration of cGMP (1 mM) was observed with Ca^{2+}-CaM compared with Ca^{2+} alone (data not shown). These results indicate that the presence of the cone photoreceptor hCNGB3 subunit conferred sensitivity to regulation by Ca^{2+}-CaM in the context of recombinant heteromeric channels.

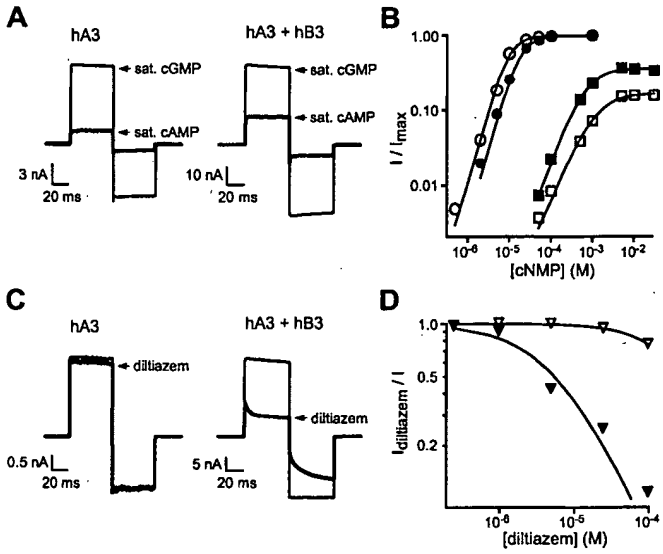

FIG. 1. **Recombinant heteromeric CNG channels containing hCNGB3 subunits differ from homomeric hCNGA3 channels.** *A*, representative current traces are shown for homomeric hCNGA3 (hA3, *left*) and heteromeric hCNGA3 + hCNGB3 (hA3 + hB3, *right*) channels after activation by 1 mM cGMP or 10 mM cAMP (*bold*). Current traces were elicited by voltage steps from a holding potential of 0 to +80 mV, then to −80 and 0 mV. Leak currents in the absence of cyclic nucleotide were subtracted for all recordings. *B*, dose-response relationships for the activation of homomeric channels (*open symbols*) and heteromeric channels (*filled symbols*) by cGMP (*circles*) and cAMP (*squares*) at +80 mV. Currents were normalized to the maximum current in saturating cGMP. *Continuous curves* represent fits of the dose-response relation to the Hill equation, $I/I_{max} = ([cNMP]^n/(K_{1/2}^n + [cNMP]^n))$. For fits to the activation of homomeric channels by cGMP and cAMP, the following parameters were used: $K_{1/2,cGMP}$ = 9.2 μM, n = 2.0; $K_{1/2,cAMP}$ = 1201 μM, n = 1.3. For activation of heteromeric channels: $K_{1/2,cGMP}$ = 17.8 μM, n = 2.0; $K_{1/2,cAMP}$ = 664 μM, n = 1.5. *C*, currents elicited by 100 μM cGMP in the absence and presence (*bold*) of 25 μM L-*cis*-diltiazem for homomeric hCNGA3 (*left*) and heteromeric hCNGA3 + hCNGB3 channels (*right*). Current traces were elicited by the same protocol described in *A*. *D*, dose-response curves for block of homomeric (*open triangles*) and heteromeric channels (*filled triangles*) by L-*cis*-diltiazem in the presence of 100 μM cGMP. *Continuous curves* represent fits of the dose-response relation to the Hill equation in the form: $I_{diltiazem}/I = (K_{1/2}^n/(K_{1/2}^n + [diltiazem]^n))$. For heteromeric channels, the $K_{1/2}$ = 5.4 μM and n = 0.92. Homomeric channels were insensitive to L-*cis*-diltiazem ($K_{1/2} \gg$ 100 μM).

Identification of Region in the hCNGB3 NH_2-terminal Domain Important for Interaction with Ca^{2+}-CaM—To test the hypothesis that hCNGB3 subunits provide sites for direct binding of Ca^{2+}-CaM, we used epitope-tagged human CaM in gel overlay and pull-down interaction assays with GST fusion proteins representing cytoplasmic domains of hCNGB3 and hCNGA3. hCNGA3 subunits are known to possess a CaM-binding site in the NH_2-terminal cytoplasmic domain that is functionally silent in the context of homomeric channels (39). As expected, the NH_2-terminal domain of hCNGA3 interacted with CaM in the presence of calcium, and deletion of a region including the previously identified Ca^{2+}-CaM-binding site prevented this interaction (Fig. 3, *B* and *C*). The NH_2-terminal cytoplasmic domain of hCNGB3 (hCNGB3 N) also was able to physically associate with Ca^{2+}-CaM (Fig. 3, *B* and *C*). Next, we localized the CaM-binding site within the hCNGB3 NH_2-terminal domain. GST fusion proteins representing various hCNGB3 N deletion constructs were generated and tested for interaction with CaM *in vitro* (Fig. 3*A*). Deletion of amino acids 2 to 107 of hCNGB3 N did not disrupt binding of Ca^{2+}-CaM. However, deletion of amino acids 108–159 in hCNGB3 N completely abolished the interaction with Ca^{2+}-CaM (Fig. 3, *B* and *C*). Moreover, a GST fusion protein including only amino acids 108–154 of hCNGB3 N was able to associate with Ca^{2+}-CaM. Thus, these results show that this region of hCNGB3 N is both necessary and sufficient for direct binding of Ca^{2+}-CaM. No CaM binding was observed for any of the fusion proteins in the absence of Ca^{2+}, confirming that the interaction was entirely Ca^{2+}-dependent (Fig. 3, *B*, *middle*, and *C*, *bottom*). Sequence alignment of the probable CaM-binding site in the hCNGB3 NH_2-terminal domain with those of CNGB1, CNGA3, and CNGA2 is shown in Fig. 3*D*. This site in hCNGB3 N resembles a 1–14 CaM-binding motif, exhibiting bulky hydrophobic residues at positions 1 and 14, a net charge of +4, and a predicted propensity to form an amphiphilic α-helix (47, 48). This pattern in hCNGB3 N appears to conform better to these common

TABLE I

Co-expression of hCNGB3 deletion mutants with hCNGA3 forms heteromeric CNG channels

$K_{1/2}$ and Hill coefficient for channel activation by cGMP or cAMP, fractional activation by a saturating concentration of cAMP compared with saturating cGMP (I_{cAMP}/I_{cGMP}), and sensitivity to block by 25 μM L-*cis*-diltiazem in the presence of 100 μM cGMP ($I_{diltiazem}/I$) were measured to confirm formation of heteromeric CNG channels (mean ± S.D.). Numbers in parentheses indicate the number of patches studied. Amino acid deletions were as follows: hA3ΔN, Δ25–106; hB3ΔN, Δ108–158; hB3ΔC, Δ669–809; hB3ΔNΔC, Δ108–158 and Δ669–809.

	cGMP		cAMP		I_{cAMP}/I_{cGMP}	$I_{diltiazem}/I$
	$K_{1/2}$	n	$K_{1/2}$	n		
	μM		μM			
hA3	13.5 ± 2.5 (39)	2.2 ± 0.2	1329 ± 369 (39)	1.3 ± 0.2	0.12 ± 0.04 (39)	0.94 ± 0.04 (6)
hA3 + hB3	19.9 ± 3.8 (56)	2.0 ± 0.2	897 ± 177 (56)	1.6 ± 0.2	0.27 ± 0.09 (59)	0.26 ± 0.11 (15)
hA3 + hB3ΔN	16.1 ± 3.4 (20)	2.0 ± 0.2	767 ± 196 (18)	1.5 ± 0.3	0.34 ± 0.08 (19)	0.26 ± 0.03 (3)
hA3 + hB3ΔC	22.0 ± 4.9 (13)	1.9 ± 0.3	973 ± 468 (13)	1.4 ± 0.2	0.30 ± 0.09 (13)	0.31 ± 0.08 (4)
hA3ΔN + hB3ΔN	17.4 ± 4.0 (10)	2.1 ± 0.2	1156 ± 367 (8)	1.6 ± 0.3	0.34 ± 0.08 (9)	0.11 (1)
hA3 + hB3ΔNΔC	24.4 ± 4.4 (14)	2.0 ± 0.2	1124 ± 283 (14)	1.4 ± 0.2	0.21 ± 0.07 (13)	0.32 ± 0.07 (4)

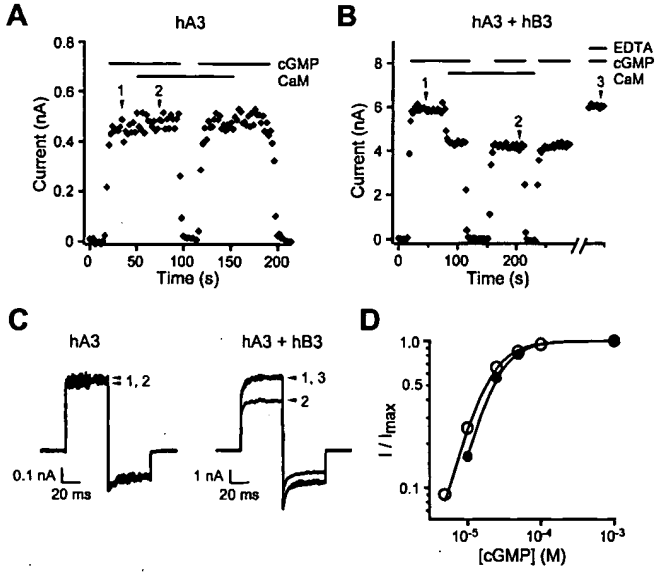

FIG. 2. **Co-expression of hCNGB3 with hCNGA3 confers sensitivity to regulation by Ca^{2+}-CaM.** *A* and *B*, time course for regulation of homomeric hCNGA3 channels (*A*) and heteromeric hCNGA3 + hCNGB3 channels (*B*) by 250 nM CaM in the presence of 50 μM Ca^{2+}. Peak currents at +80 mV were determined every 2 s. 50 μM Ca^{2+} was present for all recordings except where indicated (EDTA). *Bars above* the figures indicate the application of 10 μM cGMP and 250 nM CaM, and replacement of Ca^{2+} with 0.2 M EDTA. *C*, representative current traces from *A* and *B*. *Trace 1* in *C*, *left* and *right*, represent control currents elicited by 10 μM cGMP, corresponding to *arrow 1* in *A* and *B*, respectively. *Trace 2* in *C*, *left* and *right*, are recordings made after application of CaM, corresponding to *arrow 2* in *A* and *B*, respectively. *Trace 3* in *C*, *right*, was recorded after removal of Ca^{2+}, corresponding to *arrow 3* in *B*. *D*, dose-response relationships for activation of heteromeric channels by cGMP in the absence (*open symbols*) or presence (*filled symbols*) of 250 nM CaM (same patch as in *B* and *C*, *right*). *Continuous curves* represent fits of the dose-response relation to the Hill equation, as in Fig. 1: in the absence of CaM, $K_{1/2}$ = 17.3 μM, n = 1.9; in the presence of CaM, $K_{1/2}$ = 22.4 μM, n = 2.0.

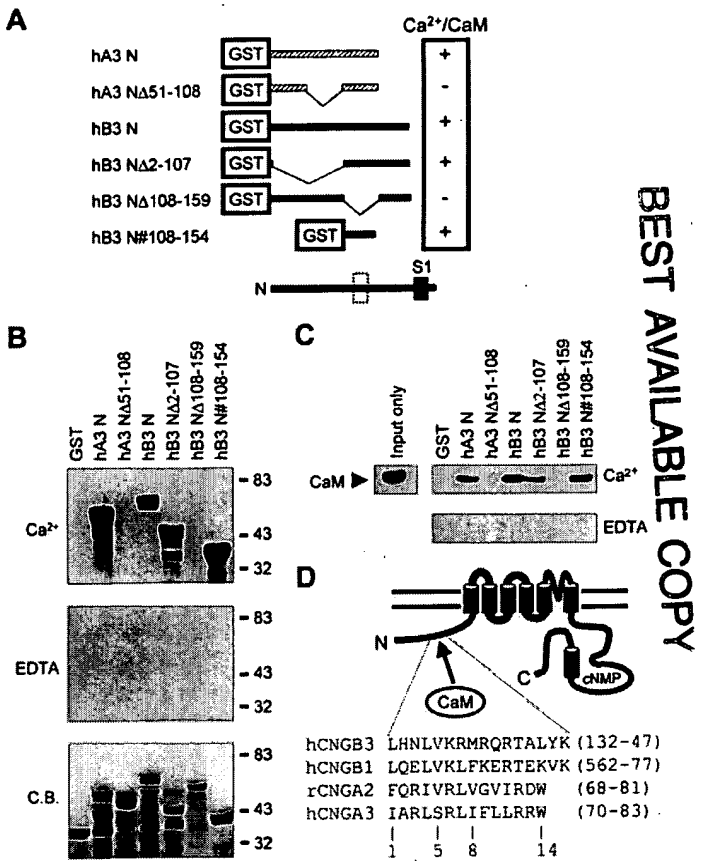

FIG. 3. **Localization of region within the hCNGB3 NH_2-terminal domain important for interaction with Ca^{2+}-CaM.** *A*, schematic representation of the GST fusion proteins of various hCNGA3 (*hatched*) and hCNGB3 (*black*) NH_2-terminal constructs. *Below*, diagram of hCNGB3 NH_2-terminal region: *S1*, putative first transmembrane domain; *open box*, putative CaM-binding site illustrated in *D*. The *box* to the *right* summarizes the presence (+) or absence (−) of *in vitro* interaction with Ca^{2+}-CaM. *B*, gel overlay assay with hCaM-FLAG and GST fusion proteins. GST fusion proteins were immunoblotted and probed with hCaM-FLAG (1 μg/ml) in the presence (1 mM, *top*) or absence of Ca^{2+} (5 mM EDTA, *middle*); hCaM-FLAG binding was detected using M2 anti-FLAG antibody and chemiluminescence. *Bottom*, Coomassie Blue-stained gel of fusion proteins used in gel overlay and GST pull-down assays. *C*, GST pull-down assay. GST fusion proteins, immobilized on glutathione-Sepharose beads, were incubated with input protein (2 μM hCaM-FLAG) in the presence (2 mM) or absence of Ca^{2+} (10 mM EDTA). After washing, bound input protein was detected via immunoblotting and M2 anti-FLAG antibody. *Arrow*, input hCaM-FLAG. *D*, cartoon of hCNGB3 subunit topology, with sequence alignment of CaM-binding sites in the NH_2-terminal regions of hCNGB3 (AF065314), hCNGB1 (AF042498), rCNGA2 (AF126808), and hCNGA3 (AF065314). The *numbers* in *parentheses* indicate the positions of the first and last residues shown.

CaM-binding motifs than the previously characterized "unconventional" CaM-binding site in the NH_2-terminal domain of CNGB1 (30, 31).

Localization of a CaM-binding Site in the hCNGB3 COOH-terminal Domain—Because a functionally silent CaM-binding site was previously identified in the COOH-terminal cytoplasmic domain of the rod CNG channel β subunit (CNGB1) (30, 31), we investigated the possibility that the carboxyl-terminal domain of hCNGB3 (hCNGB3 C) may also bind Ca^{2+}-CaM. Gel-overlay experiments with full-length hCNGB3 C demonstrated an interaction with Ca^{2+}-CaM *in vitro* (Fig. 4*B*). Similar to hCNGB3 N, CaM binding to hCNGB3 C depended on the presence of calcium. As expected, the hCNGA3 COOH-terminal domain did not interact with CaM. To localize which regions of hCNGB3 C were necessary for binding of Ca^{2+}-CaM, GST fusion proteins representing hCNGB3 C deletion mutants were engineered and tested using *in vitro* protein-protein interaction assays (Fig. 4). Assays carried out with fusion proteins including the C-linker region and the cyclic nucleotide-binding (CNB) domain, or the CNB domain alone, revealed no binding to Ca^{2+}-CaM. Instead, Ca^{2+}-CaM specifically interacted with a fusion protein representing the region of hCNGB3 C distal to the CNB domain (amino acids 637–809). A fusion protein limited to amino acids 661–757 of hCNGB3 was sufficient for interaction with Ca^{2+}-CaM, whereas proteins including amino acids 637–681 or 680–809 of hCNGB3 C were unable to bind CaM. Similar results were obtained using GST pull-down assays (data not shown). In all cases, CaM binding did not occur in the absence of calcium (Fig. 4*B*, *middle*). These results, summarized in Fig. 4*A* (*right*), identify a region distal to the cyclic nucleotide-binding domain that is necessary for Ca^{2+}-CaM binding *in vitro*. Consistent with these findings, a search for likely CaM-binding sites in hCNGB3 C highlighted this sequence as a candidate CaM target (Fig. 4*A*, *bottom*). This Ca^{2+}-CaM-binding site in hCNGB3 is positioned similar to the functionally silent CaM-binding site in the COOH-terminal domain of CNGB1, but this region of CNGB3 exhibits little sequence homology with CNGB1.

Effects of hCNGB3 NH_2- and COOH-terminal Deletions on Ca^{2+}-CaM Modulation of Heteromeric CNG Channels—To determine the functional importance of the CaM-binding sites identified within hCNGB3 NH_2- and COOH-terminal cytoplasmic domains, hCNGB3 deletion mutants were engineered and individually co-expressed with hCNGA3 in *Xenopus* oocytes. As shown in Table I, the functional properties of these channels, as indicated by the $K_{1/2}$ for cGMP, the $K_{1/2}$ for cAMP, I_{cAMP}/

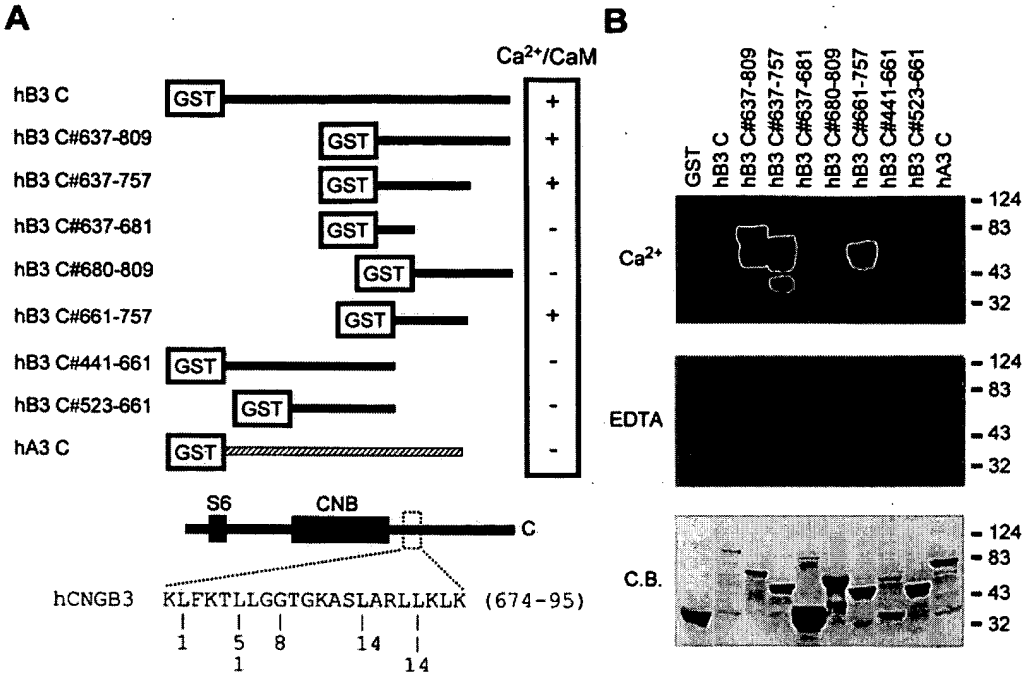

FIG. 4. **Localization of Ca^{2+}-CaM-binding site in hCNGB3 COOH-terminal domain.** *A*, schematic representation of GST fusion proteins of hCNGB3 C deletion constructs. *Box* to the *right* summarizes the results from interaction assays with Ca^{2+}-CaM. *Below*, diagram of the hCNGB3 COOH-terminal region with sequence of the putative CaM-binding site: *S6*, putative sixth transmembrane domain; *open box*, putative CaM-binding site. *B*, gel overlay assays using hCaM-FLAG were performed as described in the legend to Fig. 3 in the presence (*top*) or absence of Ca^{2+} (*middle*). *Bottom*, Coomassie Blue-stained gel of fusion proteins probed in gel overlay assays.

I_{cGMP}, and the sensitivity to block by L-*cis*-diltiazem, were roughly similar to wild type hCNGA3 + hCNGB3 channels, demonstrating that all hCNGB3 deletion mutants studied were able to participate in the formation of heteromeric channels. An α subunit with deletion of its Ca^{2+}-CaM-binding site, hCNGA3 ΔN, also formed functional homomeric channels (data not shown) as well as heteromeric channels when co-expressed with hCNGB3.

Sensitivity to regulation by CaM for these mutant CNG channels was examined in the presence of 25 μM cGMP and 50 μM Ca^{2+}. Inhibition by Ca^{2+}-CaM was still observed for heteromeric hCNGA3 + hCNGB3 ΔN, hCNGA3 + hCNGB3 ΔC, and hCNGA3 ΔN + hCNGB3 ΔN channels (Fig. 5, *A*, *C*, and *E*). For some patches, slow recovery of the current after Ca^{2+}-CaM inhibition was apparent with removal of CaM even in the presence of Ca^{2+} (Fig. 5*A*). Thus, neither individual deletion of NH_2- or COOH-terminal CaM-binding sites in hCNGB3, nor of the NH_2-terminal CaM-binding site in hCNGA3, eliminated sensitivity to regulation by Ca^{2+}-CaM. Furthermore, the extent of inhibition by Ca^{2+}-CaM of hCNGA3 + hCNGB3 ΔC and hCNGA3 ΔN + hCNGB3 ΔN channels resembled that of wild type heteromeric channels. These results suggest that either CaM-binding site in hCNGB3 is sufficient for the full range of CaM regulation of heteromeric channels. However, co-expression of hCNGA3 with hCNGB3 subunits having both NH_2- and COOH-terminal CaM-binding sites deleted (hCNGB3 ΔNΔC) gave rise to channels that were no longer sensitive to regulation by Ca^{2+}-CaM (I_{CaM}/I was 0.95 $\pm$ 0.02, n = 8) (Fig. 5, *B*, *D*, and *E*). Together, these results imply that both CaM-binding sites in hCNGB3 can contribute to modulation by CaM, but that the CaM-binding site in hCNGA3 is not sufficient for CaM regulation in the context of these heteromeric channels.

To ensure that channels arising from this combination of subunits had characteristics consistent with heteromeric rather than homomeric hCNGA3 channels, the activation properties and sensitivity to block by L-cis-diltiazem were examined more closely. hCNGA3 + hCNGB3 ΔNΔC channels displayed greater relative cAMP efficacy compared with homomeric hCNGA3 channels ($p < 0.001$) (Table I). Furthermore, the $K_{1/2}$ for L-*cis*-diltiazem block of currents at +80 mV for hCNGA3 + hCNGB3 ΔNΔC channels (6.6 $\pm$ 4.2 μM, n = 0.74 $\pm$ 0.17; n = 5) was similar to that of wild-type heteromeric channels. These results confirm that hCNGB3 ΔNΔC subunits were fully competent for assembly into functional heteromeric channels. Yet, the basic properties of hCNGB3 ΔNΔC-containing channels differed somewhat from wild-type heteromeric channels. In particular, there was a significant decrease in both apparent affinity for cGMP (p = 0.001) and relative agonist efficacy, I_{cAMP}/I_{cGMP} ($p < 0.01$) (Table I). These changes indicate that deletion of both CaM-binding sites in hCNGB3 has an effect on channel gating that parallels the effect of Ca^{2+}-CaM on the activation of wild-type heteromeric channels.

DISCUSSION

We have investigated Ca^{2+}-CaM regulation of channels formed by human retinal cone CNGB3 and CNGA3 subunits and found that the CNGB3 subunit confers sensitivity to modulation. Our results are consistent with a mechanism whereby direct binding of CaM to CNGB3 subunits of heteromeric channels reduces the sensitivity of these channels to cyclic nucleotide. The mechanism for CaM regulation appears to be similar to that of olfactory and rod CNG channels: an allosteric effect of bound CaM on the opening transition of the channel. In this way, the ligand sensitivity of human cone photoreceptor CNG channels can be regulated via a Ca^{2+}-feedback mechanism that involves binding of CaM to sites located within the NH_2- and COOH-terminal cytoplasmic domains of hCNGB3. CaM regulation of the ligand sensitivity of cone CNG channels is expected to contribute to an extension of the operating range of cone photoreceptors (49).

With completion of this study and comparison to previous studies (for review, see Ref. 50), similarities and differences in CaM binding and regulation among olfactory, rod, and cone CNG channels are now evident. All three sensory transduction

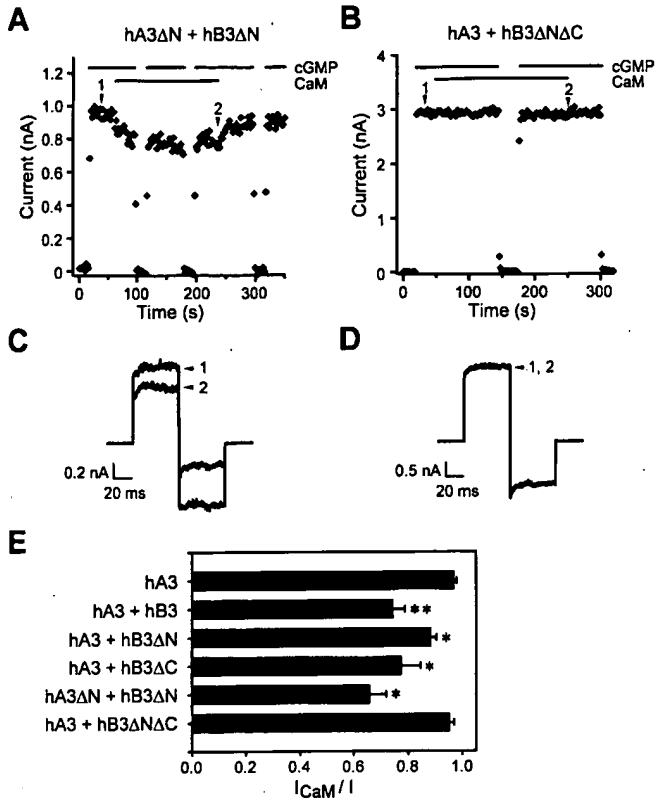

FIG. 5. **Effects of hCNGB3 NH_2- and COOH-terminal deletions on Ca^{2+}-CaM inhibition of heteromeric cone CNG channels.** *A* and *B*, time course for regulation of heteromeric hCNGA3 ΔN + hCNGB3 ΔN channels (*A*) and hCNGA3 + hCNGB3 ΔNΔC channels (*B*) by Ca^{2+}-CaM. Peak currents at +80 mV were determined every 2 s. 50 μM Ca^{2+} was present for all recordings shown. *Bars above* the figures indicate application of 25 μM cGMP and 250 nM CaM, respectively. *C* and *D*, representative current traces from *A* and *B*. *Traces* and *arrows 1* and *2* have the same meaning as Fig. 2*C*. *E*, summary of effects of hCNGB3 NH_2- and COOH-terminal deletions, and hCNGA3 NH_2-terminal deletion, on modulation of heteromeric CNG channels by Ca^{2+}-CaM. I_{CaM}/I is the current (at +80 mV) elicited by 25 μM cGMP with 250 nM CaM normalized to the current elicited by 25 μM cGMP alone, all in the presence of 50 μM Ca^{2+}. All heteromeric channels, with the exception of hCNGA3 + hCNGB3 ΔNΔC channels, exhibited a statistically significant current reduction (*, $p < 0.05$; **, $p < 0.001$; $n = 4$ to 13) compared with hCNGA3 homomeric channels.

channels contain one or more subunits with NH_2-terminal CaM-binding sites located a short distance from the first putative transmembrane domain: CNGA2 and CNGB1b for the olfactory channel, CNGB1 for the rod channel, and CNGA3 and CNGB3 for the cone channel. The cone channel is in several ways unique among these CNG channel types. First, the NH_2-terminal CaM-binding site of the human CNGA3 subunit is functionally silent not only for homomeric channels (39), but also, as shown in this paper, for heteromeric channels containing hCNGB3 subunits. Second, the sequence of the hCNGB3 NH_2-terminal CaM-binding site conforms better to typical 1–14 type motifs than the NH_2-terminal CaM-binding site of CNGB1, which has been previously described as unconventional in that its sequence is in part similar to an IQ-type motif yet CaM binding to this site is calcium-dependent (30, 31). Third, whereas CNGB3 and CNGB1 subunits both possess a COOH-terminal CaM-binding site located distal to the CNB domain, only the site in the CNGB3 subunit is functionally important for Ca^{2+}-CaM regulation. For the rod CNG channel, the CNGB1 COOH-terminal CaM-binding site is not necessary or sufficient for regulation by Ca^{2+}-CaM (30, 31). In contrast, the COOH-terminal CaM-binding site of the CNGB3 subunit contributes to the sensitivity of the cone channel to Ca^{2+}-CaM regulation and is sufficient for regulation in the absence of the NH_2-terminal CaM-binding site. Thus, our results suggest that both NH_2- and COOH-terminal CaM-binding sites of hCNGB3 are equally important for regulation. Because single deletions of the individual CaM-binding sites gave rise to heteromeric channels that exhibited sensitivity to modulation roughly similar to that of wild-type channels, we favor a model where each CaM-target site in hCNGB3 is independently capable of conferring regulation, rather than the two sites acting in a synergistic or additive manner.

CaM also decreases the ligand sensitivity of rod, cone, and olfactory CNG channels to different extents. Ca^{2+}-CaM reduces the apparent affinity of the olfactory CNG channel for cAMP by up to 20-fold (18, 20), whereas it has a more modest effect on channels formed by rod photoreceptor CNGB1 plus CNGA1 subunits (19, 22, 30–32). The magnitude of cone channel modulation by Ca^{2+}-CaM is much smaller than that of olfactory CNG channels but similar to that of rod channels. Although the sensitivity of cone photoreceptor CNG channels to regulation by CaM may vary with different species, our results indicate that channels formed by human CNGB3 and CNGA3 subunits are modulated by Ca^{2+}-CaM to an extent similar to recombinant bovine and human rod CNG channels. As previously suggested (25, 27, 32, 39, 51), CNG channel sensitivity to regulation by Ca^{2+}-CaM is dependent not merely on the presence, number, or location of CaM-binding sites but also other structural features and interactions.

As is the case for CNGA2 homomeric channels (20, 25), deletion of the CaM-binding sites in hCNGB3 subunits alters the activation properties of heteromeric channels in a way that parallels the effect of Ca^{2+}-CaM binding on gating of wild-type channels. Previous evidence suggests that an interaction occurs between NH_2- and COOH-terminal cytoplasmic domains of olfactory CNGA2 subunits that promotes channel opening and helps control gating of the channels. Ca^{2+}-CaM modulates olfactory CNG channels by direct binding to an NH_2-terminal autoexcitatory domain (20, 52, 53), disrupting interdomain coupling with the COOH-terminal CNB domain (25). For rod CNG channels, Ca^{2+}-CaM binding to an NH_2-terminal site in CNGB1 also disrupts an interaction between this domain and the distal COOH-terminal region of CNGA1 (32). It remains to be determined if a similar mechanism is involved in CaM regulation of cone CNG channels.

Whereas the simplest explanation for the observations described in this paper is that Ca^{2+}-CaM can regulate the activity of cone CNG channels by direct binding to NH_2- and COOH-terminal CaM-binding sites of hCNGB3 subunits, other mechanisms remain possible. Ca^{2+}-CaM may alter channel activity by binding to a channel-associated protein rather than, or in addition to, docking at the hCNGB3 subunit itself. In this regard, hCNGB3 deletions may prevent interactions between the channel and proteins other than CaM. Another possibility is that Ca^{2+}-CaM may stimulate patch-associated CaM-dependent kinase activity, which in turn may modulate cone CNG channels via phosphorylation. CaM kinase II activity has been implicated in circadian regulation of the ligand sensitivity of native chick cone CNG channels (54); whether the reported effect is because of direct phosphorylation of the channel protein or occurs via an indirect pathway remains to be determined. Muller and co-workers (40) have demonstrated that the ligand sensitivity of homomeric bovine CNGA3 channels is regulated by protein kinase C-mediated phosphorylation. Therefore, like rod CNG channels (Refs. 55 and 56, for review, see Ref. 57), cone CNG channels may be the targets of several regulatory pathways that include but are not limited to direct binding of CaM.

An additional consideration is that at least in some species other physiologically important effectors for Ca^{2+}-dependent regulation of cone CNG channels may act in concert with CaM. There is evidence suggesting that a Ca^{2+}-binding protein other than CaM may regulate native CNG channels of striped bass cone photoreceptors, particularly because CaM application to patches excised from cone outer segments does not completely recapitulate the effect of the endogenous calcium-dependent modulator(s) (33, 34). For CNG channels of intact cone outer segments, changes in cytoplasmic Ca^{2+} concentration can alter apparent cGMP affinity over a 4-fold range (34). The more modest extent of CaM-mediated inhibition of heterologously expressed CNGB3 plus CNGA3 channels suggests that CaM can account for some but not all of this Ca^{2+}-dependent modulation of ligand sensitivity. It has also been suggested that an unknown endogenous factor may be important for Ca^{2+}-dependent regulation of native rod (21) and olfactory (58) CNG channels. Warren and Molday (59), however, have recently shown that soluble extracts from bovine rod outer segments that have been depleted of endogenous CaM do not contain an additional endogenous factor sufficient to regulate rod CNG channel activity. Several other Ca^{2+}-binding proteins related to CaM are expressed in the retina (60). One of these, CaBP1, has recently been shown to compete with CaM for binding to a region within the cytoplasmic COOH-terminal domain of neuronal $Ca_v2.1$ channels (61). Further studies are needed to identify and characterize potential interactions between CNG channels and other calcium-sensitive regulatory proteins that may augment or compete with the action of CaM.

Acknowledgments—We are grateful to M. C. Trudeau and W. N. Zagotta for helpful comments and advice, and J. Hendrickson for technical assistance. We also thank Prof. K.-W. Yau for sharing the cDNA clone for human CNGA3.

REFERENCES

1. Zagotta, W. N. S., and Siegelbaum, S. A. (1996) *Annu. Rev. Neurosci.* **19,** 235–263
2. Richards, M. J., and Gordon, S. E. (2000) *Biochemistry* **39,** 14003–14011
3. Bradley, J., Frings, S., Yau, K. W., and Reed, R. (2001) *Science* **294,** 2095–2096
4. Liu, D. T., Tibbs, G. R., and Siegelbaum, S. A. (1996) *Neuron* **16,** 983–990
5. Varnum, M. D., and Zagotta, W. N. (1996) *Biophys. J.* **70,** 2667–2679
6. Kaupp, U. B., and Seifert, R. (2002) *Physiol. Rev.* **82,** 769–824
7. Chen, T. Y., Peng, Y. W., Dhallan, R. S., Ahamed, B., Reed, R. R., and Yau, K. W. (1993) *Nature* **362,** 764–767
8. Liman, E. R., and Buck, L. B. (1994) *Neuron* **13,** 611–621
9. Bradley, J., Li, J., Davidson, N., Lester, H. A., and Zinn, K. (1994) *Proc. Natl. Acad. Sci. U. S. A.* **91,** 8890–8894
10. Sautter, A., Zong, X., Hofmann, F., and Biel, M. (1998) *Proc. Natl. Acad. Sci. U. S. A.* **95,** 4696–4701
11. Bonigk, W., Bradley, J., Muller, F., Sesti, F., Boekhoff, I., Ronnett, G. V., Kaupp, U. B., and Frings, S. (1999) *J. Neurosci.* **19,** 5332–5347
12. Gerstner, A., Zong, X., Hofmann, F., and Biel, M. (2000) *J. Neurosci.* **20,** 1324–1332
13. Fain, G. L., Matthews, H. R., Cornwall, M. C., and Koutalos, Y. (2001) *Physiol. Rev.* **81,** 117–151
14. Menini, A. (1999) *Curr. Opin. Neurobiol.* **9,** 419–426
15. Zufall, F., and Leinders-Zufall, T. (2000) *Chem. Senses* **25,** 473–481
16. Molday, R. S. (1996) *Curr. Opin. Neurobiol.* **6,** 445–452
17. Hsu, Y. T., and Molday, R. S. (1993) *Nature* **361,** 76–79
18. Chen, T. Y., and Yau, K. W. (1994) *Nature* **368,** 545–548
19. Chen, T. Y., Illing, M., Molday, L. L., Hsu, Y. T., Yau, K. W., and Molday, R. S. (1994) *Proc. Natl. Acad. Sci. U. S. A.* **91,** 11757–11761
20. Liu, M., Chen, T. Y., Ahamed, B., Li, J., and Yau, K. W. (1994) *Science* **266,** 1348–1354
21. Gordon, S. E., Downing-Park, J., and Zimmerman, A. L. (1995) *J. Physiol.* **486,** 533–546
22. Korschen, H. G., Illing, M., Selfert, R., Sesti, F., Williams, A., Gotzes, S., Colville, C., Muller, F., Dose, A., Godde, M., Molday, L., Kaupp, U. B., and Molday, R. S. (1995) *Neuron* **15,** 627–636
23. Bauer, P. J. (1996) *J. Physiol.* **494,** 675–685
24. Kurahashi, T., and Menini, A. (1997) *Nature* **385,** 725–729
25. Varnum, M. D., and Zagotta, W. N. (1997) *Science* **278,** 110–113
26. Dhallan, R. S., Yau, K. W., Schrader, K. A., and Reed, R. R. (1990) *Nature* **347,** 184–187
27. Bradley, J., Reuter, D., and Frings, S. (2001) *Science* **294,** 2176–2178
28. Munger, S. D., Lane, A. P., Zhong, H., Leinders-Zufall, T., Yau, K. W., Zufall, F., and Reed, R. R. (2001) *Science* **294,** 2172–2175
29. Kaupp, U. B., Niidome, T., Tanabe, T., Terada, S., Bonigk, W., Stuhmer, W., Cook, N. J., Kangawa, K., Matsuo, H., Hirose, T., Miyata, T., and Numa, S. (1989) *Nature* **342,** 762–766
30. Grunwald, M. E., Yu, W. P., Yu, H. H., and Yau, K. W. (1998) *J. Biol. Chem.* **273,** 9148–9157
31. Weitz, D., Zoche, M., Muller, F., Beyermann, M., Korschen, H. G., Kaupp, U. B., and Koch, K. W. (1998) *EMBO J.* **17,** 2273–2284
32. Trudeau, M. C., and Zagotta, W. N. (2002) *Proc. Natl. Acad. Sci. U. S. A.* **99,** 8424–8429
33. Hackos, D. H., and Korenbrot, J. I. (1997) *J. Gen. Physiol.* **110,** 515–528
34. Rebrik, T. I., and Korenbrot, J. I. (1998) *J. Gen. Physiol.* **112,** 537–548
35. Rebrik, T. I., Kotelnikova, E. A., and Korenbrot, J. I. (2000) *J. Gen. Physiol.* **116,** 521–534
36. Haynes, L. W., and Stotz, S. C. (1997) *Vis. Neurosci.* **14,** 233–239
37. Bonigk, W., Muller, F., Middendorff, R., Weyand, I., and Kaupp, U. B. (1996) *J. Neurosci.* **16,** 7458–7468
38. Yu, W. P., Grunwald, M. E., and Yau, K. W. (1996) *FEBS Lett.* **393,** 211–215
39. Grunwald, M. E., Zhong, H., Lai, J., and Yau, K. W. (1999) *Proc. Natl. Acad. Sci. U. S. A.* **96,** 13444–13449
40. Muller, F., Vantler, M., Weitz, D., Eismann, E., Zoche, M., Koch, K. W., and Kaupp, U. B. (2001) *J. Physiol.* **532,** 399–409
41. Sundin, O. H., Yang, J. M., Li, Y., Zhu, D., Hurd, J. N., Mitchell, T. N., Silva, E. D., and Maumenee, I. H. (2000) *Nat. Genet.* **25,** 289–293
42. Kohl, S., Baumann, B., Broghammer, M., Jagle, H., Sieving, P., Kellner, U., Spegal, R., Anastasi, M., Zrenner, E., Sharpe, L. T., and Wissinger, B. (2000) *Hum. Mol. Genet.* **9,** 2107–2116
43. Wissinger, B., Muller, F., Weyand, I., Schuffenhauer, S., Thanos, S., Kaupp, U. B., and Zrenner, E. (1997) *Eur. J. Neurosci.* **9,** 2512–2521
44. Liman, E. R., Tytgat, J., and Hess, P. (1992) *Neuron* **9,** 861–871
45. Varnum, M. D., Black, K. D., and Zagotta, W. N. (1995) *Neuron* **15,** 619–625
46. Haynes, L. W. (1992) *J. Gen. Physiol.* **100,** 783–801
47. Crivici, A., and Ikura, M. (1995) *Annu. Rev. Biophys. Biomol. Struct.* **24,** 85–116
48. Rhoads, A. R., and Friedberg, F. (1997) *FASEB J.* **11,** 331–340
49. Pugh, E. N., Jr., Nikonov, S., and Lamb, T. D. (1999) *Curr. Opin. Neurobiol.* **9,** 410–418
50. Trudeau, M. C., and Zagotta, W. N. (2003) *J. Biol. Chem.* **278,** 18705–18708
51. Muller, F., Bonigk, W., Sesti, F., and Frings, S. (1998) *J. Neurosci.* **18,** 164–173
52. Goulding, E. H., Tibbs, G. R., and Siegelbaum, S. A. (1994) *Nature* **372,** 369–374
53. Gordon, S. E., and Zagotta, W. N. (1995) *Neuron* **14,** 857–864
54. Ko, G. Y., Ko, M. L., and Dryer, S. E. (2001) *Neuron* **29,** 255–266
55. Gordon, S. E., Brautigan, D. L., and Zimmerman, A. L. (1992) *Neuron* **9,** 739–748
56. Molokanova, E., Trivedi, B., Savchenko, A., and Kramer, R. H. (1997) *J. Neurosci.* **17,** 9068–9076
57. Kramer, R. H., and Molokanova, E. (2001) *J. Exp. Biol.* **204,** 2921–2931
58. Balasubramanian, S., Lynch, J. W., and Barry, P. H. (1996) *J. Membr. Biol.* **152,** 13–23
59. Warren, R., and Molday, R. S. (2002) *Adv. Exp. Med. Biol.* **514,** 205–223
60. Haeseleer, F., Imanishi, Y., Sokal, I., Filipek, S., and Palczewski, K. (2002) *Biochem. Biophys. Res. Commun.* **290,** 615–623
61. Lee, A., Westenbroek, R. E., Haeseleer, F., Palczewski, K., Scheuer, T., and Catterall, W. A. (2002) *Nat. Neurosci.* **5,** 210–217

THE JOURNAL OF BIOLOGICAL CHEMISTRY
Vol. 278, No. 36, Issue of September 5, pp. 34533–34540, 2003
Printed in U.S.A.

Achromatopsia-associated Mutation in the Human Cone Photoreceptor Cyclic Nucleotide-gated Channel CNGB3 Subunit Alters the Ligand Sensitivity and Pore Properties of Heteromeric Channels*

Received for publication, May 15, 2003, and in revised form, June 11, 2003
Published, JBC Papers in Press, June 18, 2003, DOI 10.1074/jbc.M305102200

Changhong Peng, Elizabeth D. Rich, and Michael D. Varnum‡

From the Department of Veterinary and Comparative Anatomy, Pharmacology, and Physiology and Program in Neuroscience, Washington State University, Pullman, Washington 99164-6520

Cone photoreceptor cyclic nucleotide-gated (CNG) channels are thought to form by assembly of two different subunit types, CNGA3 and CNGB3. Recently, mutations in the gene encoding the CNGB3 subunit have been linked to achromatopsia in humans. Here we describe the functional consequences of two achromatopsia-associated mutations in human CNGB3 (hCNGB3). Co-expression in *Xenopus* oocytes of human CNGA3 (hCNGA3) subunits with hCNGB3 subunits containing an achromatopsia-associated mutation in the S6 transmembrane domain (S435F) generated functional heteromeric channels that exhibited an increase in apparent affinity for both cAMP and cGMP compared with wild type heteromeric channels. In contrast, co-expression of a presumptive null mutation of hCNGB3 (T383f.s.ΔC) with hCNGA3 produced channels with properties indistinguishable from homomeric hCNGA3 channels. The effect of hCNGB3 S435F subunits on cell-surface expression of green fluorescent protein-tagged hCNGA3 subunits and of non-tagged hCNGA3 subunits on surface expression of green fluorescent protein-hCNGB3 S435F subunits were similar to those observed for wild type hCNGB3 subunits, suggesting that the mutation does not grossly disturb subunit assembly or plasma membrane targeting. The S435F mutation was also found to produce changes in the pore properties of the channel, including decreased single channel conductance and decreased sensitivity to block by L-*cis*-diltiazem. Overall, these results suggest that the functional properties of cone CNG channels may be altered in patients with the S435F mutation, providing evidence supporting the pathogenicity of this mutation in humans. Thus, achromatopsia may arise from a disturbance of cone CNG channel gating and permeation or from the absence of functional CNGB3 subunits.

Cyclic nucleotide-gated (CNG)[1] ion channels are fundamental to sensory transduction in retinal photoreceptor cells and in olfactory receptor neurons. CNG channels couple a change in intracellular cyclic nucleotide concentration in these cells into an electrical response underlying sensory signaling. CNG channels are part of a superfamily of ion channels whose members include voltage-gated potassium channels and channels gated by intracellular ligands (1, 2). There are six genes encoding CNG channel subunits in mammals: *CNGA1*, *CNGA2*, *CNGA3*, *CNGA4*, *CNGB1*, and *CNGB3*. Native CNG channels are thought to be tetrameric proteins formed by at least two of these subunit types. Each of these subunits exhibits six putative transmembrane domains, intracellular amino and carboxyl termini, a conserved pore domain, and a cyclic nucleotide binding domain. In cone photoreceptor cells, CNG channels are composed of CNGA3 (α) and CNGB3 (β) subunits. Similar to their rod photoreceptor counterparts, heterologous expression of CNGA3 subunits alone can generate functional homomeric channels (3–5), but CNGB3 subunits cannot (6, 7). Compared with the proteins forming rod and olfactory CNG channels, the protein subunits forming cone photoreceptor CNG channels are not as well characterized; only recently has the molecular identity of the cone CNG channel β subunit been revealed (6, 8, 9).

Mutations in the *CNGA3* and *CNGB3* genes encoding human cone photoreceptor CNG channel subunits have been found to segregate with patients having complete and incomplete achromatopsia (8–12). Achromatopsia is an autosomal recessive disease characterized by absent or limited cone function (but intact rod function), compromised visual acuity, nystagmus, and photophobia. For CNGA3-deficient mice, an animal model of complete achromatopsia, loss of cone function correlates with progressive degeneration of cone photoreceptors (13). Complete achromatopsia in humans, however, is thought to be a stationary disorder without obvious cone degeneration (but see also Ref. 14). One disease-associated mutation in humans (S435F), located in the putative S6 transmembrane domain of CNGB3, has been linked to the unusually frequent occurrence of complete achromatopsia among Pingelapese islanders (8, 9), a population described by Oliver Sachs in *The Island of the Colorblind* (15). The mechanisms underlying achromatopsia remain poorly defined. An important step toward understanding the development of the disease is determining how individual mutations in the genes that encode cone photoreceptor CNG channel subunits may alter the functional properties of these critical proteins.

Here we report the functional consequences of two mutations in hCNGB3 associated with achromatopsia in humans. Our results demonstrate that co-expression of hCNGA3 with hCNGB3 subunits containing an achromatopsia-associated frameshift mutation that truncates the pore and the carboxyl-

* This work was supported by grants from the NEI, National Institutes of Health Grant EY12836 and the Adler Foundation (to M. D. V.). Part of this work has been described previously in abstract form (Peng, C., Rich, E. D., and Varnum, M. D. (2001) *Society for Neuroscience Annual Meeting, San Diego, CA, November 10–15, 2001*, Abstr. 720.19, Society for Neuroscience, Washington, D. C.). The costs of publication of this article were defrayed in part by the payment of page charges. This article must therefore be hereby marked "*advertisement*" in accordance with 18 U.S.C. Section 1734 solely to indicate this fact.

‡ To whom correspondence should be addressed: Dept. of VCAPP, Washington State University, P. O. Box 646520, Pullman, WA 99164-6520. Tel.: 509-335-0701; Fax: 509-335-4650; E-mail: varnum@wsu.edu.

[1] The abbreviations used are: CNG channel, cyclic nucleotide-gated channel; GFP, green fluorescent protein; h-, human; cNMP, 3′,5′-cycle nucleotide monophosphate.

terminal cytoplasmic domain (T383f.s.ΔC) gave rise to channels indistinguishable from homomeric hCNGA3 channels. We also show that S435F in hCNGB3 alters both the ligand sensitivity and pore properties of heteromeric cone CNG channels. These results imply that achromatopsia can arise either from altered functional properties of cone CNG channels or from the absence of working hCNGB3 subunits. Furthermore, the effect of the S435F mutation on the properties of heteromeric channels provides insight into both the structural features important for the activation of these channels and the molecular mechanisms leading to achromatopsia in humans.

EXPERIMENTAL PROCEDURES

Molecular Biology—The human retinal cone CNG channel β subunit clone, hCNGB3, was isolated from human retinal cDNA as previously described (7). The coding sequence of this clone differs from the complete published sequence for CNGB3 of Kohl *et al.* (9) (AF272900) at two positions (nucleotide 1789g→a and nucleotide 1834a→g), representing either sequence polymorphisms or *Taq* polymerase errors; neither nucleotide change alters the amino acid sequence. It was subcloned into pGEMHE (16) for heterologous expression in *Xenopus* oocytes. Human CNGA3 (4), a generous gift of Dr. K.-W. Yau, was also subcloned into pGEMHE. To generate amino-terminal fusions of enhanced green fluorescent protein (GFP) with hCNGB3 and hCNGA3, PCR-amplified GFP (Qbiogene, Carlsbad, CA) including an additional linker sequence ($IAG_5RARLPA$) was subcloned in-frame with cDNA encoding hCNGA3 and hCNGB3 at amino acids Asp-24 and Gly-107, respectively. The essential properties of hCNGA3 and hCNGB3 plus hCNGA3 channels were unaltered by the GFP fusion (data not shown). Although the GFP tag may still have a slight influence on expression level or plasma membrane targeting, we estimate that the effect of the tag on expression level (patch current density) is small. Mutations in the hCNGB3 coding sequence were engineered using overlapping PCR mutagenesis (17). All mutations and the fidelity of PCR-amplified cassettes were confirmed by automated DNA sequencing. For expression studies, identical amounts of cDNA were linearized using *Sph*I or *Nhe*I, and capped mRNA was transcribed *in vitro* using the T-7 RNA polymerase mMessage mMachine kit (Ambion, Austin, TX). mRNA concentrations and relative amounts were determined by denaturing gel electrophoresis and one-dimensional image analysis software (Kodak, NY) and spectrophotometry.

Electrophysiology—For functional expression studies, *Xenopus laevis* oocytes were isolated and microinjected with 5–10 ng of mRNA as previously described (18). The ratio of wild type or mutant hCNGB3 mRNA to hCNGA3 mRNA was typically 5:1. Two to 7 days after microinjection of mRNA, patch-clamp experiments were performed in the inside-out configuration with an Axopatch 200B amplifier (Axon Instruments, Foster City, CA). Recordings were made at 20–23 °C. Data were acquired using Pulse software (HEKA Elektronik, Lambrecht, Germany). Initial pipette resistances were 0.4–1.5 megaohms. Intracellular and extracellular solutions contained 130 mM NaCl, 0.2 mM EDTA, and 3 mM HEPES (pH 7.2). Intracellular solutions were changed using an RSC-160 rapid solution changer (Molecular Kinetics, Pullman, WA). Currents in the absence of cyclic nucleotide were subtracted. Macroscopic patch current density was calculated after estimating the area of each patch, A (in μm^2), from the initial pipette resistance, R, using the equation $A = 12.6 \times (1/R + 0.018)$ (19). Steady-state rectification ($I_{+80\ mV}/I_{-80\ mV}$) was determined as the ratio of the current at the end of 60-ms voltage steps to +80 mV and −80 mV. For channel activation by cGMP or cAMP, dose-response data were fitted to the Hill equation, $I/I_{max} = ([cNMP]^h/(K_{1/2}{}^h + [cNMP]^h))$, where I is the current amplitude, I_{max} is the maximum current, [cNMP] is the ligand concentration, $K_{1/2}$ is the apparent affinity for ligand, and h is the Hill slope. For ion substitution experiments, the extracellular solution contained 130 mM NaOH, and the intracellular solution contained either 130 mM NaOH, KOH, RbOH, LiOH, or CsOH both with and without cGMP (100 μM or 1 mM). In addition, anhydrous EDTA was substituted for Na_2EDTA. Reversal potentials were measured by 200 ms voltage ramps from −100 to +100 mV. The permeability ratio of intracellular ion X^+ relative to extracellular Na^+, $P_X{}^+/P_{Na}{}^+$, was determined using the bi-ionic form of the Goldman-Hodgkin-Katz equation (20),

$$\frac{P_{x^+}}{P_{Na^+}} = \frac{[Na^+]_o}{[X^+]_{in}^-} e^{-\frac{zF\Delta V_{rev}}{RT}} \quad \text{(Eq. 1)}$$

where ΔV_{rev} is the change in reversal potential, $[X^+]_{in}$ and $[Na^+]_o$ are ion activities (21), and the remaining terms have their usual meanings. Conductances were determined at +80 mV. Single channel recordings were made at a 50 kHz sampling rate and filtered at 5 kHz. For single channel analysis, amplitude histograms were constructed from 1–5 s of recorded data at +80 mV. The histograms were fit with two or three gaussian functions, with one gaussian representing the closed state and the other(s) representing the open state(s) for one or two channels, respectively. For current block by L-*cis*-diltiazem, data were fit to the Hill equation in the form $I_{diltiazem}/I = (K_{1/2}{}^h/(K_{1/2}{}^h + [diltiazem]^h))$. Data were analyzed using Igor (Wavemetrics, Lake Oswego, OR), SigmaPlot, and SigmaStat (SPSS Inc.). All values are reported as the mean ± S.E. of n experiments unless otherwise indicated. Statistical significance was determined using a Student's t test or Mann-Whitney rank sum test, and a p value of < 0.05 was considered significant.

Confocal Microscopy—Confocal images were obtained using a 10× objective on a Nikon Eclipse TE 300 inverted microscope equipped with a Bio-Rad MRC-1024 confocal laser-scanning system and a krypton-argon laser. Oocytes expressing GFP-tagged CNG channel subunits 64–72 h after injection of mRNA were placed in borosilicate coverglass chambers such that the equator was approximately perpendicular to the plane of imaging. GFP fluorescence was measured using an excitation wavelength of 488 nm and a 522 DF 32 emission filter. Laser intensity, pinhole aperture, and photo-multiplier gain were kept constant for all experiments. Oocytes injected with mRNA for non-tagged subunits were included as controls for auto-fluorescence. Images were analyzed using NIH ImageJ software. Surface fluorescence was determined for a defined area positioned at the animal hemisphere of each oocyte and expressed as intensity of signal per unit area; surface fluorescence was then normalized to the mean surface fluorescence of GFP-hCNGA3-expressing oocytes within the same experiment.

Biochemistry—To assess the overall abundance of cone CNG channel subunits expressed in *Xenopus* oocytes, we used Western blot analysis of proteins from oocytes expressing GFP-tagged hCNGA3 or hCNGB3. Oocyte proteins were prepared using a protocol adapted from Rosenbaum and Gordon (22) and others (23). Briefly, oocytes were placed in buffer containing 20 mM Hepes (pH 7.5), 150 mM NaCl, 5 mM EDTA, 0.5% Triton X-100 (Surfact-Amps X-100; Pierce) and a protease inhibitor mixture (Roche Applied Science). Oocytes were subjected to trituration followed by cup sonication using a Branson Sonifier Cell Disruptor 350 (Branson Ultrasonics, Danbury, CT) repeated a total of three times. The soluble cell lysate was then separated from yolk and other insoluble material by centrifugation at 20,000 × g and 4 °C for 10 min and repeated three times. Material representing approximately two oocytes was loaded per lane and separated by SDS-PAGE using NuPage 3–8% Tris acetate gels (Invitrogen). Proteins were then transferred to nitrocellulose using the NuPage transfer buffer system (Invitrogen). Immunoblots were probed with anti-GFP *Aequorea victoria* peptide polyclonal antibody (Clontech, Palo Alto, CA) at a concentration of 1:250 in Tris-buffered saline with 1% nonfat dry milk. GFP-tagged channel subunits were visualized using SuperSignal West Dura substrate (Pierce) and autoradiography film (Kodak X-Omat Blue XB-1, Eastman Kodak Co.). The approximate molecular weights of the GFP-tagged subunits were calculated by interpolation using the linear relationship between the log of molecular weight for protein standards (Invitrogen), as reported by the manufacturer for these buffer conditions, and the migration distance of the proteins.

RESULTS

Functional Expression of Mutant Human CNGB3 Subunits—To investigate the functional consequences of two achromatopsia-associated mutations in the human cone photoreceptor CNG channel β subunit gene (*CNGB3*) (8, 9), we introduced these mutations into cDNA encoding the human CNGB3 subunit and co-expressed mutant or wild type CNGB3 with human cone CNG channel α subunits (hCNGA3) (4) in *Xenopus* oocytes. Fig. 1*A* illustrates the approximate positions in hCNGB3 of the two mutations examined in this study, 1) S435F, located within the S6 transmembrane domain, and 2) T383f.s.ΔC, a 1-base pair deletion at nucleotide 1148 generating a frameshift and premature stop codon at Leu-395 with truncation of the carboxyl terminus of the CNGB3 subunit (8, 9). Similar to other CNG channel β subunits (6, 24–26), human CNGB3 failed to generate functional cyclic nucleotide-activated channels when expressed alone in oocytes (data not shown). As previously demonstrated (7), co-expression of wild type human CNGB3 subunits with human CNGA3 subunits

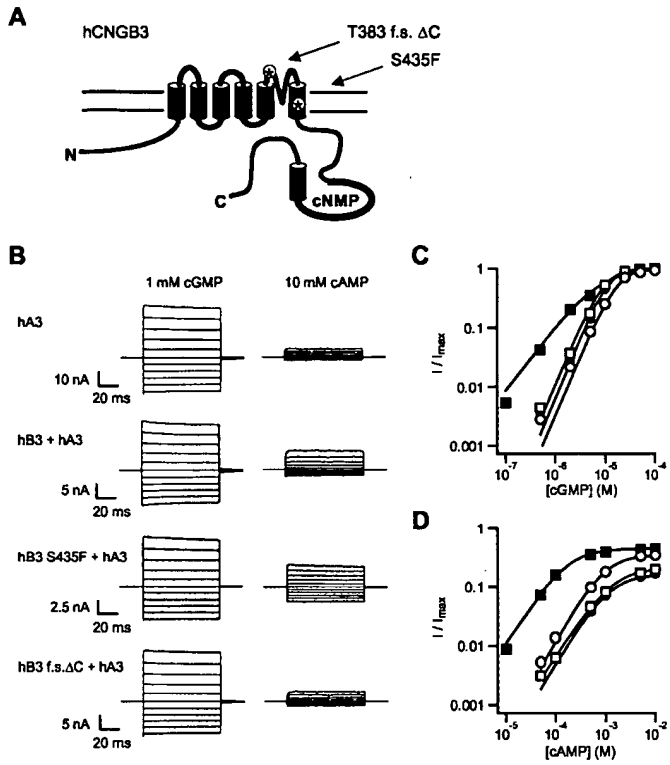

FIG. 1. **Functional characterization of recombinant cone CNG channels containing achromatopsia-associated mutations in hCNGB3.** *A*, schematic of human CNGB3 subunit topology with the approximate locations of two mutations (*) linked to achromatopsia in humans, T383f.s.ΔC and S435F. *B*, current families recorded from inside-out patches excised from *Xenopus* oocytes expressing homomeric hCNGA3 (hA3) channels or heteromeric channels generated by co-injection of mRNA encoding wild type or mutant hCNGB3 (hB3) with hCNGA3 subunits. Current sweeps were elicited at a saturating concentration of cGMP (1 mM) or cAMP (10 mM) by voltage steps from 0 mV to potentials between −100 mV and 100 mV, in 20-mV increments. Currents in the absence of cyclic nucleotide were subtracted. *C*, representative dose-response relationships for channel activation by cGMP for homomeric hCNGA3 channels (*filled circles*), wild type heteromeric hCNGB3 + hCNGA3 channels (*open circles*), heteromeric channels containing hCNGB3-S435F subunits (*filled squares*), and channels formed after co-expression of hCNGB3-T383f.s.ΔC subunits with hCNGA3 subunits (*open squares*). Currents were measured after voltage steps to +80 mV and were normalized to the maximum current elicited by a saturating concentration of cGMP. Continuous curves represent fits of the dose-response relation with the Hill equation, $I/I_{max} = ([cNMP]^h/(K_{1/2}{}^h + [cNMP]^h))$. For these fits, the following parameters were used. For homomeric hCNGA3 channels, $K_{1/2} = 11$ μM, $h = 2.1$; for wild type hCNGB3 + hCNGA3 channels, $K_{1/2} = 18$ μM, $h = 2.0$; for hCNGB3 S435F + hCNGA3 channels, $K_{1/2} = 7.6$ μM, $h = 1.1$; for hCNGB3 T383f.s.Δ + hCNGA3, $K_{1/2} = 10$ μM, $h = 2.0$. *D*, representative dose-response relationships for activation of homomeric and heteromeric channels by cAMP; symbols are the same as in *C*. Currents were normalized to the maximum current elicited by a saturating concentration of cGMP. For these fits, the following parameters were used. For homomeric hCNGA3 channels, $K_{1/2} = 1209$ μM, $h = 1.4$, $I_{max\ cAMP} = 0.16$; for wild type hCNGB3 + hCNGA3 channels, $K_{1/2} = 954$ μM, $h = 1.5$, $I_{max\ cAMP} = 0.35$; for hCNGB3 S435F + hCNGA3 channels, $K_{1/2} = 170$ μM, $h = 1.3$, $I_{max\ cAMP} = 0.45$; for hCNGB3 T383f.s.Δ + hCNGA3, $K_{1/2\ cAMP} = 1214$ μM, $h = 1.3$, $I_{max\ cAMP} = 0.20$.

generates heteromeric channels with properties that differ from channels formed by hCNGA3 subunits alone. The altered functional properties include an increase in the relative agonist efficacy for cAMP (Fig. 1*B*), a small but significant decrease in the apparent affinity for cGMP and increase in apparent affinity for cAMP (Fig. 1, *C* and *D*), and sensitivity to regulation by calcium-calmodulin (7). In addition, wild type heteromeric channels exhibited significantly altered steady-state outward rectification for currents elicited by saturating concentrations of cGMP and cAMP (Fig. 1*B*). $I_{+80\ mV}/I_{-80\ mV}$ in 1 mM cGMP was 1.30 ± 0.02 ($n = 53$) for heteromeric channels and 1.50 ± 0.03 ($n = 12$) for homomeric CNGA3 channels ($p < 0.05$); in 10 mM cAMP, $I_{+80\ mV}/I_{-80\ mV}$ was 2.81 ± 0.11 ($n = 42$) for heteromeric channels and 2.00 ± 0.05 ($n = 12$) for homomeric CNGA3 channels ($p < 0.05$). Thus, the presence of the human CNGB3 subunit tunes the activation properties of recombinant heteromeric cone CNG channels.

Co-expression of CNGB3 subunits containing the achromatopsia-associated S435F mutation with CNGA3 subunits generated channels exhibiting robust cyclic nucleotide-activated currents (Fig. 1*B*) but with properties differing from both wild type heteromeric channels and homomeric CNGA3 channels. The level of functional expression for mutant heteromeric channels was somewhat reduced compared with channels including wild type CNGB3 subunits; the mean patch current density was 580 ± 82 pA/μm^2 ($n = 42$) for wild type heteromeric channels and 390 ± 106 pA/μm^2 ($n = 10$) for S435F-containing channels ($p < 0.05$) when co-injected with hCNGA3 under identical conditions. For S435F-containing channels, the relative agonist efficacy for channel activation by a saturating concentration of cAMP compared with maximal activation by cGMP ($I_{max\ cAMP}/I_{max\ cGMP} = 0.33 \pm 0.03$; $n = 23$) resembled wild type heteromeric channels (0.36 ± 0.01; $n = 37$) but not homomeric hCNGA3 channels (0.12 ± 0.01; $n = 48$) (Fig. 1*B*), confirming that these mutant CNGB3 subunits combined with CNGA3 subunits to form functional heteromeric channels. The macroscopic current records do not reveal if the mutation altered the absolute efficacy of cAMP or cGMP. Steady-state rectification in the presence of a saturating concentration of cAMP (1.34 ± 0.04; $n = 17$) was significantly reduced ($p < 0.001$) compared with both homomeric CNGA3 channels and wild type heteromeric channels. Steady-state rectification in saturating cGMP (1.42 ± 0.02; $n = 36$) was intermediate between that of homomeric hCNGA3 channels and wild type heteromeric channels (Fig. 1*B*). Furthermore, fits with the Hill equation of the dose-response relationships for activation of S435F-containing heteromeric channels (Fig. 1, *C* and *D*) demonstrated an increase in the apparent affinity for both cAMP ($K_{1/2} = 184 \pm 12$ μM; $n = 14$) and cGMP ($K_{1/2} = 9.2 \pm 0.4$ μM; $n = 25$) compared with activation of wild type heteromeric channels (for cAMP, $K_{1/2} = 846 \pm 33$ μM, $n = 54$; for cGMP, $K_{1/2} = 15.8 \pm 0.3$ μM, $n = 61$). In addition to the change in apparent affinity for cAMP and cGMP, the S435F mutation reduced the Hill slope from 1.5 ± 0.3 ($n = 54$) and 2.0 ± 0.2 ($n = 61$), respectively, for wild type heteromeric channels, to 1.1 ± 0.2 ($n = 14$) and 1.4 ± 0.3 ($n = 25$), respectively, for mutant heteromeric channels. The apparent affinities also differed significantly from those of homomeric CNGA3 channels for both cAMP ($K_{1/2} = 1212 \pm 37$ μM; $n = 53$) and cGMP ($K_{1/2} = 12.9 \pm 0.5$ μM; $n = 62$) ($p < 0.001$) (Fig. 1, *C* and *D*). These results indicate that the activation properties of heteromeric cone CNG channels are modified by the S435F mutation in the CNGB3 subunit.

In contrast, co-expression of hCNGA3 subunits with hCNGB3 subunits containing a different achromatopsia mutation, T383f.s.ΔC, generated CNG channels with properties indistinguishable from homomeric CNGA3 channels. First, the steady-state rectification properties of the expressed channels were similar to those of homomeric CNGA3 channels; $I_{+80\ mV}/I_{-80\ mV}$ in 1 mM cGMP was 1.46 ± 0.04 ($n = 8$) and 2.26 ± 0.06 ($n = 8$) in 10 mM cAMP (Fig. 1*B*). Second, the relative efficacy of cAMP (0.13 ± 0.01; $n = 8$) and the apparent affinities for cAMP ($K_{1/2} = 12.3 \pm 0.2$ μM; $n = 8$) and cGMP ($K_{1/2} = 1230 \pm 77$ μM; $n = 8$) were not significantly changed by the truncated hCNGB3 subunit (Fig. 1, *B–D*). Third, functional expression level for the hCNGA3-like channels was qualita-

tively unaffected by the presence of hCNGB3-T383f.s.ΔC subunits; under the same experimental conditions, patch current density was 591 ± 137 pA/μm^2 (n = 9) for hCNGA3 plus hCNGB3 T383f.s.ΔC and 589 ± 156 pA/μm^2 (n = 18) for hCNGA3 alone. Thus, not only did the basic properties of CNG channels generated by co-injection of mRNA encoding hCNGA3 and hCNGB3-T383f.s.ΔC subunits resemble homomeric hCNGA3 channels, but also no apparent dominant-negative effect of the truncated hCNGB3 subunit was evident. These results are consistent with the idea that complete functional absence of the modulatory CNGB3 subunit can be critical for the development of achromatopsia and that homomeric hCNGA3 channels are not sufficient for normal cone photoreceptor function.

Plasma Membrane Targeting of Recombinant Cone CNG Channel Subunits—The pathological basis of many disease-associated mutations in the genes that encode ion channels has been attributed to impaired folding, assembly, and/or plasma membrane targeting of channel subunits or complexes. In addition, photoreceptor dysfunction and degeneration have been associated with mutations that disrupt the processing and trafficking of proteins normally targeted to the photoreceptor outer segment (for review, see Ref. 27). Furthermore, a mutation in CNGA1 linked to retinitis pigmentosa has been shown to dramatically alter the plasma membrane targeting of recombinant rod CNG channel subunits (28–30). Thus, we were interested in determining whether achromatopsia-associated mutations in hCNGB3 impaired the assembly and cell-surface localization of recombinant cone CNG channels.

To address this question we engineered gene fusions of GFP with the amino-terminal regions of the respective human cone CNG channel subunits, generating GFP-hCNGA3 and GFP-hCNGB3. GFP-tagged subunits provide a convenient means to assess cell-surface localization of CNG channel subunits in oocytes using confocal microscopy. The functional properties of GFP-tagged subunits in the context of both homomeric (for hCNGA3) and heteromeric channels were indistinguishable from those of non-tagged subunits (data not shown). We first investigated the effect of co-expression of wild type or mutant hCNGB3 subunits on the surface expression of GFP-tagged hCNGA3 subunits (Fig. 2, *A* and *B*). GFP-hCNGA3 mRNA was injected into oocytes either alone or in combination with mRNAs encoding non-tagged hCNGB3 subunits. For these experiments, the amount of GFP-hCNGA3 mRNA injected was held constant, and the ratio of GFP-hCNGA3 to non-tagged hCNGB3 or control mRNA was fixed at 3:1, a ratio fully effective for the formation of heteromeric channels (data not shown). Compared with the expression of hCNGA3 subunits alone, co-expression of wild-type hCNGB3 subunits attenuated plasma membrane localization of the GFP-tagged hCNGA3 subunits (Fig. 2, *A* and *B*). hCNGB3-S435F subunits similarly attenuated surface fluorescence of GFP-hCNGA3 subunits, indicating that these mutant β subunits are competent for assembly with α subunits. In contrast, co-expression of hCNGB3 T383f.s.ΔC did not significantly alter GFP-hCNGA3 surface fluorescence, suggesting that the carboxyl-terminal region of hCNGB3 may be important for assembly with hCNGA3 subunits or for trafficking control of cone CNG channels. Co-injection of either an irrelevant mRNA species transcribed from a *lac*Z gene construct in the same vector or of mRNA for non-tagged hCNGA3 had no significant effect on surface fluorescence of GFP-hCNGA3 (Fig. 2*B*). These controls confirm that attenuation of GFP-hCNGA3 surface expression by hCNGB3 did not arise from a nonspecific effect, such as overwhelming the oocyte protein synthesis machinery.

Reduced surface fluorescence of GFP-hCNGA3 subunits may result from intracellular retention or recycling of channel complexes or from reduced hCNGA3 protein levels. To help discriminate between these possibilities, we used immunoblots of total solubilized oocyte protein probed with anti-GFP antibody to qualitatively assess the relative levels of GFP-hCNGA3 protein in the absence or presence of hCNGB3 subunits. Western blotting suggested that GFP-hCNGA3 protein levels were not substantially altered by co-expression of wild type or mutant hCNGB3 subunits (n = 3; Fig. 2*C*). Together, these results imply that CNGB3 subunits may provide a brake, regulating

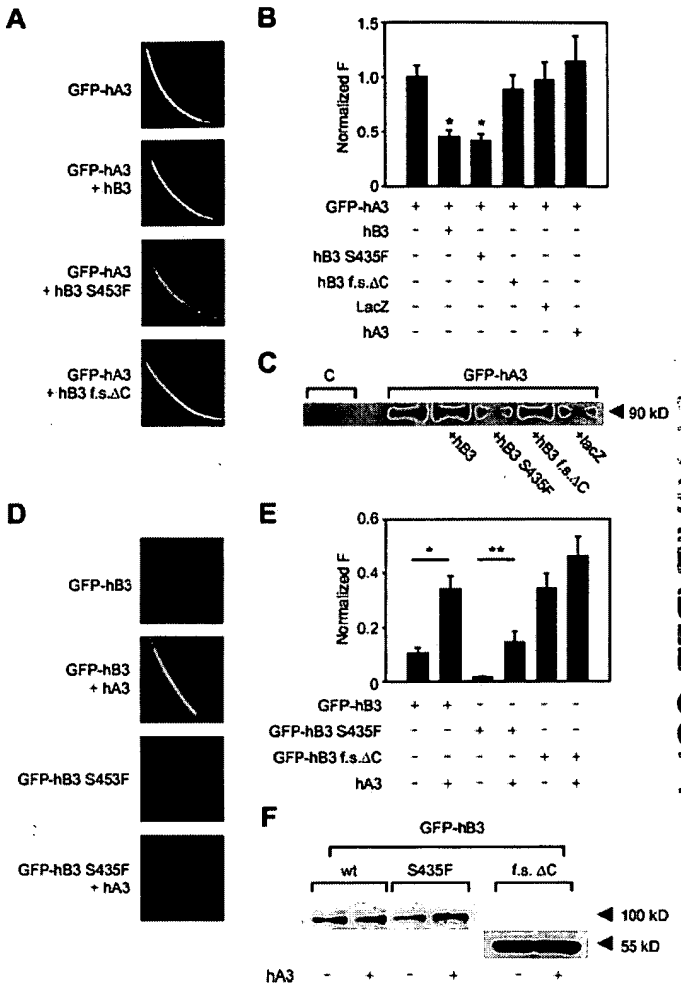

FIG. 2. **Assembly and plasma membrane targeting of hCNGA3 and hCNGB3 subunits.** *A*, confocal images of *Xenopus* oocytes injected with mRNA encoding GFP-tagged hCNGA3 (hA3) subunits and non-tagged hCNGB3 (*hB3*) wild type or achromatopsia-mutant subunits. The amount of GFP-hCNGA3 mRNA injected was held constant, and the ratio of GFP-hCNGA3 to other mRNA was 3:1. *B*, bar graph of surface fluorescence (n = 21–48). The fluorescent signal was normalized to the mean fluorescence of oocytes expressing GFP-hCNGA3 alone from the same experimental group. hCNGB3 wild type and S435F significantly reduced surface expression of GFP-hCNGA3 (*, $p \leq 0.001$). Co-injection of an equal amount of hCNGB3-T383f.s.Δ mRNA, an irrelevant mRNA species (*lacZ*), or mRNA for non-tagged hCNGA3 had no significant effect on GFP-hCNGA3 surface fluorescence. *C*, representative immunoblot of lysates from oocytes expressing GFP-hCNGA3 alone or with wild type or mutant hCNGB3 subunits, as in *B*. *D*, confocal images of oocytes injected with mRNA encoding GFP-tagged hCNGB3 wild type or S435F subunits with or without non-tagged hCNGA3 subunits. The amount of wild type or mutant GFP-hCNGB3 mRNA was kept constant, and the ratio of GFP-hCNGB3 to hCNGA3 mRNA was 5:1. *E*, bar graph of surface fluorescence (n = 9–57) as shown in *D*. The fluorescent signal was normalized to the mean fluorescence of GFP-hCNGA3-expressing oocytes from the same experimental group. hCNGA3 promoted surface localization of GFP-tagged wild type and S435F hCNGB3 subunits (*, $p < 0.01$; **, $p < 0.001$). *F*, Western blot of lysates from oocytes expressing GFP-tagged wild type (*wt*) or mutant hCNGB3 subunits with and without hCNGA3, as in *E*.

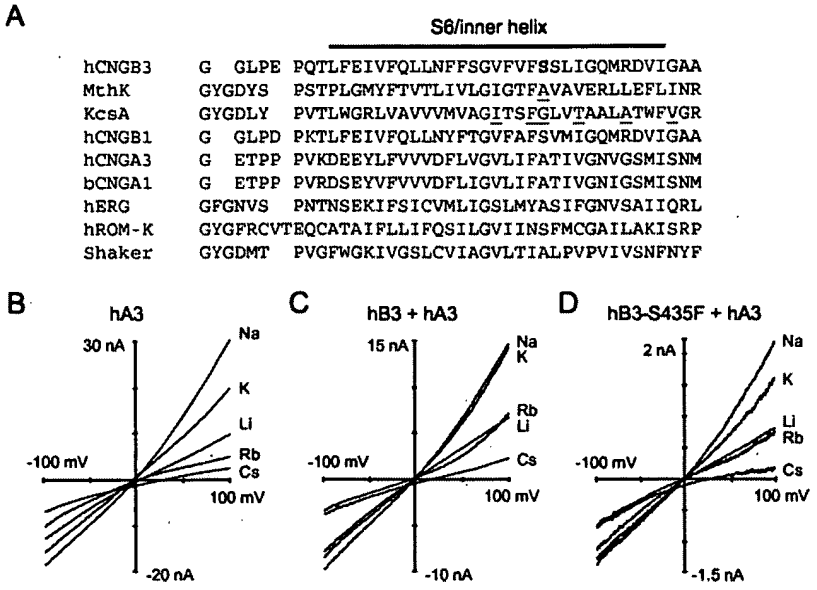

FIG. 3. **Effect of S435F mutation in hCNGB3 on the monovalent cation selectivity of heteromeric cone CNG channels.** *A*, sequence alignment of the S6 region of hCNGB3 with other CNG channel subunits and various K^+ channels. *Highlighted* in *gray shadow* are small volume side chains aligned with Ser-435 (*bold*) in hCNGB3; *underlined residues* in the KcsA and MthK sequences extend side chains into the pore in the respective crystal structures (31, 32). *B–D*, representative I-V relationships under symmetrical bi-ionic conditions with the indicated test ion on the cytoplasmic face of the inside-out patch and Na^+ on the extracellular side, for homomeric hCNGA3 (*hA3*) channels (*B*), wild-type heteromeric channels (*C*), and heteromeric channels formed with hCNGB3 (*hB3*)-S435F subunits (*D*).

trafficking of heteromeric cone CNG channels.

Next we examined the cell-surface localization of wild type and mutant GFP-hCNGB3 subunits in the absence or presence of non-tagged hCNGA3 subunits. For these experiments, the amount of wild type or mutant GFP-hCNGB3 mRNA injected was held constant, and the ratio of GFP-hCNGB3 mRNA to non-tagged hCNGA3 mRNA was 5:1. Only low level surface fluorescence for GFP-hCNGB3 was detected when these subunits were expressed alone (Fig. 2, *D* and *E*). This result implies that hCNGB3 subunits are only marginally competent to traffic to the plasma membrane of oocytes in the absence of hCNGA3 subunits, perhaps contributing to their failure to form functional channels when expressed alone. Co-expression of hCNGA3 subunits promoted surface expression of GFP-hCNGB3 subunits. GFP-tagged hCNGB3 S435F subunits also exhibited little surface fluorescence when expressed alone, and surface expression of S435F subunits was similarly enhanced by hCNGA3 (Fig. 2, *D* and *E*). Surface fluorescence of GFP-hCNGB3 S435F subunits was reduced compared with wild type GFP-hCNGB3 subunits under identical conditions both in the absence and presence of hCNGA3 subunits, paralleling the reduced level of functional expression observed for S435F macroscopic currents. Furthermore, immunoblots of total oocyte protein probed with anti-GFP antibody suggested that the relative amounts of GFP-tagged hCNGB3 and hCNGB3-S435F protein were qualitatively similar and that protein levels were obviously changed by co-expression of hCNGA3 ($n = 3$; Fig. 2*F*). In contrast to hCNGB3 wild type and S435F subunits, GFP-tagged hCNGB3 T383f.s.ΔC subunits exhibited greater surface fluorescence when expressed alone, and surface fluorescence was not significantly enhanced by hCNGA3 subunits. Overall, results shown in Fig. 2 indicate that (*a*) hCNGA3 subunits promote or stabilize plasma membrane localization of hCNGB3 subunits, (*b*) the S435F mutation in hCNGB3 does not impede assembly with hCNGA3 subunits but may instead hinder trafficking of subunits to the plasma membrane, and (c) the carboxyl-terminal region of hCNGB3 may participate in channel assembly and/or may be important for subunit trafficking.

Pore Properties of Wild Type and Mutant Heteromeric Cone CNG Channels—Sequence homology between hCNGB3 and related potassium-selective channels such as KcsA (31) and MthK (32) (Fig. 3*A*) suggests that Ser-435 may contribute to the pore of cone CNG channels. Thus, we were interested in determining if the S435F mutation in hCNGB3 influences the pore properties of recombinant cone CNG channels. First we examined the monovalent cation selectivity of homomeric and heteromeric cone CNG channels by measuring the reversal potential under symmetrical bi-ionic conditions, substituting intracellular Na^+ with K^+, Li^+, Rb^+, or Cs^+ (Fig. 3, *B–D*). The relative monovalent cation permeabilities for recombinant cone CNG channels, determined using the Goldman-Hodgkin-Katz equation, are shown in Table I. For homomeric hCNGA3 channels, $K^+ \geq Na^+ \geq Rb^+ > Li^+ > Cs^+$; for heteromeric hCNGB3 + hCNGA3 channels, $Rb^+ > K^+ \geq Na^+ > Li^+ > Cs^+$; for hCNGB3 S435F + hCNGA3 channels, $Na^+ \geq K^+ \geq Rb^+ > Li^+ > Cs^+$. The relative conductance sequences for outward currents measured at +80 mV were as follows: for homomeric hCNGA3 channels, $Na^+ > K^+ > Li^+ > Rb^+ > Cs^+$; for heteromeric hCNGB3 + hCNGA3 channels, $Na^+ \geq K^+ > Li^+ \geq Rb^+ > Cs^+$; for hCNGB3 S435F + hCNGA3 channels, $Na^+ > K^+ > Li^+ \geq Rb^+ > Cs^+$. Overall, channels formed with hCNGB3-S435F subunits exhibited subtle differences in relative monovalent ion selectivity and conductance compared with both wild type heteromeric channels and homomeric hCNGA3 channels. Small changes in ion selectivity and conductance might arise from a local structural perturbation of the pore due to the S435F mutation. Minimally, these results are consistent with the participation of mutant hCNGB3 subunits in the formation of the cone CNG channel ion conduction pathway.

We also investigated the effect of the S435F mutation on the single channel properties of recombinant cone CNG channels. The single channel current amplitude at +80 mV for wild type hCNGB3 plus hCNGA3 heteromeric channels was 3.26 ± 0.08 pA ($n = 4$ patches) (Fig. 4*A*). The corresponding single channel conductance (~41 picosiemens) was similar to that reported previously for mouse CNGB3 plus CNGA3 channels (6). For S435F-containing heteromeric channels, the single channel current amplitude at +80 mV was reduced to 2.55 ± 0.19 pA ($n = 4$ patches) (Fig. 4*B*), representing a single channel conductance of ~32 picosiemens. Furthermore, for activation of heteromeric channels by a saturating concentration of ligand, the maximum open probability (P_{max}) increased from 0.76 ± 0.02 in 1 mM cGMP and 0.31 ± 0.02 in 10 mM cAMP for wild-type heteromeric channels (Fig. 4*A*) to 0.88 ± 0.03 and 0.39 ± 0.04, respectively, for channels containing S435F subunits (Fig. 4*B*). Thus, the absolute agonist efficacy of cAMP and of cGMP increased for S435F-containing heteromeric channels, but the agonist efficacy of cAMP relative to cGMP ($P_{max\ cAMP}/P_{max\ cGMP}$) remained similar to that of wild type heteromeric channels (~0.4) and was in reasonable agreement with the

TABLE I
Permeability and conductance ratios

Data are the mean ± S.D.; n = 6–12 patches.

Ion	hCNGA3		hCNGB3 + hCNGA3		hCNGB3 S435F + hCNGA3	
	P_x/P_{Na}	G_x/G_{Na}	P_x/P_{Na}	G_x/G_{Na}	P_x/P_{Na}	G_x/G_{Na}
Na^+	1.0	1.0	1.0	1.0	1.0	1.0
K^+	1.04 ± 0.04	0.66 ± 0.14	1.06 ± 0.09	0.97 ± 0.06	0.97 ± 0.06	0.68 ± 0.07
Li^+	0.56 ± 0.02	0.36 ± 0.18	0.74 ± 0.10	0.48 ± 0.10	0.61 ± 0.03	0.35 ± 0.07
Rb^+	0.96 ± 0.08	0.20 ± 0.11	1.27 ± 0.11	0.45 ± 0.10	0.94 ± 0.30	0.31 ± 0.11
Cs^+	0.37 ± 0.15	0.13 ± 0.12	0.55 ± 0.07	0.14 ± 0.03	0.43 ± 0.15	0.13 ± 0.08

relative agonist efficacy observed with macroscopic current recordings. These results indicate that the achromatopsia-associated S435F mutation decreased the single channel conductance and increased the open probability (at saturating ligand concentrations) of recombinant heteromeric cone CNG channels.

Next we examined the sensitivity of wild type and mutant cone CNG channels to block by L-*cis*-diltiazem. L-*cis*-Diltiazem, applied to the cytoplasmic face of the membrane, blocks native photoreceptor CNG channels in a voltage-dependent manner, consistent with this agent binding within the membrane electric field (33–35). For recombinant CNG channels, sensitivity to L-*cis*-diltiazem depends on the presence of CNGB1 or CNGB3 subunits (6, 7, 24, 36). Like homomeric hCNGA3 channels (4, 7), channels formed after co-injection of mRNA encoding hCNGB3 T383f.s.ΔC and hCNGA3 were insensitive to L-*cis*-diltiazem (Fig. 5, *A* and *B*). Surprisingly, heteromeric channels generated by co-expression of hCNGB3-S435F and hCNGA3 subunits were less sensitive to L-*cis*-diltiazem block than channels containing wild type hCNGB3 subunits (7) but more sensitive than hCNGA3 homomeric channels (Fig. 5), suggesting that the mutation may directly or indirectly alter the binding site for the drug. In addition, S435F-containing channels were found to be more sensitive to block by 25 μM L-*cis*-diltiazem in low [cGMP] than in the presence of a saturating concentration of cGMP (Fig. 5*C*). Consistent with this observation, S435F-containing heteromeric channels were also more sensitive to L-*cis*-diltiazem in the presence of a saturating concentration of the partial agonist cAMP; in 10 mM cAMP, $I_{diltiazem}/I$ was 0.42 ± 0.11 (n = 4) (data not shown). Homomeric hCNG3 channels were also somewhat more sensitive to L-*cis*-diltiazem in low [cGMP] (Fig. 5*C*). Wild type heteromeric channels were blocked equally well in low or high [cGMP]. These results provide evidence indicating that a block by L-*cis*-diltiazem of cone CNG channels can exhibit closed-state dependence, as is the case in the tetracaine block of homomeric CNG channels (37), and that the altered gating properties of S435F-containing heteromeric channels may contribute to decreased sensitivity to L-*cis*-diltiazem.

DISCUSSION

We have characterized achromatopsia-associated S435F and T383f.s.ΔC mutations in human CNGB3 using heterologous expression in *Xenopus* oocytes and have identified changes in both ligand sensitivity and pore properties for S435F-containing channels. CNGB3-S435F subunits formed functional heteromeric channels with altered properties when co-expressed with hCNGA3 subunits, whereas CNGB3-T383f.s.ΔC subunits did not participate in channel formation. One of the most dramatic changes observed with S435F-containing channels was a greater than 4-fold increase in cAMP sensitivity. S435F-containing channels also exhibited a modest increase in apparent affinity for cGMP. In addition, single channel recordings revealed an increase in open probability for both cGMP- and cAMP-bound mutant heteromeric channels. These results indicate that the gating properties of heteromeric channels are altered by the S435F mutation.

Most members of the superfamily of ion channels that includes potassium-selective channels and CNG channels present small volume amino acid side chains (Ala, Ser, or Gly) at positions aligning with Ser-435 in hCNGB3 (Fig. 3*A*). The Van der Waals volumes (in Å^3) of the amino acids alanine, serine, and glycine are 67, 73, and 48, respectively (38). For the recently described crystal structure of the open MthK potassium channel, the residue in MthK (Ala-88, Fig. 3*A*) that aligns with Ser-435 in hCNGB3 forms the narrowest part of the MthK intracellular "entryway" (32). Jiang *et al.* (32) argue that a small side chain at this position seems important to prevent interference with ion conduction. If Ser-435 is similarly positioned in open cone CNG channels, then the reduced single channel conductance (Fig. 4) and altered sensitivity to block by L-cis-diltiazem (Fig. 5) that we have observed for mutant heteromeric channels may arise at least in part from the increased size of the substituted amino acid (135 Å^3 for phenylalanine) in the hCNGB3 subunit. Furthermore, the inner helix (S6) bundle of CNG channels is thought to undergo a conformational change during channel activation (39, 40) that may be similar to the outward displacement proposed for K^+ channels (32, 41, 42). We hypothesize that S435F may effectively destabilize the closed state of the channel if the bulky aromatic side chain is more difficult to accommodate in the closed conformation, perhaps because the smaller side chain normally found at this position in CNG channels is packed or buried when channels close (see Ref 43). This would account for the increase in ligand sensitivity seen with S435F-containing heteromeric channels.

The increase in ligand sensitivity reported here for recombinant cone CNG channels containing the S435F mutation in the CNGB3 subunit would be consistent with a phenotype of enhanced channel activity. This suggests that in cone photoreceptors of patients with this mutation, CNG channels may fail to close appropriately as intracellular concentrations of cGMP (or cAMP) fall in response to light stimulation or other, slower adaptive processes. Elevated photoreceptor cyclic nucleotide levels have been previously associated with other congenital retinal disorders (44). In addition, native cone CNG channels and recombinant homomeric CNGA3 channels display remarkably high calcium permeability (45–49). Possible cellular mechanisms for impaired cone photoreceptor function in achromatopsia may depend on altered calcium homeostasis. Because calcium is a universally critical intracellular signaling molecule and plays a particularly important role for recovery and adaptation in cone photoreceptors (50, 51), even subtle changes in CNG channel function may have profound cellular consequences. Also, future studies should address the question of whether the S435F mutation in hCNGB3 may alter the calcium permeability of heteromeric CNG channels.

Co-expression of hCNGB3-T383f.s.ΔC subunits with hCNGA3 subunits generated CNG channels indistinguishable from expression of hCNGA3 subunits alone. Unlike wild type or S435F CNGB3 subunits, T383f.s.ΔC subunits did not suppress cell-surface fluorescence of GFP-tagged hCNGA3 subunits. Further-

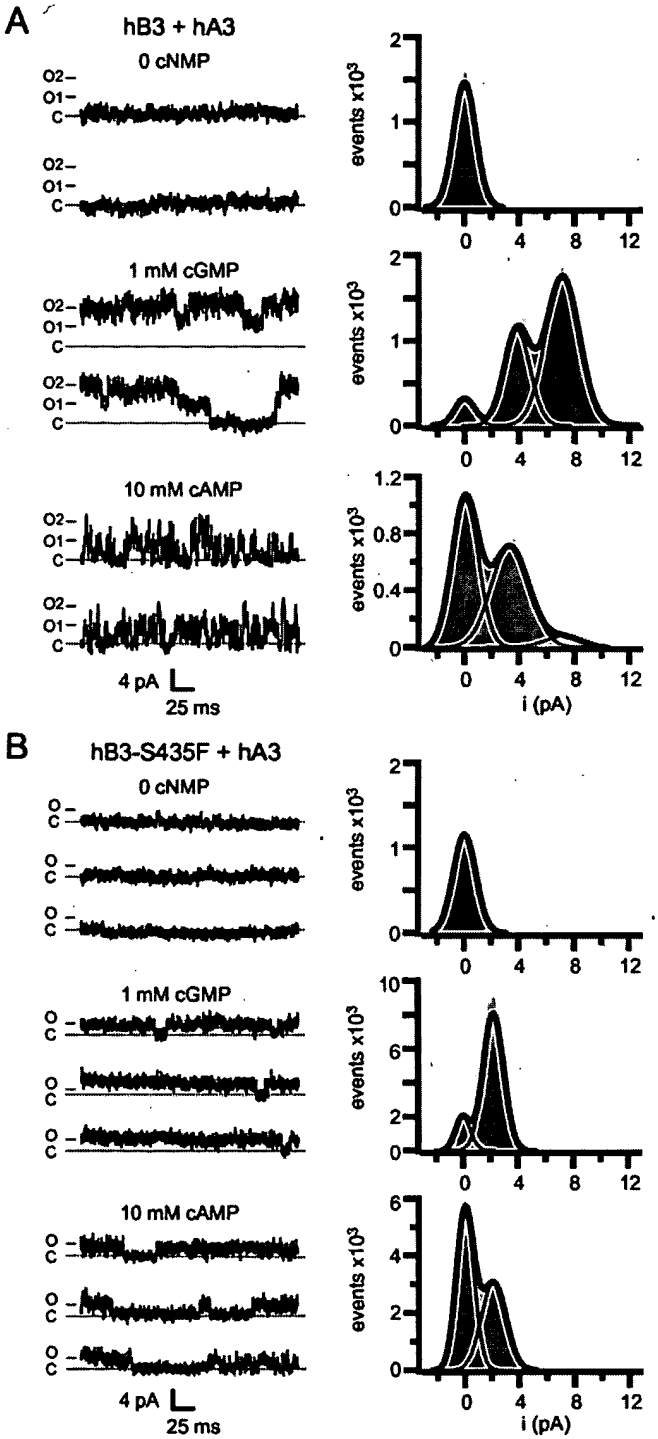

FIG. 4. **Single channel activity of wild type and S435F-containing heteromeric cone CNG channels.** Examples of inside-out patches containing one or two CNG channels are shown, excised from oocytes expressing hCNGB3 (*hB3*) + hCNGA3 (*hA3*) (*A*) or hCNGB3 S435F + hCNGA3 (*B*) heteromeric channels. Currents were elicited at a membrane potential of +80 mV by a saturating concentration of cGMP (1 mM) or cAMP (10 mM). *C*, closed channel mean current level. *O*, current level(s) for open channel(s). *Scale bars* are identical for *A* and *B*. Amplitude histograms (*right*) were accumulated from 1 to 5 s of recording and fit by the sum of two (*B*) or three (*A*) gaussian functions. For wild type hCNGB3 + hCNGA3 channels (*A*) in the presence of a saturating concentration of cGMP (1 mM), i = 3.33 pA, and P_o = 0.78; in a saturating concentration of cAMP (10 mM), i = 3.37 pA and P_o = 0.28. For hCNGB3 S435F + hCNGA3 channels (*B*), in 1 mM cGMP, i = 2.41 pA, and P_o = 0.86, and in 10 mM cAMP, i = 2.13 pA, and P_o = 0.43.

more, no dominant-negative effect on functional hCNGA3 expression was observed, in contrast to the current suppression effects reported for similarly truncated K^+ channel subunits (52).

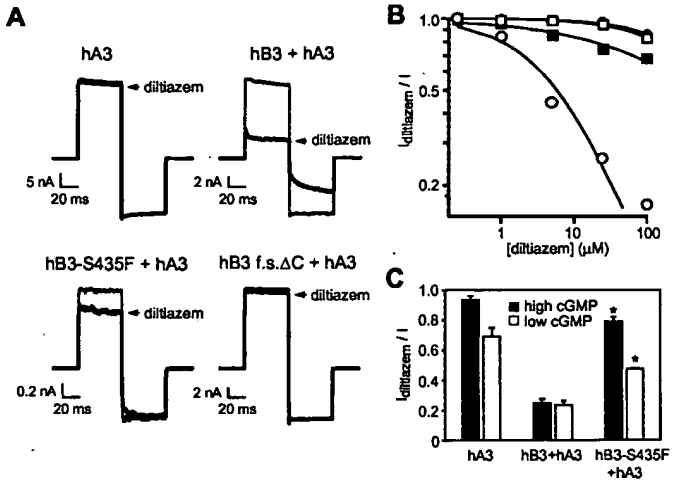

FIG. 5. **L-*cis*-Diltiazem block of heteromeric channels formed by co-expression of hCNGA3 with wild type or mutant hCNGB3 subunits.** *A*, representative current traces elicited by 100 μM cGMP in the absence or presence (*thick line*) of 25 μM L-*cis*-diltiazem for homomeric hCNGA3 (*hA3*) channels and for channels generated by co-expression of hCNGA3 with wild type or mutant hCNGB3 (*hB3*) subunits. Current traces were elicited by voltage steps from a holding potential of 0 mV to +80 mV, then to −80 and 0 mV. Leak currents in the absence of cyclic nucleotide were subtracted for all recordings. *B*, dose-response relationships for block by L-*cis*-diltiazem in the presence of 100 μM cGMP of homomeric hCNGA3 channels (*filled circles*) and channels produced by co-injection of hCNGA3 with wild type hCNGB3 (*open circles*), hCNGB3 S435F (*filled squares*), or hCNGB3 T383f.s.ΔC (*open squares*) (same representative patches as in *A*). Currents were normalized to the current elicited by 100 μM cGMP in the absence of L-*cis*-diltiazem. Continuous curves represent fits of the dose-response relation to the Hill equation in the form: $I_{diltiazem}/I = (K_{1/2}{}^h/(K_{1/2}{}^h + [\text{diltiazem}]^h))$. For heteromeric hCNGB3 + hCNGA3 channels, $K_{1/2}$ diltiazem = 5.8 μM, and h = 0.8. Both homomeric hCNGA3 channels and channels formed by co-expression of hCNGA3 with hCNGB3 T383f.s.ΔC were insensitive to L-*cis*-diltiazem ($K_{1/2} \gg 100$ μM). Channels formed by co-injecting hCNGA3 with hCNGB3 S435F exhibited intermediate sensitivity to block by L-*cis*-diltiazem. *C*, state dependence of cone CNG channel block by L-*cis*-diltiazem. S435F-containing channels were more sensitive to block by 25 μM L-*cis*-diltiazem in 10 μM cGMP (*open bars*) than in 100 μM cGMP (*closed bars*) (*, $p < 0.01$) and more sensitive than homomeric hCNGA3 channels at the corresponding concentrations ($p < 0.05$ and $p < 0.01$, respectively).

One possible explanation is that the cytoplasmic carboxyl-terminal domain of CNGB3 may be critical for assembly with CNGA3 subunits. In relation to this possibility, it has been proposed previously that intersubunit interactions between cytoplasmic amino- and carboxyl-terminal domains may be involved in assembly of olfactory (53) and rod (22, 29, 54, 55) CNG channels. In addition, homotypic interactions among the carboxyl-terminal domains of CNGA1, CNGA2, or CNGA3 subunits have been recently demonstrated (56). Further experiments are needed to define the important intersubunit contacts that control the assembly of cone CNGB3 and CNGA3 subunits. Data presented here for hCNGB3 T383f.s.ΔC are consistent with the recessive inheritance pattern of the disease and with the likelihood that channels made up of hCNGA3 subunits alone are not sufficient for normal cone photoreceptor function. Although heterologous expression studies indicate that hCNGA3 subunits can form functional channels by themselves, cone photoreceptors probably require specialized CNG channels composed of both CNGA3 and CNGB3 subunits. Thus, in patients with this frameshift mutation, cone dysfunction may arise from the complete lack of serviceable hCNGB3 subunits.

For GFP-tagged hCNGB3 T383f.s.ΔC, enhanced surface fluorescence of these truncated subunits when expressed alone suggests that the cytoplasmic carboxyl-terminal domain of CNGB3 may contain a control signal that limits plasma mem-

brane localization of CNGB3 subunits in the absence of CNGA3 subunits. Because CNGB3 subunits do not form functional homomeric channels, we do not expect these truncated CNGB3 subunits to form tetramers. It is possible that aberrant targeting of hCNGB3-T383f.s.ΔC subunits in cone photoreceptors may contribute to the development of achromatopsia. Elegant experiments with inwardly rectifying potassium channels have recently identified distinct signals that control the trafficking of the subunits to the plasma membrane; these signals include sequence motifs for endoplasmic reticulum retention/retrieval (57) and other motifs that promote endoplasmic reticulum exit and cell-surface expression (58, 59). Such signals are thought to be vital for the control of channel makeup (heteromultimerization) and of the density of channels at the plasma membrane (57, 59). Human CNGB3 subunits may possess similar trafficking signals within the carboxyl-terminal domain that lead to intracellular retention of CNGB3 subunits (in the absence of CNGA3 subunits) and of incompletely assembled channels.

Overall our results indicate that T383f.s.ΔC is effectively a null mutation, whereas the pathogenicity of the S435F mutation may arise from a complex of effects, an increase in ligand sensitivity, changes in the pore properties, and a decrease in functional expression level of heteromeric channels. A subtle decrease in patch current density and cell-surface localization after heterologous expression, however, cannot be readily extrapolated to predict the effect of mutations on cone CNG channel density or makeup *in vivo*. Thus, animal models expressing achromatopsia-associated mutations may be required to address this question more definitively. Results presented here provide a rational basis for the generation of mutant mice containing select achromatopsia mutations in the CNGB3 subunit.

Acknowledgments—We are grateful to S. E. Gordon for helpful advice and comments, to C. A. Thor for excellent technical assistance, and D. A. Hess and C. Liu for comments on the manuscript. We also thank Prof. K.-W. Yau for providing the cDNA clone for human CNGA3.

REFERENCES

1. Zagotta, W. N., and Siegelbaum, S. A. (1996) *Annu. Rev. Neurosci.* **19,** 235–263
2. Kaupp, U. B., and Seifert, R. (2002) *Physiol. Rev.* **82,** 769–824
3. Bonigk, W., Altenhofen, W., Muller, F., Dose, A., Illing, M., Molday, R. S., and Kaupp, U. B. (1993) *Neuron* **10,** 865–877
4. Yu, W. P., Grunwald, M. E., and Yau, K. W. (1996) *FEBS Lett.* **393,** 211–215
5. Wissinger, B., Muller, F., Weyand, I., Schuffenhauer, S., Thanos, S., Kaupp, U. B., and Zrenner, E. (1997) *Eur. J. Neurosci.* **9,** 2512–2521
6. Gerstner, A., Zong, X., Hofmann, F., and Biel, M. (2000) *J. Neurosci.* **20,** 1324–1332
7. Peng, C., Rich, E. D., Thor, C. A., and Varnum, M. D. (2003) *J. Biol. Chem.* **278,** 24617–24623
8. Sundin, O. H., Yang, J. M., Li, Y., Zhu, D., Hurd, J. N., Mitchell, T. N., Silva, E. D., and Maumenee, I. H. (2000) *Nat. Genet.* **25,** 289–293
9. Kohl, S., Baumann, B., Broghammer, M., Jagle, H., Sieving, P., Kellner, U., Spegal, R., Anastasi, M., Zrenner, E., Sharpe, L. T., and Wissinger, B. (2000) *Hum. Mol. Genet.* **9,** 2107–2116
10. Kohl, S., Marx, T., Giddings, I., Jagle, H., Jacobson, S. G., Apfelstedt-Sylla, E., Zrenner, E., Sharpe, L. T., and Wissinger, B. (1998) *Nat. Genet.* **19,** 257–259
11. Wissinger, B., Gamer, D., Jagle, H., Giorda, R., Marx, T., Mayer, S., Tippmann, S., Broghammer, M., Jurklies, B., Rosenberg, T., Jacobson, S. G., Sener, E. C., Tatlipinar, S., Hoyng, C. B., Castellan, C., Bitoun, P., Andreasson, S., Rudolph, G., Kellner, U., Lorenz, B., Wolff, G., Verellen-Dumoulin, C., Schwartz, M., Cremers, F. P., Apfelstedt-Sylla, E., Zrenner, E., Salati, R., Sharpe, L. T., and Kohl, S. (2001) *Am. J. Hum. Genet.* **69,** 722–737
12. Rojas, C. V., Maria, L. S., Santos, J. L., Cortes, F., and Alliende, M. A. (2002) *Eur. J. Hum. Genet.* **10,** 638–642
13. Biel, M., Seeliger, M., Pfeifer, A., Kohler, K., Gerstner, A., Ludwig, A., Jaissle, G., Fauser, S., Zrenner, E., and Hofmann, F. (1999) *Proc. Natl. Acad. Sci. U. S. A.* **96,** 7553–7557
14. Eksandh, L., Kohl, S., and Wissinger, B. (2002) *Ophthalmic Genet.* **23,** 109–120
15. Sachs, O. W. (1997) *The Island of the Colorblind*, Knopf, New York
16. Liman, E. R., Tytgat, J., and Hess, P. (1992) *Neuron* **9,** 861–871
17. Ho, S. N., Hunt, H. D., Horton, R. M., Pullen, J. K., and Pease, L. R. (1989) *Gene (Amst.)* **77,** 51–59
18. Varnum, M. D., Black, K. D., and Zagotta, W. N. (1995) *Neuron* **15,** 619–625
19. Sakmann, B., and Neher, E. (eds) (1995) *Single-channel Recording*, 2nd Ed., pp. 643–649, Plenum Press, New York
20. Hille, B. (2001) *Ion Channels of Excitable Membranes*, 3rd Ed., pp. 1–22, Sinauer Associates, Sunderland, MA
21. Robinson, R., and Stokes, R. (1959) *Electrolyte Solutions*, 2nd Ed., Butterworth and Co., London
22. Rosenbaum, T., and Gordon, S. E. (2002) *Neuron* **33,** 703–713
23. Rho, S., Lee, H. M., Lee, K., and Park, C. (2000) *FEBS Lett.* **478,** 246–252
24. Chen, T. Y., Peng, Y. W., Dhallan, R. S., Ahamed, B., Reed, R. R., and Yau, K. W. (1993) *Nature* **362,** 764–767
25. Liman, E. R., and Buck, L. B. (1994) *Neuron* **13,** 611–621
26. Bradley, J., Li, J., Davidson, N., Lester, H. A., and Zinn, K. (1994) *Proc. Natl. Acad. Sci. U. S. A.* **91,** 8890–8894
27. Rattner, A., Sun, H., and Nathans, J. (1999) *Annu. Rev. Genet.* **33,** 89–131
28. Dryja, T. P., Finn, J. T., Peng, Y. W., McGee, T. L., Berson, E. L., and Yau, K. W. (1995) *Proc. Natl. Acad. Sci. U. S. A.* **92,** 10177–10181
29. Trudeau, M. C., and Zagotta, W. N. (2002) *Neuron* **34,** 197–207
30. Mallouk, N., Ildefonse, M., Pages, F., Ragno, M., and Bennett, N. (2002) *J. Membr. Biol.* **185,** 129–136
31. Doyle, D. A., Morais Cabral, J., Pfuetzner, R. A., Kuo, A., Gulbis, J. M., Cohen, S. L., Chait, B. T., and MacKinnon, R. (1998) *Science* **280,** 69–77
32. Jiang, Y., Lee, A., Chen, J., Cadene, M., Chait, B. T., and MacKinnon, R. (2002) *Nature* **417,** 523–526
33. Stern, J. H., Kaupp, U. B., and MacLeish, P. R. (1986) *Proc. Natl. Acad. Sci. U. S. A.* **83,** 1163–1167
34. McLatchie, L. M., and Matthews, H. R. (1992) *Proc. R. Soc. Lond. B Biol. Sci.* **247,** 113–119
35. Haynes, L. W. (1992) *J. Gen. Physiol.* **100,** 783–801
36. Korschen, H. G., Illing, M., Selfert, R., Sesti, F., Williams, A., Gotzes, S., Colville, C., Muller, F., Dose, A., Godde, M., Molday, L., Kaupp, U. B., and Molday, R. S. (1995) *Neuron* **15,** 627–636
37. Fodor, A. A., Black, K. D., and Zagotta, W. N. (1997) *J. Gen. Physiol.* **110,** 591–600
38. Richards, F. M. (1974) *J. Mol. Biol.* **82,** 1–14
39. Flynn, G. E., and Zagotta, W. N. (2001) *Neuron* **30,** 689–698
40. Flynn, G. E., Johnson, J. P., Jr., and Zagotta, W. N. (2001) *Nat. Rev. Neurosci.* **2,** 643–651
41. Liu, Y., Holmgren, M., Jurman, M. E., and Yellen, G. (1997) *Neuron* **19,** 175–184
42. Perozo, E., Cortes, D. M., and Cuello, L. G. (1999) *Science* **285,** 73–78
43. Yifrach, O., and MacKinnon, R. (2002) *Cell* **111,** 231–239
44. Dizhoor, A. M. (2000) *Cell. Signal.* **12,** 711–719
45. Frings, S., Seifert, R., Godde, M., and Kaupp, U. B. (1995) *Neuron* **15,** 169–179
46. Picones, A., and Korenbrot, J. I. (1995) *Biophys. J.* **69,** 120–127
47. Korenbrot, J. I. (1995) *Cell Calcium* **18,** 285–300
48. Dzeja, C., Hagen, V., Kaupp, U. B., and Frings, S. (1999) *EMBO J.* **18,** 131–144
49. Ohyama, T., Hackos, D. H., Frings, S., Hagen, V., Kaupp, U. B., and Korenbrot, J. I. (2000) *J. Gen. Physiol.* **116,** 735–754
50. Miller, J. L., and Korenbrot, J. I. (1994) *J. Gen. Physiol.* **104,** 909–940
51. Pugh, E. N., Jr., Nikonov, S., and Lamb, T. D. (1999) *Curr. Opin. Neurobiol.* **9,** 410–418
52. Tu, L., Santarelli, V., Sheng, Z., Skach, W., Pain, D., and Deutsch, C. (1996) *J. Biol. Chem.* **271,** 18904–18911
53. Varnum, M. D., and Zagotta, W. N. (1997) *Science* **278,** 110–113
54. Gordon, S. E., Varnum, M. D., and Zagotta, W. N. (1997) *Neuron* **19,** 431–441
55. Trudeau, M. C., and Zagotta, W. N. (2002) *Proc. Natl. Acad. Sci. U. S. A.* **99,** 8424–8429
56. Zhong, H., Molday, L. L., Molday, R. S., and Yau, K. W. (2002) *Nature* **420,** 193–198
57. Zerangue, N., Schwappach, B., Jan, Y. N., and Jan, L. Y. (1999) *Neuron* **22,** 537–548
58. Ma, D., Zerangue, N., Lin, Y. F., Collins, A., Yu, M., Jan, Y. N., and Jan, L. Y. (2001) *Science* **291,** 316–319
59. Ma, D., Zerangue, N., Raab-Graham, K., Fried, S. R., Jan, Y. N., and Jan, L. Y. (2002) *Neuron* **33,** 715–729